uOttawa

L'Université canadienne
Canada's university

FACULTÉ DES ÉTUDES SUPÉRIEURES ET POSTOCTORALES

uOttawa

L'Université canadienne
Canada's university

FACULTY OF GRADUATE AND POSDOCTORAL STUDIES

Ali Abbas

AUTEUR DE LA THÈSE / AUTHOR OF THESIS

Ph.D. (Electrical and Computer Engineering)

GRADE / DEGREE

School of Information Technology and Engineering

FACULTÉ, ÉCOLE, DÉPARTEMENT / FACULTY, SCHOOL, DEPARTMENT

Concept Development, Design, Analysis, and Performance Evaluation of an Automated Computerized Auscultation and Diagnostic System for Respiratory Sound

TITRE DE LA THÈSE / TITLE OF THESIS

Atef Fahim

DIRECTEUR (DIRECTRICE) DE LA THÈSE / THESIS SUPERVISOR

CO-DIRECTEUR (CO-DIRECTRICE) DE LA THÈSE / THESIS CO-SUPERVISOR

Rafik Goubran

Tet Yeap

Thomas Doyle (McMaster Univeristy)

Abdulmotaleb El Saddik

Gary W. Slater

Le Doyen de la Faculté des études supérieures et postdoctorales / Dean of the Faculty of Graduate and Postdoctoral Studies

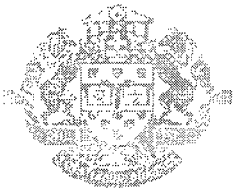

University of Ottawa
Electrical and Computer Engineering

Concept Development, Design, Analysis, and Performance Evaluation of An Automated Computerized Auscultation and Diagnostic System For Respiratory Sound

By

Ali Abbas

A Thesis submitted to
The Faculty of Graduate and Postgraduate Studies
In Partial Fulfillment of the degree of
Ph.D. of Electrical and Computer Engineering

School of Information Technology and Engineering
Electrical and Computer Engineering
University of Ottawa

Your file Votre référence
ISBN: 978-0-494-66252-6
Our file Notre référence
ISBN: 978-0-494-66252-6

To my wife Sausan;
To my kids, Al-Hassan, Tabarek, and Amir;
Those from whom the time was stolen
To make this work possible

Acknowledgments

The accomplishment of this work is greatly due to the huge encouragement, unconditional support and wonderful guidance that I have received from my supervisor ***Dr. Atef Fahim****. Therefore, I would like to offer my greatest thanks to him for his generous giving of his time and expertise.*

Last but certainly not least, I must extend a special thanks to my family; wife and kids, whose amazing support and ability to cope with the difficulties have been vital in such a journey of study and research.

TABLE OF CONTENTS

LIST OF FIGURES

LIST OF TABLES

Abstract:

Respiratory sounds are of significance as they provide valuable information on the health of the respiratory system. Sounds emanating from the respiratory system are uneven, and vary significantly from one individual to another and for the same individual over time. In and of themselves they are not a direct proof of an ailment, but rather an inference that one exists. Auscultation diagnosis is an art/skill that is acquired and honed by practice; hence it is common to seek confirmation using invasive and potentially harmful imaging diagnosis techniques like x-rays. This research focuses on developing an automated auscultation diagnostic system that overcomes the limitations inherent in traditional auscultation techniques. The system uses a front end sound signal filtering module that uses adaptive Neural Networks (NN) noise cancellation to eliminate spurious sound signals like those from the heart, intestine, and ambient noise. The core diagnosis module of the system is capable of identifying lung sounds from non-lung sounds, normal lung sounds from abnormal ones, and identifying wheezes from crackles as indicators of different ailments. Furthermore, the system is capable of identifying the location of different infected sites of the diseased lungs. An approach for generating virtual patients auscultation sounds by isolating the adventitious signals from lung sounds and injecting them into healthy lung sounds has been developed. Forty distinct virtual patients were generated and used to test the performance of the identification and localization modules of the system. Test results using real and virtual auscultation sounds show the high efficacy of the conceived system.

CHAPTER I
Introduction

1.1 Introduction

Breathing is the process of inhaling oxygen and exhaling carbon dioxide. The respiration system performs the breathing process through the mouth, nose, trachea, and lungs. Air inters the respiratory system through the mouth and the nose, it then travels through the different airways towards its final destination, the lungs. The trachea is divided into two smaller tubes, the bronchi. Each bronchus then divides again forming the bronchial tubes. The bronchial tubes enter the lungs where they divide many times over into smaller tubes which finally terminate into tiny sacs, the alveoli. The inhaled air enters the alveoli where oxygen diffuses into arterial blood through the alveoli walls and their arterial capillaries. Meanwhile, the waste-rich blood from the veins releases its carbon dioxide into the alveoli. The carbon dioxide go though the same passageways out of the lungs during the exhalation cycle [1]. Through the process of inhalation and exhale air flow through the series of respiratory structures resulting in the familiar pulmonary sounds. Due to the complexity of the respiratory system structure, and the possibility of presence of restrictions and obstructions, the nature and quality of pulmonary sounds tend to be complex and the process of diagnosis using auscultation tends to be difficult [2].

Auscultation is a procedure of listening and detecting the acoustical signals, "sounds", produced by the human body. It can help classify and identify normal or abnormal sounds in order to assist in making a medical diagnosis. In general, auscultation can be used as an assessment tool to determine medical conditions. This research is limited to those sounds generated in the lungs. In order for the auscultation process to be successfully carried out, the breathing has to be performed normally and smoothly by the patient. Although asking a patient to take a deep breath is commonly requested from a patient during auscultation, it is hard for a child to breathe deeply for a long time when he/she has any respiratory disease. Deep breathing amplifies the sounds emanating from the lung and allows for better diagnosis. The difficulty of repeatedly breathing deeply experienced by sick children adds to the difficulty experienced by the diagnosing physician, because, in such a case,

the physician can not get the full profile of the respiratory sound signals. This difficulty can be mitigated by a computerized and automated auscultation system such as the one subject of this research, because the system is designed to acquire signals from 20 different locations simultaneously. The decision to monitor 20 different locations is based on the lung physiology and medical practices. The right lung, as will be seen later, is composed of 10 segments. The left lung is composed to 10 segments and sub-segments. Each segment and sub-segment is monitored by an auscultation channel.

The auscultation of the respiratory system is one of the oldest diagnostic techniques used by physicians to diagnose different pulmonary diseases. It is broadly utilized because it is inexpensive, noninvasive, safe, and easy for medical professionals to use. The stethoscope was one of the first medical diagnostic instrument ever used. Auscultation of the respiratory system has been confirmed to be a significant diagnostic tool for identifying and observing different types of the respiratory diseases. Many researches and studies utilized computer based approaches to design a system that can be used for the measurement and/or analysis of acoustic respiratory signals [16-54]. In general, most of such systems have features that enable them to digitally record the acoustical signals of the respiratory system. Such computerized systems use an electronic stethoscope for acquiring the respiratory acoustic signals. In most cases the recorded respiratory sounds can be replayed, edited, modified, filtered, and analyzed in order to show the features and characteristics available within these signals. However, the system conceived and constructed during this research is well above the capabilities of other known auscultation systems in the scope, precision, technologies and in over all functionality.

The respiratory system of children is easily accessible for clinical examination. The chest wall is thin and far more elastic than that of adults, thus allowing for better sound transmission. A complete and careful physical examination provides valuable information and is a sound basis for comparison with diagnostic imagery findings. To diagnose respiratory diseases by the auscultation method, one should listen for variation in breathing sounds from all over the chest. Such breath sounds may include: wheezes, crackles, murmurs, muffling of the baby's crying, and displacement

of the heart sounds [2]. Such a variety in respiratory sounds will impose a challenge when the signals being classified, filtered, identified and diagnosed. Therefore, there are many research directions are being pursued in order to construct an auscultation system that would form a framework for respiratory disease analysis and diagnosis.

1.1.1 Research Motivations, Objectives and Contributions

Pulmonary and pulmonary-related infections are the most common causes of illness in North America [3]. Statistics Canada data show that influenza and pneumonia are the sixth most common cause of death in Canada. For the age-standardized mortality rate per 100,000, both together account for approximately 8,000 deaths per year [4]. In the USA, it is estimated that 10 to 20 percent of the population contract influenza and pneumonia each year, and that together they rank as the seventh leading cause of death [5]. This translates to approximately 200,000 hospitalizations and 36,000 deaths each year. The initial step in diagnosing a pulmonary disease is for the physician to perform a medical auscultation to acquire acoustic signals from the structures of the lungs during breathing and classify these as normal or abnormal [6].

Auscultated respiratory acoustical signals have long been significant reflection of respiratory health and disease. Acoustical observation of the breathing sound signals has been used by medical professionals and other researchers for a variety of diagnostic rationales. In the early days of auscultation, medical doctors depended on simple instruments and their hearing to perceive any symptomatic indicators in respiratory sound signals of their patients. However, in recent years, and due to advances in digital signal processing equipment and techniques, interest in further research for new methodologies for diagnosis through auscultation have emerged. These advancements in the science and applications of signal processing allow for efficient and rapid identification, quantification, and categorization of respiratory sound signals. In addition, digital recording of the respiratory sounds of a patient would allow for comparative analysis with later recordings in order to track the progress of the disease or the recovery.

Signal processing techniques of the respiratory sounds will be used in this research to derive characteristics features of the lung sounds for both diagnostic and assessment for treatment purposes. Although the analytical techniques of signal processing are largely independent of the application, interpretation of their results on biological data, i.e. respiratory sounds, requires substantial understanding of the involved physiological system.

Auscultation is recognized as an efficient and safe method for early detection of lung diseases and is easy to apply to patients irrespective of their age and severity of disease [7]. Auscultation diagnosis is an art/skill that is acquired and honed by practice. Hence it is common to seek conformation using deterministic imaging diagnosis techniques like x-rays even though they are invasive and potentially harmful. To achieve fast, inexpensive, and precise diagnosis of the pulmonary disease through a medical auscultation, an automated and computerized method is developed in this work. The system is capable of distinguishing between normal and abnormal lung sounds, and categorizing abnormal sounds as containing crackles or wheezes. These two are the most commonly used acoustic descriptors in pulmonary medicine [8]. The ultimate goal of the work is to develop a fully automated accurate and easy to use auscultation system as an adjunct for a physician diagnostic techniques in order to reduce the necessity for invasive medical imaging techniques. A primary design criteria adhered to strictly when constructing the system was to ensure that it does not take over the diagnosis function from a physician, but to become an adjunct to their diagnosis expertise. The research of this thesis focuses on the development of a computerized and automated auscultation system for the acquiring, recording, conditioning, classification and identification of respiratory sound signals and the anomalous sounds. It also focuses on the recognition of their characteristics and the diagnose of the respiratory medical condition.

For the accurate and reliable lung sounds acquisition , the hardware is constructed to be able to precisely and efficiently acquire lung sound signals from the patient's chest. The design objective is to acquire 20 channels of lung sound signals simultaneously. Hence, the respiratory acoustical signals should be acquired by an array of transducers (electronic stethoscopes) and converted into a digital data stream. The transducers are constructed in house using tiny microphone

elements (omni-direction electret microphones) and are housed in specially shaped chest pieces that are strung together to form the multi-channel electronic stethoscope. The omni-direction electret condenser microphones form the core sensing elements of the electronic stethoscope, see Figure 6.3. Different software modules (Digital Signal Processing (DSP) and filtration modules, identification and diagnosing NN modules, localization of the source of infection modules, and Graphical User Interface module) are integrated together in order to automate the diagnosis process. The design of the auscultation core software is modular to allow effective development, modification, and maintenance. The designed graphical user interface (GUI) is able to provide the auscultation physician with an easy access mechanism to monitor and control the functionality of the different system hardware and software modules, see Figure 3.8. Audio inspection of the auscultation sounds, analysis and diagnosis can be practiced in real time or off line. The user can listen to each channel individually by browsing through and selecting from a drop down menu. The position of each channel is displayed on a generic upper body view. For efficient analysis and diagnose of the healthy and adventitious lung sounds, the user can control all the parameters of the low-pass, high-pass, band pass, and band stop filters, as well as the operation of the heartbeat filter. The system can be commanded to perform a diagnostic process on any one of the channels or a general diagnosis of the entire set of channels. The user can view the sound signals for any of the 20 channel in one of three formats; time base-domain , frequency domain, and Power Spectral Density (PSD). By using this system, the medical doctor should be able as well to locate the source(s) of the adventitious lung sounds which reflect the identification of the different infected location(s) of the lungs. The diagnosing neural network is trained using two sources of data; data recorded using the developed automatic auscultation system, data from clinically recorded lung sounds used for training medical students [57- 59]. In this research no target group is stated, even though initially the system was targeted at children. This is because the profile and age of patients whose lung sounds are included in the publically available lung sounds data bases used for training medical students intention were not stated.

1.2 Thesis Outline

Chapter 2 provides the necessary background of the respiratory system structure, lung sound origination and transmission, and the classification and characteristics of the breath sounds. It also describes devices used for auscultation, the auscultation process, and the conventional locations for listening to lung sounds In addition, the chapter provides a detailed literature review of the related works. Description of the developed computerized auscultation system architecture, hardware, and software are provided in Chapter 3. Chapter 4 describe the process of filtering and analyzing respiratory acoustical signals using conventional signal processing techniques and explains the strengths and weaknesses of these methods. Chapter 5 details the Neural Network approaches used in this work for processing and identifying anomalies in respiratory acoustical signals. In addition, the chapter explains the process of identifying the location of different infection sites of a diseased lungs. Chapter 6 describes a novel process for generating virtual patients. The chapter also presents results of the diagnosis, identification of auscultated sounds, and the localization of infection sites performed on these patients. Finally, Chapter 7 present the conclusion of the thesis, summary of the contributions and future works.

CHAPTER II

Auscultation of the Respiratory System

2.1 Respiratory System

The primary function of the respiratory system is the exchange of oxygen and carbon dioxide between the inhaled air and the blood . During inspiration, air enters the upper airway and travels through the lower airways until it reaches the alveoli [9]. Each alveolus is surrounded by multiple capillaries. During systoles, de-oxygenated blood returning from the body's cells is pumped from the right ventricle through the arterial pulmonary circulation to the alveolar capillaries. Carbon dioxide diffuses from the capillary blood across the alveolar capillary membrane and enters the alveolar air. Simultaneously, oxygen from the inspired atmospheric air in the alveolus crosses the alveolar capillary membrane and enters the pulmonary capillary blood. Oxygenated capillary blood travels to the left side of the heart and is pumped from the ventricle into arterial circulation to the cells of the body, where cellular respiration occurs [9].

2.1.1 Lung Structure and Physiology

With reference to Figure 2.1, the upper airway consists of the nasal cavities and the pharynx. Air enters the body through the nose and passes through the nasal cavities. Hairs located in the nostrils filter out foreign particles. The lateral walls of the nasal cavities curve causing turbulent airflow. Seromucous glands secretes a mixture of watery and mucinous material over the passage lining to trap particles against it during airflow. The pharynx is divided into three sections: the nasopharynx, the oropharynx, and the hypopharynx. In children, the larynx and glottis (vocal apparatus of the larynx) are positioned higher in the nick creating a grater risk for aspiration [9].

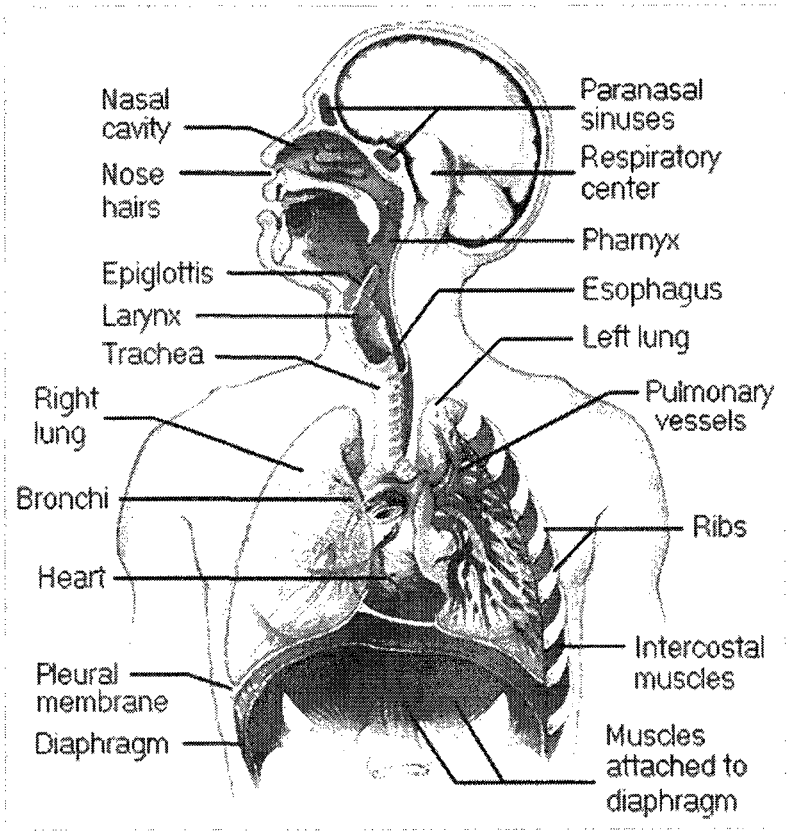

Figure 2.1: Respiratory System [10]

The lower airway, the tracheo-bronchial tree, begins at the level of the cartilage of the larynx and ends at the distal bronchioles that open into the alveoli. The larynx, which contains the epiglottis and vocal cords, has a role in ventilation and phonation and helps protect the lower airway from aspiration. The adult trachea is about 25 mm (1") in diameter and 100 mm (4") long to the division when it becomes bronchus. In children, the trachea is shorter with a more acute angle at the division of the right bronchus. The smaller diameter of the trachea results in increased airway resistance [11].

The trachea divides into a right and left main stem bronchus. The left main stem bronchus leaves the trachea at a sharper angle than the right main stem bronchus and passes under the aortic arch before entering the lung. The bronchi course downward and immediately divided into lobar

bronchi, which subdivide into segmental bronchi, Figure (2.2), shows the subdivision of the airway passages . The airways continue to systematically branch, narrow, shorten, and increase in number toward the lung edge. They divide about 25 times before ultimately opening into the terminal, or respiratory, bronchioles [11].

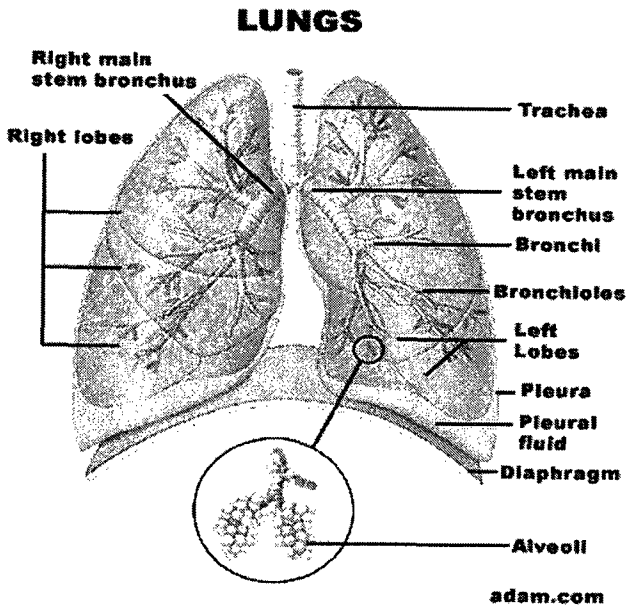

Figure 2.2: Lungs Physiology Showing Airways[12]

The terminal bronchioles, which have a few alveoli growing from their walls, branch into alveolar channels that are completely lined with alveoli. These airways and their alveoli form the respiratory lobules of the lungs. The distance from the terminal bronchiole to the most distal alveolus is only about 5mm; however, most of the lung surface area available for gas exchange is contained in these spaces. The airways between the nose and the terminal bronchioles are called the conducting airways. The large airways below the glottis contain cartilage, smooth muscle, elastic fibers, connective tissue, and mucous glands [9] [11]. With reference to Figure 2.3, each lung is divided into lobes. The right lung has three lobes; upper, middle, and lower. The left lung has only an upper and a lower lobe. The lung's apex is located near the clavicle, and its base is located near the diaphragm [9].

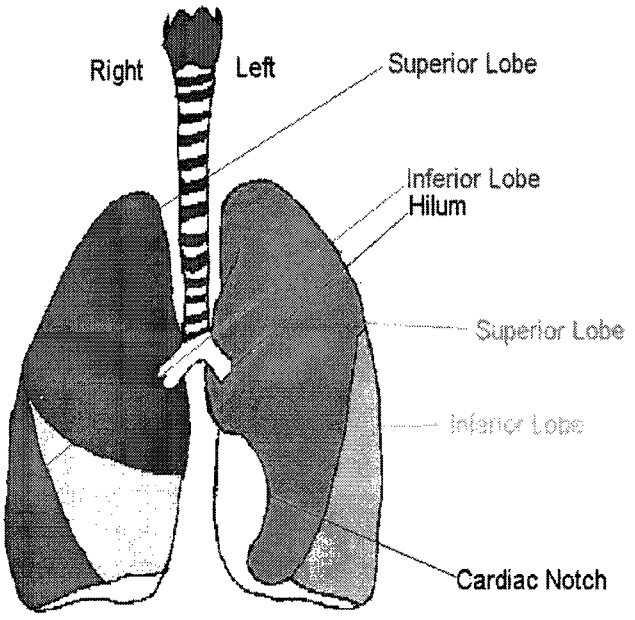

Figure 2.3: The Lungs Lobs [10]

2.2 Respiratory Sounds

2.2.1 Mechanics of Breathing

The respiratory muscles help the chest area to expand and contract. Pressure difference between atmospheric air and the lungs help produce air movement. The diaphragm is the primary muscle of respiration; it is composed of two dome-shaped hemi-diaphragms that are attached to the lower edge of the rib cage. The diaphragm forms the lower ground of the thorax. During inspiration, the diaphragm flattens and descends toward the abdomen. During expiration, it relaxes, and ascends to its resting dome shape configuration [9] [13]. Figure 2.4 shows the diaphragm in its relaxed position.

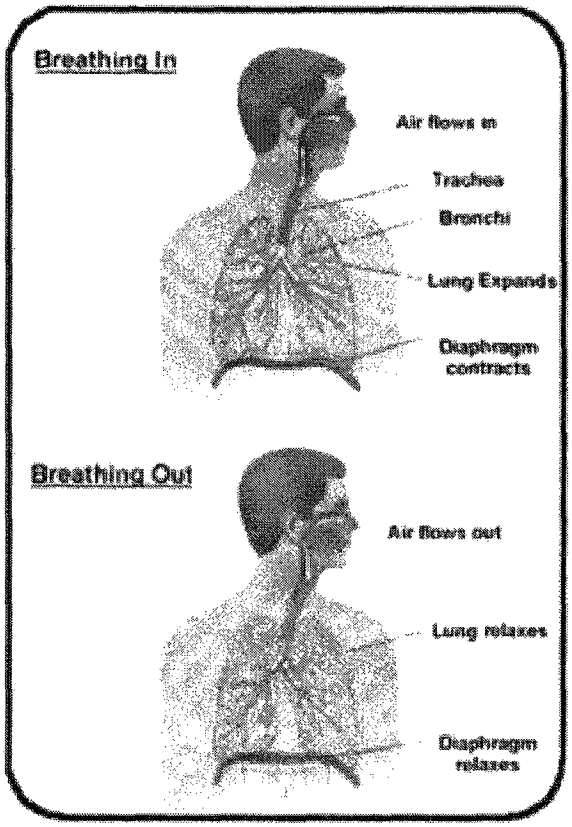

Figure 2.4: Diaphragm Function[14]

Normal Breathing

During inspiration, the diaphragm and external intercostal muscles (muscles between the ribs) are activated. Diaphragmatic contraction flattens the domed diaphragm and expands the lower rib cage, forcing the abdominal contents downward and out, thus increasing the longitudinal lung size. External intercostal muscle contraction stabilizes the rib cage and moves it outward and upward. As the thorax expands, it results in lung expansion and decreased pulmonary system pressures. Inspired air flows from higher atmospheric pressure into the airways. At the end of inspiration, diaphragmatic movement declines and the air inflow gradually slows. During expiration, the thorax and the elastic recoil force of the lungs return to their resting position, increasing the pulmonary system pressure. This increased pressure forces air to flow out of the lower and upper

airways. At the end of expiration, during quiet breathing, all muscles are relaxed and the diaphragm has return to its resting position. During normal breathing in the upright position, air movement (ventilation) is greatest in the lung bases or dependent lung regions. Because of the pull of gravity, the alveoli in the lung bases collapse to a smaller size during expiration than do the alveoli in the lung apices. During inspiration, the alveoli in the lung bases open more easily, causing ventilation in the bases to be greater than in the apices.

In older adults, airway closure and a loss of surface area results in decreased ventilation at the bases of the lung, this phenomena does not happen in the children. All the air movements and ventilation through different parts of the respiratory system produce a specific and recognizable breath sounds [9][15]. In general, the respiratory system pressure and alveolar elastic recoil pressures drive expiratory airflow. At the beginning of expiration, lung pressure cause the alveolar pressures to rise and push the air through the airways and out through the mouth. Air pressures fall as the air flows through the airways from the alveoli to the mouth. A point is reached, particularly during forceful expiration, when intrapleural and intrapulmonary pressures are equal; this normally occurs in the segmental bronchi and is called the equal pressure point. Downstream from this point, pressures outside of the airways can compress and further narrow the airways, causing increased resistance to airflow.

2.2.2 Breath Sounds Origination

The places where breath sounds originate are not obviously defined. For example, sounds heard over the trachea and large airways are characterized as loud and tubular with a long duration in the expiration phase. Sounds heard over other chest wall areas are softer and have a shorter duration in the expiration phase. These sounds may also be created by turbulent airflow in the first few divisions of the large airways; however, the fact that these sounds vary with changing airflow rates and distribution of ventilation in the lungs suggests that they are produced in very narrow airways. Also, inspiration sounds may be created in the narrow airways, and sounds in the expiration phase may be created in the larger airways. Breath sounds are not produced in the terminal

bronchioles because of minimal airflow rate. Any cause of alteration of the airflow dynamics, such as diseases, may create abnormal breath sounds or adventitious sounds. These sounds are generated by the vibration of solid structures, by airflow through narrowed airways, or by sudden changes in airway pressure.

The interaction among the elastic properties, the intrapulmonary airways, and the pressures will impose an influence on the shape and size of the lungs during inspiration and expiration. During the respiratory cycle, and as the chest expands during inspiration, intra-pleural pressure falls; at the same time, the lung's elastic recoil increases, exerting traction on airway walls. This traction increases the airway's diameter and decreases the resistance to airflow. The pressure gradient between the alveolar and atmospheric pressures increases, driving air through the airways toward the alveoli.

In older persons, pulmonary function decreases due to many factors, primary among there are; ventilation capacity diminishes because of a decline in the lung's diffusion , decrease in lung's vital capacity due to a decrease in inspiration and expiration muscle, strength, decrease in the lung's elastic recoil capacity which results in an elevated residual volume caused by lung tissue degeneration.

Variations in airflow patterns are affected by the intricate network of branching airways, the various airway diameters, and the potential for irregular airway wall surfaces within the tracheobronchial tree. During rapid, or turbulent airflow, air molecules and suspended particles move randomly, colliding against airway walls and each other. They may move across or against the general direction of airflow. The colliding molecules produce rapid pressure changes within the airway, and these rapid pressure changes produce sounds. Turbulent airflow occurs in the trachea, main stem bronchi, and other larger airways.

As airflow is forced to change directions abruptly in the branching airways, the airstreams separates into layers and moves at different velocities. The shearing force of high-velocity airstreams,

along with slower airstreams, precipitates opposing circular airflow, or vortices. This airflow pattern generates sounds as the flow of air carries the vortices downstream. In the terminal or small airways and respiratory bronchioles, airflow is slow and laminar, or non-turbulent. No abrupt changes in pressure or airway wall movements occur to generate sound. Consequently, air movement in these areas produces no sound.

Breath sounds are also produced by mechanical vibrations of solid tissue. These vibrations travel through the different media of air, fluid, or tissue at varying speeds. Different frequencies produce the different pitch sounds heard during auscultation. The Intensity of the breath sounds is affected by the type of vibrating structure producing the sound, the distance the sound travels, and the transmission pathway. The duration of the vibrations that produce breath sounds can be measured, however, in general the human ear perceives sounds during auscultation as long or short and as continuous or discontinuous. The airflow has a direct impact on the amplitude and the frequency contents of the respiratory acoustic signals [16].

2.2.3 Breath Sounds Transmission

Breath sounds are usually influenced by the environment when they're transmitted through air, fluid, and tissue. However, when these sounds are transmitted sequentially through media with different acoustic properties, the sounds' vibrations are filtered and reflected at the interface of the different media. The amount of filtration that takes place depends on the nature of resistance of the media to sound transmission, i.e. its impedance. When the media impedance match, breath sound transmission is better, and when the impedance mismatch breath sound attenuation occur. For example, consolidated areas improve the transmission of breath sounds to the chest wall, because the fluid produced by some diseases will fill airless lung tissue and the chest wall is acoustically a good media for sound transmission, therefore the breath sounds are transmitted more easily. Some other disease and even obesity may increase the impedance mismatch, this result in diminish of breath sounds [17][18].

2.2.4 Quantifying of the Respiratory Sounds.

Acoustical signals acquired through different channels present different energy quantity and patterns. This is due to the fact that the variations in airflow patterns are affected by the intricate network of branching airways, the various airway diameters, and the potential for irregular airway wall surfaces within the tracheobronchial tree. During rapid, or turbulent airflow, air molecules and suspended particles move randomly, colliding against airway walls and each other. They may move across or against the general direction of airflow. The colliding molecules produce rapid pressure changes within the airway, and these rapid pressure changes produce sounds. Breath sounds are also produced by mechanical vibrations of solid tissue. These vibrations travel through the different media of air, fluid, or tissue at varying speeds. Different frequencies produce the different pitch sounds heard during auscultation. The intensity of the breath sounds is affected by the type of vibrating structure producing the sound, the distance the sound travels, and the transmission pathway. The duration of the vibrations that produce breath sounds can be measured, however, in general the human ear perceives sounds during auscultation as long or short and as continuous or discontinuous. The airflow has a direct impact on the amplitude and the frequency contents of the respiratory acoustic signals.

Measuring the intensity of the respiratory sound signals provide definite quantities which describe and rate sounds. Sound measurements permit precise and objective means for comparison of the diversity of signals acquired through deferent auscultation channels. In fact, the measurement and analysis of sound is a powerful tool that would help us in the process of diagnostic and distinguish the source of the sounds. The pressure variations on the eardrum perceive by human ear as sound are the same pressure variations which are detected on the diaphragm of a condenser microphone. Any piece of machinery that vibrates radiates acoustical energy. Sound power is the rate at which energy is radiated (energy per unit time). A sound source radiates power and these results in a sound pressure. The lung sound power is the cause and the lung sound pressure to quantify is the effect. The sound pressure that acquired by the electronic stethoscope and measured after is dependent on the distance from the source and the acoustic environment (or sound field) in which

the lung sound waves are present. This in turn depends on the size of the lungs and the health condition of the patient.

The intensity of the respirator sound signals will be measured and quantified. All the acoustic quantity will be presented in Sound Pressure Level (SPL) terms. It is a relative quantity in that it is the ratio between the actual sound pressure (pressure caused by the sound wave), and a fixed reference pressure. The commonly used reference sound pressure is the threshold of hearing. The most common approach to sound measurement is to use the decibel scale (dB).

$$SPL = 10\log(p / p_{ref})^2 = 20\log(p / p_{ref}) \quad \textbf{(1)}$$

The pressure P here is to be understood as the amplitude of the pressure wave. The power carried by a traveling wave is proportional to the square of the amplitude. The factor of 20 comes from the fact that the logarithm of the square of a quantity is equal to 2 times the logarithm of the quantity. Sound intensity is the time-averaged product of the pressure and particle velocity or the sound power per unit area . Therefore, the threshold of the hearing can be sated in term of the sound intensity:

$$I_0 = 10^{-12}\ watts / m^2 = 10^{-16}\ watts / cm^2 \quad \textbf{(2)}$$

This value has wide acceptance as a nominal standard threshold and corresponds to 0 decibels. It represents a pressure change of less than one billionth of standard atmospheric pressure. This is indicative of the incredible sensitivity of human hearing.

2.3 Auscultation of the Respiratory System

Breath sounds have a wide range of frequencies, many near the lower threshold of human hearing. Consequently, the environment for auscultation should be as quiet as possible so that breath sounds can be heard clearly and distinctly. During auscultation, the stethoscope should be pressed firmly against the patient's chest wall. The breath sounds should be acquired though bare skin, to eliminate the external effect of clothing.

2.3.1 Locations of the Auscultation

Accurate interpretation of breath sounds depends on a systematic approach to auscultation; it also requires the ability to describe the location of abnormal finding in relation to bony structures and anatomic landmark lines. Breath sounds are auscultated over the anterior chest wall surface, the lateral chest wall surfaces, and posterior chest wall surface. For the anterior chest wall surface, the ribs and intercostal spaces provide precise landmarks to describe the location of breath sounds; the second rib and second intercostal on each side space serve as reference points [15]. Figure 2.5 A and B shows the auscultation area of the anterior chest wall surface, where the RUL, LUL, RLL, LLL and RML are respectively the right upper lobe, left upper lobe, right lower lobe, left lower lobe, and right middle lobe.

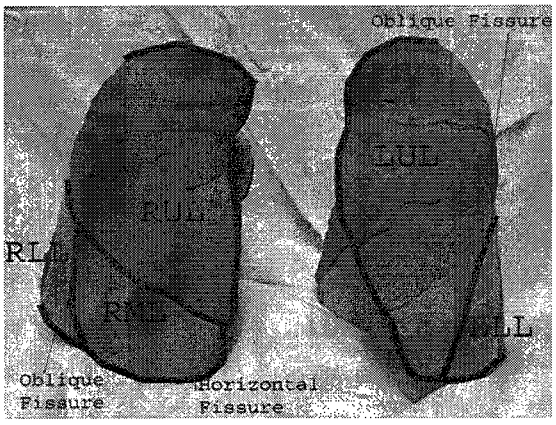

Figure 2.5 A : Auscultation area of the anterior chest wall surface

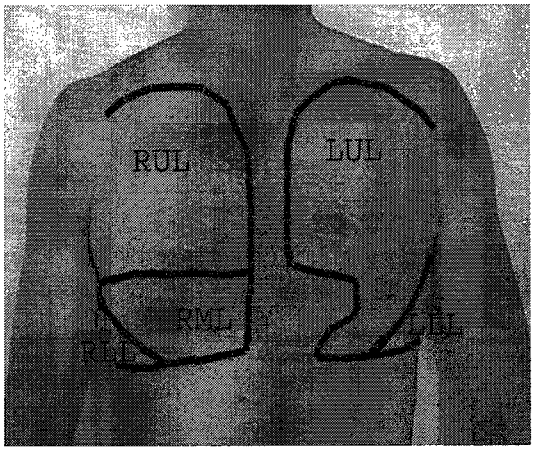

Figure 2.5 B : Auscultation area of the anterior chest wall surface

The posterior chest wall surface, and its underlying structure provide landmarks to locate breath sounds. The scapulae's inferior borders, located at about the same level as the seventh ribs, serve as reference points. With reference to Figure 2.6 B, the right and left lower lobes cover most of the area of the posterior chest wall. Therefore, When making an auscultation on the posterior chest wall, one would mostly hear the lower lobes due to the anatomical position of the lobes [9][15]. Figures 2.6 A and B show the auscultation area of the posterior chest wall surface.

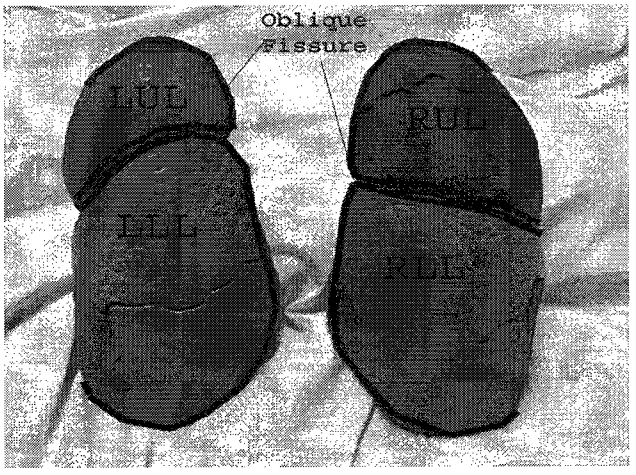

Figure 2.6 A : Auscultation area of the Posterior chest wall surface

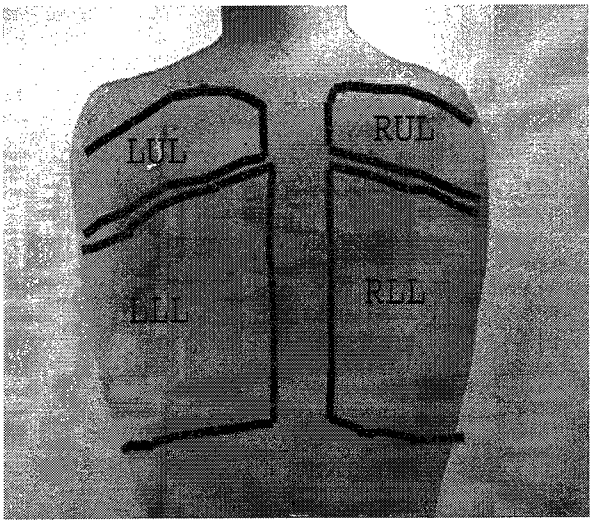

Figure 2.6 B : Auscultation area of the Posterior chest wall surface

Each lung lobe is further subdivided into smaller segments. These segments are attached to each other. They are named according to the segmental bronchus that supplies them. A lung segment is therefore an area of lung tissue that is supplied by that segmental bronchus. With reference to the figure; the lobe's segments and sub-segments are identified as follows [85]: the upper lobes are subdivides into; 1-apical, 2-posterior and 3-interior segments. The right middle lobe is subdivided into; 4-lateral and 5-medial. The left angular lobes include; 4-superior and 5-inferior. The lower lobes are subdivides into; 6-apical, 7-interior basal, 8-lateral basal, 9-posterior basal, and 10-subapical segment. Knowledge of the position of the lung segments is useful and important during the auscultation and diagnosis of the lung diseases. Usually the medical doctors give the location of the infection a segmental position reference.

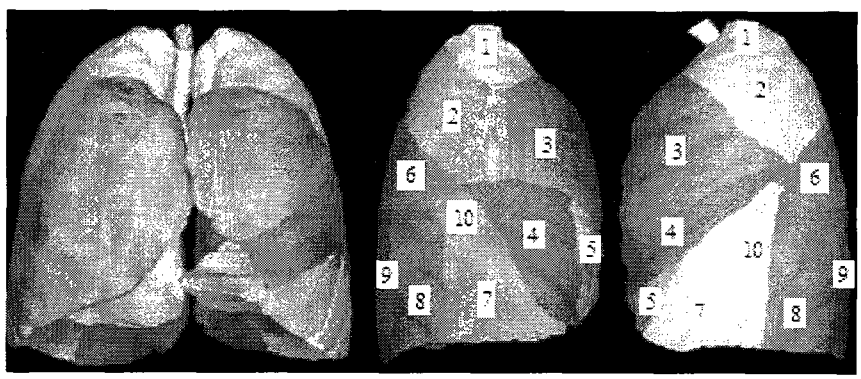

Figure 2.7: Segments of the Lungs [85]

With reference to the next figure, the position of the lung segments in respect with the chest ribs is essential during the auscultation process in order to locate the source of infection.

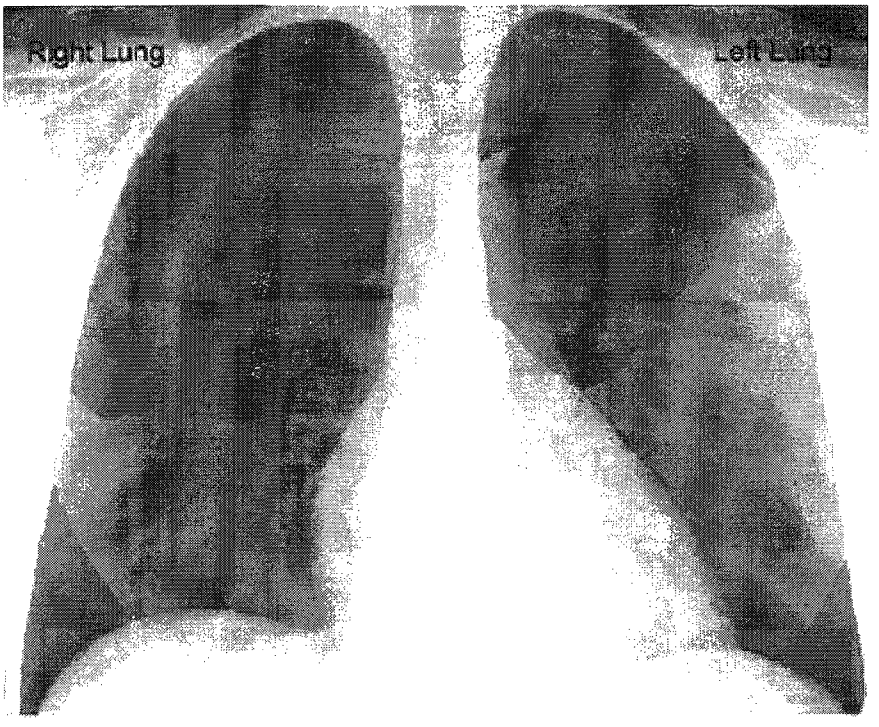

Figure 2.8: Positions of the Lung's Segments in Respect with the Chest's Ribs [86]

The lung lobes are not harmonically positioned across the chest but they overlap each other. For example, LLL, and LUL overlap each other on the anterior and posterior side. The LUL is dominant in the anterior view, while the LLL is dominant in the posterior view. With reference to Figure 2.9, the relative sizes of the lobes and their segments are uneven and shaped like a triangle from the side view. Hence, when calculating the propagating pathways, the distance is proportionate with the different allotment of the lung segments.

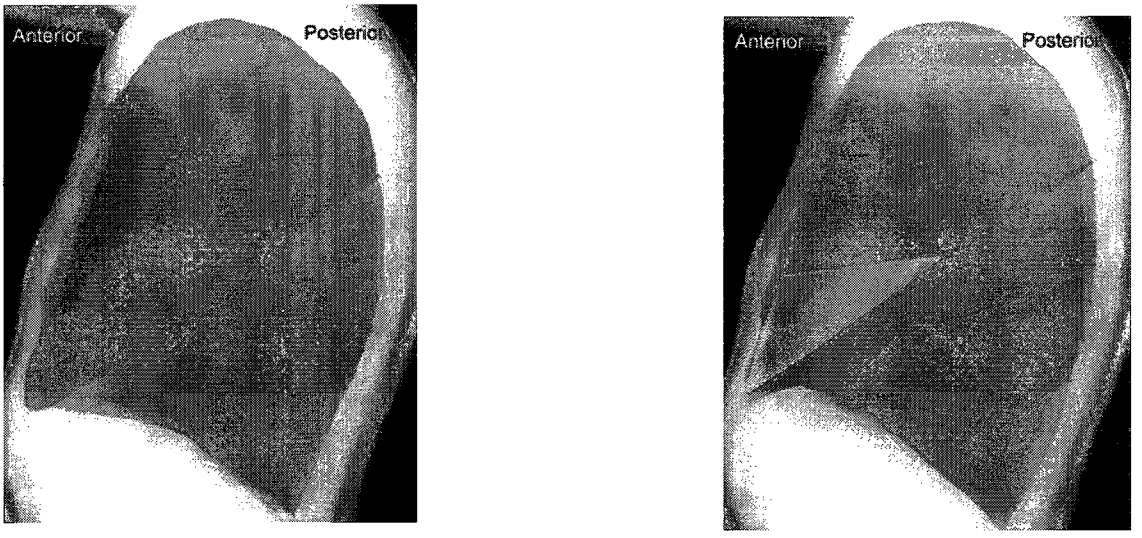

Figure 2.9: Width of the Upper and Lower Lobes of the Lungs [86]

2.3.2 Techniques of Auscultation

There are many different auscultation techniques and methods that has been practiced during the course of the history of medicine.

2.3.2.1 Traditional Stethoscopes

A traditional stethoscope conveys sound from the chest piece, via air filled hollow tubes, to be listened to by an attending medical professional. The chest piece is designed, in general, to have two sides with different sound pick up characteristic for auscultation of the chest or abdomen; a diaphragm side and bell side. When the bell is used on the patient, the vibrations of the skin directly produce acoustic pressure waves that travel to the physician ear canal directly through the stethoscope tubes [19].

The diaphragm is used to listen to high-pitched breath sounds, while the bell is used to listen to low-pitched breath sounds. Applying the stethoscope firmly to the chest wall amplifies high-frequency sounds. However, if too much pressure is applied when using the bell, the stretched skin function as a diaphragm and filters out low-pitched sounds. The earpieces at the end of the tubes should fit tightly into the ears in an anterior direction so that they conform to the direction of the ear canals [19].

2.3.2.2 Electronic Medical Sensors and Electronic Stethoscope

Electronic stethoscopes perform a conversion of acoustic signals into electrical signals that can then be filtered, amplified and processed for the best possible quality of the sound signals. Different types of sound pick up transducers in a variety of configuration are used. The simplest method of sound detection is achieved by placing a microphone in the chest piece. Another employs a piezoelectric crystal attached to one end of a metal shaft while the other end of the shaft contacts a diaphragm. Sound pressure waves cause the piezoelectric material to generate proportional voltage [19].

2.4 Classification and Characteristics of Breath Sounds

Generally speaking, breath sounds can be classified as normal and abnormal (adventitious); discussion of these follow.

2.4.1 Normal Breath Sounds

Breath sounds can be classified as tracheal and main stem bronchi sounds or as lung sounds heard over chest wall areas. The tracheal and main stem bronchi sounds are produced by turbulent airflow in the airways, they are loud and can be heard throughout inspiration and expiration. Lung sounds are heard over other chest wall areas, they are week and can be heard throughout inspiration and at the beginning of expiration. Breath sounds are affected by three variables; the distance

between the source of the sound and the chest wall, the path of sound transmission, and the sound's location. Normal breath sounds are shaped by airways acoustical characteristics and by solid tissue vibrations. Breath sounds heard over large airways are produced by turbulent airflow in those airways. The breath sounds heard over most of the chest wall surface are soft and low pitched; they are softer and of shorter duration during expiration than during inspiration. The sound frequency distribution of these normal breath sounds is in the range between 100 to 600 Hz. Tracheal breath sounds are described as harsh and high pitched and can be heard over the trachea. The sound frequency distribution of these breath sounds is 200 to 2,000 Hz [20][37]. Breath sounds have definite identifiable characteristics. Their amplitude and intensity are believed to be affected by airflow patterns, regional lung volume or distribution of air, body position, and the sound production site.

The sounds are normally diminished and filtered when they are transmitted through air-filled alveoli, fluid accumulations in the pleura, and solid structures, such as bone. In general during auscultation, ambient sounds are presented and overlap the auscultated sound. G.R Pasterkamp et al studied the effect of ambient sounds on auscultation. Their research showed the general impact of the noise on the analysis of acoustical respiratory signals [21].

2.4.2 Adventitious Breath Sounds

In cases of a lung inflammation such as pneumonia, fluid accumulates in spaces that are normally filled by air producing a consolidated spot or spots in the lungs. These consolidations cause a change in the airways and airflow pattern and consequently produces adventitious sounds. For example, when consolidation is present in an upper lung lobe, wheezing and loud tracheal breath sounds may be heard over that lobe, whereas in the absence of these consolidations these sounds would not be heard at that location. This is because in this condition the upper lobe surfaces are in direct contact with the trachea and these sounds are transmitted directly to the dense, airless upper lobe tissues [22-24].

Adventitious sounds are classified qualitatively based on their acoustic qualities or their similarities to musical tones. A more scientific classification is based on acoustical qualities, timing, and frequency of the waveforms. Accordingly, the adventitious sounds being classified as wheezes, crackles, rhonchi, and grunts[22-24]. Each class of the adventitious lung sounds is further sub-classified. For example, the discontinuous crackle sounds that are loud and low in frequency (low pitched) are mainly referenced as coarse crackles. While a discontinuous sounds that is shorter in duration, with higher frequency (higher in pitch), softer and less loud than coarse crackles are usually called fine crackles.

Crackles are discontinuous, nonmusical, brief sounds heard more commonly on inspiration with a major contribution frequency from 200 Hz to 1200 Hz. They can be classified as fine or coarse based on their characteristics such as loudness, pitch, and duration in the respiratory cycle [25].These characteristics change, depending on the underlying cause like fluid movement in the lung or lung structures that lead up to changes in the airways. Crackles are heard primarily through the chest wall with a stethoscope, but they may also be heard at the mouth with or without a stethoscope [22-24].

Wheezes, are high-pitched continuous sounds with a major contribution frequencies from 600 Hz to 2000 Hz and a duration of 250 msec or more. Their duration is long enough to carry an audible pitch similar to a musical tone. Wheezes are described by their timing within the respiratory cycle; they may be heard during inspiration or expiration or continuously throughout the respiratory cycles. The differences in wheeze's frequency are attributed to the airway size and elasticity and to airflow rates through the narrowed bronchus. Soft, narrowed airways generate low frequency wheeze sound signals, while stiff and narrowed airways generate high frequency wheeze sound signals. Wheezes of different frequencies may occur simultaneously or may overlap, and the frequency of a single wheeze may change during inspiration and expiration [9-11].

Rhonchus is used to describe a rough, rumbling low-pitched sound that is heard primarily on expiration, although, at times, rhonchi may also be heard with inspiration. Rhonchi are generally caused by fluid or secretions partially blocking the large airways and typically undergo change in sound, or disappear with coughing [11].

Grunts is a sound that occurs primarily in neonates when the infant exhales air against a partially closed epiglottis. It is a natural function which generates back pressure to keep smaller airways open. In general, it occurs because of underdeveloped accessory muscles, and is observed for infants with respiratory distress, or infections. Grunts are considered a sign that a child is having trouble breathing [11].

2.5 Literature review of the Automated System for the Auscultation of Respiratory Sound Signals

Conventional auscultation using traditional stethoscopes have limitations that may affect the accuracy of the diagnosis. As has been discussed above, the descriptors of lung sounds are non-precise and subjective in nature, and the sounds vary noticeably from one person to another. In addition, the diagnosing procedure depends heavily on the hearing ability and the experience of the medical professional carrying it. Moreover, the presence of the noise will add difficulties for making an accurate medical analysis and diagnose.

Electronic auscultation systems offer the possibility of targeted filtering of noise (like heart beat and ambient noise cancellation) and targeted enhancement of relevant waveforms. Furthermore, recent advances in the fields of signal processing and artificial neural networks provide an opportunity to develop an automated auscultation system that can assist in different aspects of medical diagnosis and training.

2.5.1 Computerized Analysis, classification and identification of Respiratory Acoustical Signals

Huseyin Polat and Inan Guler [26] developed a computerized system for the acquisition and analysis of the acoustic lung signals. This system includes a portable computer, electronic hardware and software. The system can record and play back the lung sounds and analyze them in the time and frequency domains. This system uses an electret microphone for the acquisition of the lung sounds. The microphone output is amplified and digitized with a sampling frequency of 8000 Hz at 16-bit resolution. A graphical user interface (GUI) for the end user interaction was developed and the software part of the system provides the users with the ability to visually analyze the lung sounds in order to get the spectral analysis of the signals. The software can perform a real time monitoring and offline analysis of the lung signals.

F. Schuttler, T. Penzel, and P. Von Wiichert [27] developed a system for digitally acquiring and studying of the respiratory sound signals. This system includes a three channels hard disk recording instrument with high sampling rates. The lung sounds are recorded using two air-coupled condenser microphones and then the sound signals are digitized using an analog-to-digital converter. One of the microphones is taped on the infected spot and the other one is placed on the opposite spot. After that, the system will be set to start acquiring the lung acoustic signals, then the signals are amplified, and then band-pass filtered (75-2000) for clearer lung sounds. At the same time the airflow is also recorded using a mouthpiece and a flow sensor. The system is able to record three channels simultaneously, two lung sounds and the airflow, with a sampling rate of 11025 Hz at 12-bit resolution. All the recorded lung sounds and airflow are consecutively analyzed and the lung sound signals are visually presented in the frequency domain.

H. A. Mansy, T.J. Royston, R.A. Balk and R.H. Sandier [28] produced a system that measure the influence of Pneumothorax (PTX) on a lung sounds. This work in the development of a method that can pattern the lung sound in order to diagnose the PTX. PTX causes the lung to collapse, hence the lung sound will be altered due to the air or gas accumulated in the pleural cavity caused by the disease [29]. The outcome of this research has concluded that Pneumothorax causes a decline in

sound amplitude, a decline in high-frequency acoustic components and a reduction in sound amplitude variation during the respiration cycle. Such characteristic changes are useful in diagnosing the PTX.

Alsmadi, S.S. and Kahya, Y.P., [30] developed a system for online lung sounds identification. The hardware of this system consists of a Motorola's 56311 digital signal processor and electrete microphones. The main purpose of this system is to perform a real time preliminary classification of the acoustical lung signals. This work provides a general approach that can only identify two classes of signals: healthy or pathological. The system uses two inputs that work collectively and bring the signals simultaneously into the system. The first input is a microphone placed on the chest of the patient in order to acquire the acoustic signals of the respiratory system. The second input is a flow meter that is utilized to mark the inspiration phase or expiration phase of the breath cycle. The recorded lung sounds of the full breath cycle are separated into 6 phases. "Each phase is divided further into 10 overlapping segments. Each segment is modeled by an auto regressive (AR) model of order 6 by means of the Levinson-Durbin algorithm. The classification process is done using two classifiers: k-nearest neighbor (k-NN) classifier with Itakura and Euclidean distance measures, and minimum distance classifier with the Mahalanobis distance measure. The software was written entirely in assembly language and the result of the classification process is displayed on a character display (LCD)" [30].

Yasemin Kahyq Ugur and Cini Cerid. [31] developed a respiratory sounds diagnosis instrument. In this research a 4-channels electronic stethoscope was constructed to acquire and process the lung sounds in real time. This instrument can classify the lung sounds only as a normal or pathological. The classification is performed by processing the acoustic respiratory signals obtained from 4 different locations on the posterior part of the patient's chest. The condition of the lung sounds is assessed based on the FFT of the recorded pulmonary signals. The diagnosis produced by making a comparison between the frequency parameters of the healthy and the pathological lung sound signals. A user interface was developed to make it easier and more efficient for the end user to operate the system. The hardware components of this system consisted of; four electret

microphones, fleisch-type pneumotachograph for measuring the airflow, amplifier card, filter card, analog-to-digital converter, Motorola digital signal processor, and a PC. The percentage of the frequency points of the total area under the power spectrum density curve is calculated and presented as the percentile frequencies. A threshold percentile frequency value is set to distinguish a healthy recording from a pathological one.

Yasemin P. Kahya, and Cagatay E. Guler [32] developed a system to identify anomalous lung sounds. The system compares sound features of an acquired lung sound with those from a static historical database of features of anomalous lung sounds for the identification process. Each lung sound is divided into two phases based on their occurrence during the breath cycle; inspiration phase and expiration phase. Each of these phases are then sub divided into early, middle and late expiration/inspiration phases. Each of these are further split into 11 segments with up to a 25% overlapping ratio between adjacent segments. In order to measure and specify the feature vectors of the segments that can represent the respiratory sound signals, different order autoregression filters are used. Crackle parameters are added into the feature vectors of the lung sound segments of the database to improve classification. These parameter are extracted separately from the three phases of the expiration and inspiration, and are separated into raising and falling patterns.

Zahra Moussavi, Mary Leopando, Hans Pasterkamp, and Gina Rempel [33] developed an automated method for breath cycle phase detection without the need for the measurement of airflow. The developed system provides users with a spectral portrait of the lung sound so as to monitor the different characteristics of the respiratory signals. The system operates on recorded acoustical respiratory signals whereby the signals are segmented evenly with 50% overlap between the consecutive segments. Each segment has a duration of 100 ms and the power spectrum of each segment is calculated. The chest sounds and tracheal sounds average power are calculated over the frequency range from 150 to 300 Hz and 150 to 600 Hz respectively. The average chest power spectra are used by the phase detection algorithm for respiratory phase detection, while the tracheal power spectra are used to determine the onset of breathing cycle. To evaluate the general performance of the phase detection of the respiratory acoustical signals performed by this system,

the percentage of the correctly detected respiratory phase and the percentage of the correctly detected onset points were calculated. The system was developed to work in two modes: semi-automated mode, and fully automated mode. When working in semi-automated mode, the system can detect the inspiration peak with 100% accuracy, but the percentage of the accuracy detection is 93% when the system works in the fully automated mode.

M. Yeginer, K. Ciftci, U. Cini, I. Sen, G. Kilinc, and Y. P. Kahya [34] developed a system to identify and classify the pulmonary diseases using respiratory sub-phases classification. Similar to the approach adopted in [32], the two respiration phases, inspiration and expiration, are divided into early, middle and late inspiration and expiration sub-phases. This work proposes that such a respiration phases division can help make a diagnosis. However the diagnosing process is limited only to identify the subject as either healthy or pathological. A neural classifier is used to achieve the classification of the sub-phases of the respiratory sound signals. Figure 2.10 shows the segmentation of the inspiration and expiration cycle phases utilized in this research.

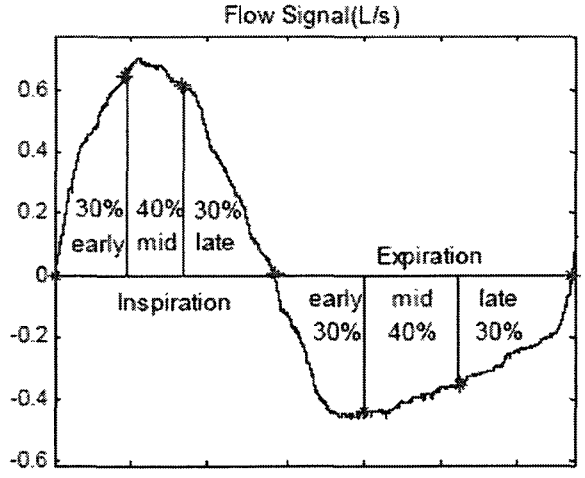

Figure 2.10: A respiratory sound cycle consists of inspiratory and expiratory phases

The division of the respiratory cycle sub-phases facilitates modeling the signals using autoregrassion (AR) analysis. A neural network (NN) classifier is used for the diagnosis. The NN classifier uses a variety of features including the AR parameters, prediction error, and ratio of expiration/inspiration durations to distinguish between normal and pathological diagnosis. Radiological and traditional medical auscultation were performed on the subjects to confirm the NN findings. The system was used on subjects with different respirator ailments including asthma, COPD, bronchiectasis, pneumonia, however the system outcome was either healthy or not healthy. The authors report the accuracy of the diagnosing based on the number of segments that were accurately classified for all the patients. The result of this classification, except for the late inspiration phase, was about 70% accuracy. The diagnosis was more accurate when dealing with the mid-inspiration and mid-expiration phases.

N. Gavriely et al [103], have explored in their research whether the addition of lung sound analysis, in coordination with spirometry provides a more efficient and sensitive tool for pulmonary illness screening. Spirometry and phonopneumography (PPG) are, respectively, proven and effective methods for testing pulmonary function and analyzing lung sound. To test the author's suggested screening process; patients were given a pulmonary function test (PFT), asked to fill out a questionnaire, and then subjected to PPG. PFT results were evaluated in real time, questionnaires evaluated by an online algorithm, and PPG results were tabulated by an offline system, as well as subjectively diagnosed by experienced listeners. This research was conducted by involving mostly blue-collar workers, ages 21-77, smokers and nonsmokers. Also, care was taken to adhere to standards set forth by the American Thoracic Society. From the screening, it was determined that 21% of the patients had pulmonary problems. Only two thirds of these patients' illnesses were indicated by the PFT results. The other third of these patients' illnesses were indicated by PPG results, despite the patients having tested negative for pulmonary problems in the PFT screening. The spirometry setup involved a differential-pressure-transducer connected to a pneumotachograph. Analog-to-digital convertersion is done at 100 Hz. It was calibrated daily, using a 3 L syringe. The acoustic setup used the pneumotachograph as a trigger for data acquisition. Four piezoelectric sensors were placed on the trachea, right chest, and each lung base. Acoustic signals were amplified,

bandpass filtered for 75-2000 Hz, and digitized at 4 kHz. Readings were taken for six to fifteen inhale/exhale cycles, and the signals were averaged and displayed as a log power versus frequency plot. The data was stored, and magnetic tapes were made for experienced listeners, as a control. Slope, intercept, and regression coefficients were tabulated for log amplitude vs. log frequency graphs and compared to previously established "normal" plots. The regression coefficient of the best-fit line, and the ratio between the total power in an actual spectrum and the power under the regression line were tabulated. If both values were above 0.75 or their sum was above 1.7, the PPG was considered normal. If not, it was considered abnormal. The PPG was determined to be a useful add-on for pulmonary illness screening. However, it needs to be limited to an add-on until improvements are made. The high percentage of false positives could be decreased. Also, the PPG measures wheezes, but cannot measure crackles or any other type of sound that has been proven important in diagnosing pulmonary disorders.

T. Orihasi et al [104], established a method of objectively diagnosing lung sounds because there is no current standard. They focused their interest only on crackle. The typical classifications of crackle; coarse crackles and fine crackles were the targets. These crackles have been identified through time expanded waveform analysis based upon their initial deflection width and the two-cycle duration. These characteristics were difficult for computers to identify. Due to the identification difficulty, the authors built a CAD (computer-aided diagnosis) system for classifying lung sounds into coarse crackles, fine crackles, or normal breaths. Effectively, coarse crackles are high amplitude, low frequency, and long in duration, while fine crackles are low amplitude, high frequency, and short in duration. Based upon these characteristic differences, representative histograms are produced for coarse crackles, fine crackles, or normal breath. These are built using average values from known digitized examples collected from a database of these sounds. Input signals are then discriminated into the three types of sounds, based upon their statistical distance from each of the average histograms. In order to identify the crackle and its position in the time segment, the sounds are digitized and the program uses statistics of the waveform intervals around the crackle. To test this CAD system, examples of known sound type were input into the program, and comparisons were made between output and expected value. Overall, the CAD system correctly predicted the coarse

crackle 94% of the time, and the fine crackle and normal breath 86% of the time. Also importantly, there were very few false negatives. The incorrect fine crackles were often mistaken for coarse crackles and would be flagged either way. As a result, the authors decided that their CAD system had obtained good performance and there would be more studies to come. The authors plan to improve performance.

L. Bentur et al [105], had studied and assessed the response to the asthma therapy during night. In their work, the author describe how it is difficult to obtain direct measurements of airflow obstruction during sleep as it would require significant instrumentation and is not practical for longer, clinical tests. Preliminary tests showed a large increase in the airflow obstruction during sleep. The authors concluded that a simpler, less invasive quantitative method to assess NA is needed. The hypothesis tested by the authors was that quantification of wheezes would provide information on nocturnal asthma activity and severity. A new wheeze-detecting device called the PulmoTrack was used to automatically monitor asthmatic and healthy patients. The Pulmo Track is a specially designed set of sensors for detecting wheeze sound signals of the lungs. The test was designed to view the effects of montelukast (singulair) before and during treatment in a noninvasive manner. Patients were given 5mg of montelukast each night and were attached to the wheeze-detecting device. This testing along with spirometry were conducted again 2 days later and again 6 weeks later to observe the early and delayed effects of the medication. The respiratory acoustic signals were recorded with the use of five piezoelectric contact sensors with built-in passive ambient noise rejection. The system also rejects speech, crying and vocal cord sounds. Wheezing was measured and quantified in real time as a percent of wheezing time to breathing time, called the wheeze rate and plotted on a Wheezogram. Characteristics such as amplitude, frequency, duration and chest distribution were measured and recorded. Lung sounds were recorded every 30s throughout the night and a Nocturnal Wheeze Index was calculated. The study showed that computerized nocturnal wheeze monitoring is an efficient noninvasive way of assessing asthma activity and data correlates well with traditional data from spirometry indices and bronchial reactivity, and symptom scores. A main finding was that most patients were unaware of nocturnal symptoms and that all patients tested had some form of persistent nocturnal asthma. Since healthy patients do not wheeze

during sleep, the presence of wheezes is therefore a symptom of the disease. 75% of patients had a significant drop in nocturnal wheezing with the continued use of montelukast. The study showed, as well, the effectiveness of nocturnal wheeze monitoring in assessing asthma severity and response to treatment, in a quantitative and noninvasive manner. This type of testing is ideal for young children, infants, and elderly patients who cannot perform spirometry. The results correlated well with conventional indices of asthma activity, and more importantly can be used to assess efficiency of treatment.

S. Tejman-Yarden et al [106], studied the acoustic performance of the lung sounds to detect One-Lung Intubation (OLI). It occurs due to an improperly placed endotracheal (ET) tube, often due to migration. Only one lung is ventilated leading to insufficient ventilation and can cause complications such as collapsed lung, hypoxemia, and hypotension. It is difficult to predict the position of the tube. A preliminary test was done analyzing gas passing through a narrow gap between the ET tube and bronchial wall generating sound signals. A multi input multi output (MIMO) system was developed with an auto-regressive model relating the lung inputs and recorded sound outputs, and a classifier that indicates the number of ventilated lungs. This paper introduced a new acoustic monitoring system for detecting OLI and was tested on patients scheduled for routine surgical procedures. The system has four sensors with piezoelectric microphones and record breath sounds from the back during anesthesia. To achieve OLI, the ET tube was inserted all the way down until no breath sounds were heard on the left side. The tube was then withdrawn stepwise until distinct breath sounds could be heard with a stethoscope. Fiberoptic bronchoscopy was then used to verify the correct position of the ET tube. Lung sound samples were collected in real time for analysis. The algorithm contains four eigenvalues that represent the sound sources of the right lung, left lung, echoes, and ambient noise. For OLI to be detected, the sound source must be below a specific threshold, which is set based on a distribution curve of bilateral ventilation values from sound signals of patients. The study was done on a small scale and many additional tests still need to be done, requiring further validation in order to broaden the application of these results. In this study, data obtained during ET tube placement indicates that this method can discriminate one-lung ventilation from bilateral ventilation with high reliability. The algorithm achieved an OLI detection

probability of 95.2%, significantly higher than other present methods but a 4.8% incidence of false positives.

A. Yadollahi and et al [107], had developed an integrated remote assessment tool for swallowing and respiratory sounds. Therefore, their work was focused on speech signal compression techniques. Sounds with a bandwidth of over 5kHz were required to be transferred online, therefore, data compression was desirable for fast and reliable online data transfer. Within this study, a compression method founded on DCT (discrete cosine transform) coding was researched for swallowing and respiratory sound signals. In addition, the study of bit allocation to different transform coefficients was conducted to find optimum transfer coding applications. Generally, swallowing sounds are considered non-stationary signals, while respiratory sounds are considered wide-sense stationary signals. Thus, a new adaptive bit allocation technique was researched, in this study, that utilized the difference between the properties of the DCT coefficients of the stationary and non-stationary components of the swallowing and respiratory sound signal. Within this study, 12 healthy children provided 14 recordings of swallowing and respiratory sounds. Each child swallowed 180 ml of juice (thin liquid) and diluted pudding (thick liquid) in single boluses of 5ml each. A Siemens accelerometer was placed over a suprasternal notch in order to record sound signals. The sound signals of the swallowing and respiratory functions were amplified, bandpass filtered between a frequency range of 30-2500 Hz, and digitized at 10240Hz sampling rate and 12bits/sample. The frequency components of the sounds signal were then extracted using suitable transform coding techniques. The signal is coded in two steps during transform coding. The first step applies a linear transformation to the signal and then individually quantizes the transform coefficients. A major challenge in transform coding is the choice of transform function and bit allocation technique. Minimum quantization error was achieved using KLT (the Karhunen-Loeve transform). Additional transform techniques were studied and compared such as the discrete slant transform (DST), the Walsh-Hadamard transform (WHT), the discrete Fourier transform (DFT) and the discrete cosine transform (DCT). Throughout the study, the performance of DCT was better than the other transforms and it had a minimum quantization error very close to that found for KLT. The bit allocation method chosen is important as it defines the accuracy of transform coefficient

encoding. Three bit allocation techniques were studied within this investigation. These include uniform bit allocation, bit allocation that takes into account coefficient variance assuming similar pdf (probability density function), and bit allocation that takes into account varying pdfs for coefficients. Finally, the possibility of removing the requirement of updating the bit allocation method for each subject was studied. Within this portion of the study, results demonstrated that the proposed method could be used in fully automated mode without the need to adjust the adaptive bit allocation for every individual signal. Thus, allowing for fast online coding applications.

U. Frey et al [108], were interested in determining whether the changes in respiratory input impedances (Zin) that were measured over a wide range of frequencies were sensitive to alterations in the airway mechanics in infants. Methacholine was used to induce changes in airway mechanics, which were then verified using a reference lung function technique. Another aim of the study was to determining whether the induced changes in the Zin match those found in adults with airway obstruction. At low frequencies, the Zin is primarily a function of the viscoelastic properties of the airway resistance and tissues. Thus, Zin measurements at the low frequency range can be useful for measuring the mechanical properties of tissues, lungs, and the chest wall. Some argue that the parameters derived from Zin measurements at low frequencies are more relevant to natural breathing conditions. At high frequencies, the Zin is equivalently influenced by airway resistance, less by tissue properties, and more by the airway wall characteristics. The Zin measurements data can be analyzed by considering properties of the Zin spectra or using systems identification techniques. Researchers of this study were interested in evaluating whether induced airway obstruction resulted in changes in the frequency of the resonance and/or anti-resonance and also whether it resulted in increased frequency dependence in the real part of the Zin measurements. Results of this study concluded that in wheezy infants, anti-resonant frequency is highly sensitive to lung mechanic changes. A simple lumped parameter model cannot be used to fully explain resonant frequency. Researchers of this study assume that it is most likely caused due to wave propagation phenomena.

H.Kiyokawa et al [109], were able to detect acoustically the simulated crackle in the breath sounds. The main purpose of the study was to examine the audibility of various simulated crackles,

to define their characteristics, and to investigate the ability of human observers to detect them. Based on the findings, it was concluded that the agreement of crackle detection by different human observers was quite high, except under specific conditions. According to Greenberg et al., fine, medium, and coarse crackles with large and small amplitudes can be generated using mathematical functions developed in a numerical computing environment such as MATLAB. The amplitude of a medium crackle is between that of a fine and coarse crackle. A small amplitude crackle was defined to be just above the threshold of audibility for simulated crackles that are recorded during a held breath. The amplitude of a large crackle is equal to twice the amplitude of a small crackle. The respiratory sounds were recorded in a sound insulated chamber. An electric microphone was attached by double sided adhesive tape to the left lower back of a healthy male. A pneumotachometer was used to measure the airflow at the mouth. The recorded sounds were then amplified and filtered. An analog to digital converter was used to digitize the signals. These signals were then stored in a computer. Using the digitized data, audio files were then generated using MATLAB and simulated crackles were placed on top of the recorded sounds. The work concluded that the airflow plays a major role in a physician's ability to detect crackles, since the greater the airflow, the more difficult it is for physicians to detect crackles that can provide meaningful information about a patient's condition. Therefore, it is recommended that when examining a patient for crackles in their respiratory sounds, patients should be advised to take slow, deep breaths to minimize the amount of noise created by their airflow intake and out take, thus making crackles more audible.

T. Kawamura et al [110], were interested in analyzing the characteristics of crackle sound signals. They used a digital stethoscope to record respiratory sounds in 41 patients with crackles. Eighteen patients had interstitial pneumonia and the other twenty three did not. The examinations were conducted in a quiet room. Patients were auscultated in a sitting position. The data was then recorded from 12 sites on their chests. Using a personal computer, the data was converted into digital signals. The recorded sounds were then examined using computer analysis. The characteristics of the crackle sound signals were evaluated in details using Time Expanded Waveform Analysis (TEWA). The values of Initial Detection Width (IDW) and Two Cycle Duration (2CD) were measured from the duration of fixed waveforms of a crackle. The mean of the IDW and 2CD

parameters were calculated for the 41 patients. Based on the findings in the research, shorter parameters identified higher pitched crackles and longer parameters identified lower pitched crackles. Coarse crackles tended to have a low pitch, whereas fine crackles tended to have a high pitch.

Michael Savic [114] developed a medical apparatus and a technique by which lung diseases can be recognized and diagnosed without depending on medical doctors' abilities and experience in hearing and interpreting the respiratory sound signals. This researchers applied digital signal processing techniques to analyze lung sound signals acquired from the chest of patients. Initially a classifier verifies if the lungs are healthy or not. If the classifier concludes that the lungs are not healthy, then anartificial Neural Networks (NN) classifier is used. While the reported device and techniques were developed to detect chronic bronchitis and fibrosis, the authors claim it can be used to detect many different lung diseases. Autoregressive modeling is used for features extraction of the lung diseases. The developed medical apparatus consists of a regular acoustical stethoscope for acquiring the lung sounds from the subject, a transducer operatively connected to the stethoscope for converting the lung sounds to an electric signal, and a computer-based analyzer for analyzing the signal and to identify the lung disease.

Mazic, S. Sovilj, and R. Magjarevic [35] developed an asthma monitoring system in conjunction with a wheezing detection in phonopneumograms using an electronic auscultation system base on electrete microphones. The auscultation was performed on asthmatic patients under the age of seven. This system was developed to sense the occurrence of wheezing and analyze the respiratory spectra characteristic for early discovery of the asthmatic symptoms. The system detected the wheezing in 70% of the patients that were asthmatic prone and had symptoms, however, the system was unable to identify asthmatic prone patients with no symptoms. More general, the system did not identify pathological subjects with no symptoms.

V. Gross and et al [36] developed a lung sound analysis system using a WAVELET Transformation (WT) based method combined with filtering and spectral analysis. The objective of

this system is to extract parameters from recorded lung sound signals in order to detect typical pneumonia lung sounds. The system hardware consists of air coupled microphones, pneumotachograph, amplifier, and a computer monitor to display the signals. All signals were acquired and digitalized at 5512 Hz with 12 bit resolution. In addition, all sound signals were bandpass filtered at 60-2100 Hz. The respiratory signals were analyzed with WT based frequency band analysis between 345-690 Hz, using MATLAB 6.0, wavelet-toolbox. This system was able to identify 50 percent of the bronchial breathing and 62 percent of the crackles recorded sounds.

Noam Gavriely, Yoram Palti, and Gideon Alroy [37] developed a system for obtaining the spectral analysis of normal breath sounds. In this work, the respiratory signals was acquired over the trachea and then characterized using the power spectral density of the signals. The finding shows that the power spectrum of breath sounds has a sharp decrease of power at a cut-off frequency that varied between 850 and 1,600 Hz among the 10 healthy subjects studied.

Volker Gross, Anke Dittmar, Thomas Penzel and Frank Shutter [38] developed a statistical procedure to relate and formulate a connection and relation between normal lung sounds, age , and gender. Overall, this work provides a quantitative method for an objective assessment of lung sounds. Through the statistical relation approach, this work concluded that lung sounds are age-dependent and gender-dependent. Hence, such a dependency must be considered during auscultation, analysis, and diagnostic process.

Pdityi Piiri [39] developed a system that can detect the crackle sounds in auscultation signals. This research focused primarily on the changes in crackle characteristics during the clinical course of pneumonia. The crackling lung sounds of 11 patients with pneumonia were recorded and then analyzed using phonopneumography, FFT spectrography and time-expanded waveform display. Through the analysis and by comparing the different FFT display of the signals, the system was able to detect the crackle.

George R. Wodicka, Kenneth N. Stevens, Howard L. Golub, Ernest G. Cravalho, and Daniel C. Shannon [40] developed a system to model the transmission of the acoustical signals through the lung structure. This work produced a theoretical model of sound transmission from within the respiratory region to the chest wall. The model estimates the magnitude of acceleration over the extra-thoracic trachea and over the other locations on the posterior chest wall in the same vertical plane. Different spectal analysis were applied on the model to compare it with the real lung sound transition.

Lea Bentur, Raphael Beck and et al [41] developed a system to look at the effect of night time on the severeness of wheeze lung sound in asthmatic children. The objective of this study was to analyze the relationship between subjective complaints of nocturnal asthma symptoms, by objectively recording wheezes and spirometry values. Wheezing was identified and quantified by an FFT-based computer algorithm.

A. H. Leung and S. Sehati [42] developed a system to analyze different influences on the lung sounds transmission through normal and diseased human lungs. In this work, a system for monitoring sound transmission through the human lung was described and the possibility of using this information in order to construct a functional map of the lung was investigated.

T. Richard Fenton, Hans Pasterkamp and et al [43] developed an automated spectral analysis and characterization of wheezing in asthmatic children. This system can record the breath sounds in normal and asthmatic children over the chest and trachea. The power spectra of the sounds were analyzed for peaks of high amplitude and high frequency as an indication of wheezing.

T. Rosqvist and E. Paajanen [44] developed a toolkit for lung sound analysis . The major objective of this toolkit was the integration of different signal processing methods in a versatile prototype toolkit to support non-invasive scientific studies of the lung sounds. The study involved the recording of 30 crackling and 10 wheezing lung sounds, which were used as the basic data in the development and the end evaluation of different signal processing algorithms.

P. Piirilä, and A. Sovijärv [45] developed a process for crackle measurements. This work concentrated mainly on the the timing of crackles in the breathing cycles, which can be assessed with phonopneumography. The specification of crackle and its duration was measured through the time-expanded waveform analysis and through the crackle pitch analysis of frequency spectra.

H. Pasterkamp, G.R. Wodicka and S.S. Kraman [46] investigated the effects that can be imposed by the ambient respiratory noise on the measurement of the normal lung sounds. In this study the researchers compared the typical pattern of the healthy lung sounds with the ones that have ambient noise associated with them. They concluded that the ambient noise increased the amplitude of the normal lung sound and extent its frequency range.

Noam Garviely and David W. Cugell [47] studied the airflow effects on the amplitude and frequency content of normal breath sounds. Even though it is well known that breath-sound amplitude (BSA) increases with airflow, the exact quantitative relationships and their distribution within the relevant frequency range have not been determined. This research evaluated these relationships using the measurement of spectral content of tracheal and chest wall breath sounds during breath hold, inspiration, and expiration in six normal men. They concluded that the increase in the volume of the airflow would increase the amplitude of the acoustical signal of the lung sounds.

George R. Wodicka, Kenneth N. Stevens and et al [48] analyzed the characteristics of sound transmission in the human respiratory system. An acoustic driver and a rigid tube were employed to introduce sound into the mouths of the subjects to be propagated through the lung, and the transmission measurements were performed using light weight accelerometers. This work assessed the measurement of the speed of sound through the lungs that can possibly provide an indication of collapsed alveoli.

Yee Leng Yap and Zahra Moussavi [49] developed a system for respiratory onset detection. The system detects the respiratory phases without using airflow measurement. In this work , the average power of tracheal breath sounds were used to detect the onset of breathing.

Earis, J. E., and Cheetham, B. M. [50] studied the importance of modern technology in the respiratory acoustical signal analysis and diagnosis. They reviewed the efficiency and advantages of modern technologies for the capture, storage, analysis, and communication of sounds that are heard through a stethoscope. This study explored the use of digital signal processing equipment and computerized systems in clinical respiratory signals analysis, remote monitoring, data exchange, tele-medicine, and diagnosis evaluation. The study concluded that the limiting factors are no longer the storage capacity, the computing power, the signal processing nor the capability or speed of readily available personal computers. However, the study stated that a further development is required for a computerized diagnostic system of the respiratory signals to be utilized in clinical medicine.

A.S. Brown, D.M. Harvey, and G.Jamieson, Dr. D.R. Graham [51] developed a Physiological Signal Analysis System (PhiSAS) for the observation of lung sounds. The system consisted of a personal computer (PC) supported with dedicated software and hardware. Lung sounds could be recorded via chest microphones into the computer system for post processing using software-based digital signal processing (DSP) techniques that can mathematically manipulate lung sounds to extract important features. Data and result can be presented audibly by sound playback or graphically by using spectrographs. PhiSAS has the ability to present three types of analyses based on conventional techniques: Fourier, Wavelet, and Time-Frequency Analysis. The system consists of the application software written for Microsoft Windows. PhiSAS is written in C++, and exploits a graphical user interface (GUI) environment. The design of the software is modular, allowing effective maintenance. Transducers and signal conditioning electronics were designed in-house using conventional hardware to reduce costs. Signal acquisition is provided using a SoundBlaster compatible 16-bit sound card interface. Software control of sound acquisition and playback is provided using the Microsoft DirectX interface. PhiSAS integrates an Intel signal processing library which reduces computation time without the need for additional DSP hardware.

Antoni Homs-Corbera, Raimon Antonio and Fiz Morera [52] developed an algorithm, they called grouping algorithm, to detect wheezes by means of a time-frequency analysis technique.

Through this algorithm, the authors tried to objectively characterize how wheezes evolve in time. The short-in-time frequency peaks are eliminated, so crackles and microphone clicks are no longer detected as wheezing peaks. The result is more close to what a medical doctor would perceive as a wheeze during an auscultation. The grouping algorithm scans the time-frequency plane searching for a wheezing peak that is not grouped at a time distance of 25.6 ms. If there are peaks at this distance, the algorithm performs a frequency proximity check. As a result, only the peaks that are closer than 50 Hz to the original wheezing were kept. If there are no peaks meeting those conditions, the algorithm looks for peaks that are not grouped at a time distance of 51.2 ms. A frequency proximity check is also performed and only the peaks closer than 65 Hz to the original wheezing are kept. Of the peaks that are kept, only those that have an amplitude close to the original wheezing peak are grouped with it. The process starts all over again taking the last grouped peak as the original peak until none close to this one are found. At this time, the entire wheeze is defined. After applying the algorithm to the entire time-frequency plane, the possible wheezes with duration shorter than 80 ms are eliminated.

Hong Wang and Le Yi Wang [53] developed multiple acoustic sensors (accelerometers) system to measure respiratory sounds at designated auscultation sites. Sensor signals are scaled, synchronized and amplified by a multi-channel sound adaptor, and then fed to a computer. The signals are first processed for noise attenuation and signal separation. The clarified signals are then combined with other measured signals for information processing and diagnosis. This work attempt to develop an auscultation system for monitoring and recording of the lung sounds as well as computer-assisted signal processing of respiratory sounds. The researchers stated that a prototype of the system was developed, however they emphasized that the validity of this system remains to be extensively studied and verified.

Meng-Lun Hsueh, and et al [54] developed a low cost lung sound recording system that adheres to the Standardized Recording Protocol of CORSA. The study subjects were divided into two groups. The first group consisted of 12 nonsmoking asthmatic patients with various wheeze episodes. The second group was composed of 4 subjects with no reported respiratory pathology. The

recording site in all cases was the thorax. Patients were in a sitting position when their tidal breathing was recorded for about 7-10 respiratory cycles. The hardware of the system consisted of an electrical condenser type omni-directional microphone (ECM) and was mounted within a stethoscope. It provided a fairly high SNR and sensitivity, and flat response in the band of interest. A band-pass filter, made up of a high-pass filter and low-pass , was used. The digitalization of the acquired signals was performed via a commercial sound card.

Yang-sheng Lu, Wen-hui Liu and Guang-xia Qin [55] attempted to remove heartbeat noise from breath sounds using an adaptive filter. They stated in the result section of their work that several kinds of breath sounds with less heartbeat noise have been recorded. However, they indicated as well that their work provides a good base for further studies.

A. I. D'yachenko and G. A. Lyubimov [99] studied the propagation of the sound through the pulmonary parenchyma. For the purpose of analyzing the sound, this study employed a system model of pulmonary air passages, which include a bronchial part that consists of rigid tubes. This model was constructed on the basis of a formerly developed model of the dynamics of the parenchyma when treated as a multi-phase continuum. The speed of sounds, in this model was chosen to be close to the speed of sound in the gas, even though, the authors were stating that experimental data had showed the speed of sound in the pulmonary parenchyma with a frequency spectrum of 100 - 1000 Hz was about 30-60 m/s. The authors showed that the sound intensity decreases with the distance as it propagates through the parenchyma. The damping over a distance of the order of the dimension of the lungs, which was taken as 25 cm, results in a decrease in the sound pressure level for about 4.3 dB, which is much less than the attenuation sound in parenchyma derived from some experimental values that will be explained in the next literature review.

U. H. Cegla [100] studied different aspects of sound transmission in the lungs. The paper showed that the experiment was performed by generating a sound signal at the mouth and recording it by using a stethoscope attached to different parts of the chest. The attenuation was evaluated by analyzing the recorded sound signals. With reference to the Figure 2.11, the sound pressure level

acquired by the stethoscope decreased rapidly when the frequency of the sound was more than 500 Hz. The same figure illustrates the sound transmission from the mouth through the airways and parenchyma up to the chest wall, at frequencies up to 500 Hz, without being damped. However, at a frequency of 1 kHz the attenuation is equal to 18 dB and at 2 kHz to about 36 dB.

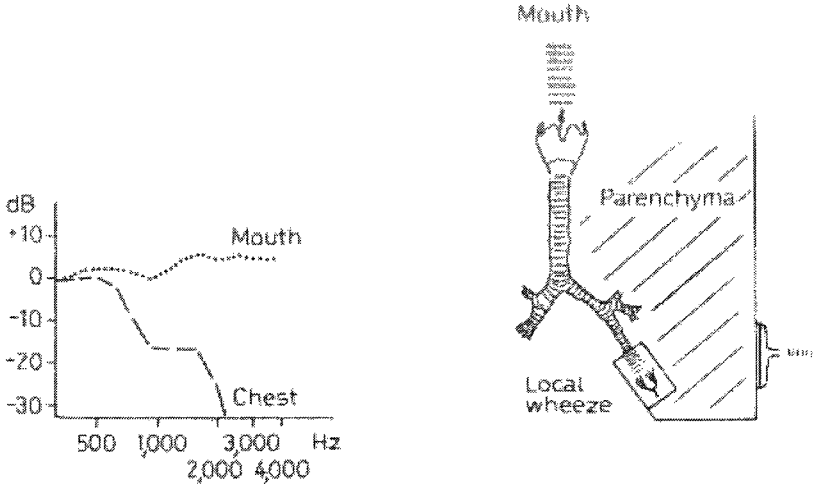

Figure 2.11: Attenuation of Lung Sounds Through Parenchyma

George R. Wodicka et al [101] developed a system for evaluating the frequency characteristics of sound transmission from the mouth to the chest wall. In this research, the experiments were performed by introducing a sound into the mouths of eight healthy individuals. Acceleration measurements of the chest wall were performed at resting lung volume using calibrated contact transducers. The authors analyzed the sound signals and realized that the attenuation in the sound intensity due to wave propagation through the parenchyma is a function of frequency; it is negligible at 100 Hz and greater than 30 dB at 600 Hz. Figure 2.12 demonstrate the set up of the experiment, illustrating the position of the transducers for recording the sound introduced from the mouth, propagated through the airways and parenchyma and then recorded.

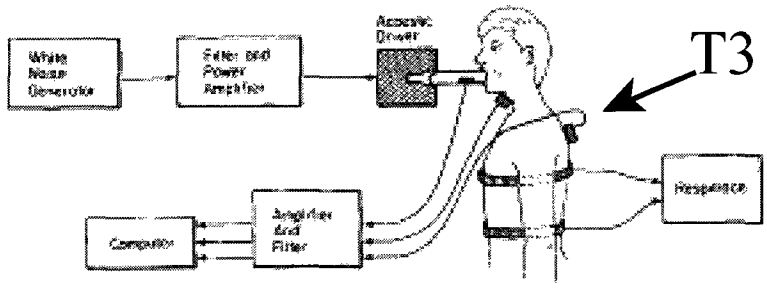

Figure 2.12: System for Measuring the Attenuation

Philip J. Berger and et al [102], carried out experiments on the isolated lung of the lategestation fetal sheep in order to evaluate whether the acoustic properties of the lung reflect the volume of gas that the lung contains. The researchers started from a point at which the lung is completely free of gas. Their approach had allowed the velocity and attenuation of audible sound in the isolated lung to be characterized as it is inflated from the liquid-filled state up to total lung capacity with air. The first measurement of the acoustic properties of the lung was made with fetal lung liquid occupying the potential air space of the lung, i.e., there was no air present in the lung. The researchers used CLIO software (AUDIOMATICA SRL, Firenze, Italy) to generate a pseudorandom voltage to actuate the electromagnetic sound transducer, producing a pseudorandom noise signal that passed through the lung to the microphone on the opposite side. The microphone output was amplified and filtered using a fourth-order linear phase band-pass filter with a lower cutoff frequency of 100 Hz and an upper cutoff frequency of 20 kHz. The strong filtering applied at 100 Hz was used to limit potential interference from low-frequency room noise and the upper frequency limit to satisfy the Nyquist criterion for sampling at 48 kHz. In all experiments, the sound intensity input to the lung produced by the electromagnetic sound transducer was set at 120 dB. With reference to Figure 2.10, the authors stated that the measurements of excess attenuation vs. inflation are illustrated for four frequencies between 1,500 Hz and 3 kHz. The research stated that the attenuation in the parenchyma is a function of the frequency and inflation. At 1,500 Hz there was no significant change in attenuation with inflation. The results at 1,500 Hz show a more or less linear

increase in attenuation with inflation between 40 and 240 ml with (excess) attenuation rising significantly from 0.2 - 0.5 to 3.6 - 4.0 dB/cm over this inflation range. At 2 , 2.4 an d 3 kHz, the rate of increase of attenuation is significantly higher than at 1,500 Hz.

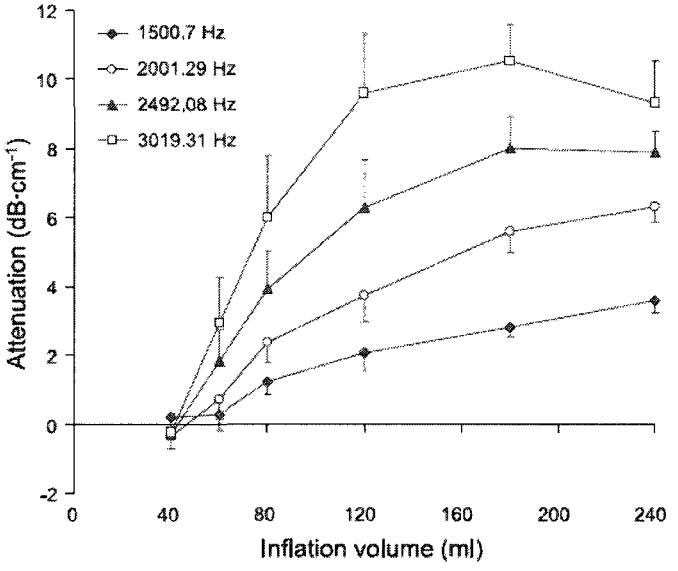

Figure 2.13: Lung Sounds Attenuation vs Inflation

2.5.2 Summery of the Literature Review

There was a great deal of research conducted that concentrated mainly on the auscultation and identification of the lung sound signals. Different methods and approaches were used in order to develop systems that would form frameworks for respiratory sound signal analysis and identification. However, the focus was mainly on the analysis and at a very limited extent on the classification and identification of the lung sound signals. However the identification processes were mostly able to only tell whether the lung signals were healthy or pathological. In addition the degree of the identification accuracy was not suitable for a medical diagnosis. The other shortcomings of the previous research conducted were that they tackled specific problems instead of structuring a

more complete approach for auscultation, recording, analysis, identification and diagnose of the lung sounds. These shortcomings are primarily due to the amount of effort required and the complexity of handling different areas of the technologies. The aim of this thesis research is to overcome the shortcomings mentioned above by advancing a structured and comprehensive methodology for constructing a computerized and automated auscultation system. This system can be used for monitoring, recording, conditioning, classifying, identifying, and diagnosing respiratory sound signals. In addition, the newly developed system provides a high degree of accuracy which is better than any other previously "developed system", even though the comparison is not equivalent. The system diagnoses mainly the two most popular adventitious lung sound signals, wheeze and crackle, however, it can easily be extended to include another type of adventitious lung signals, such as Rhonchus and Grunts.

CHAPTER III

Computerized Auscultation and Diagnostic System: Architecture and Design

3.1 Introduction

The objective of this research is to develop a computerized auscultation and diagnostic system, that would be able to acquire, amplify, filter, analyze, identify, and diagnose lung sound and its anomalies. The system would be able to provide an initial diagnosis that an attending physician would take into account when assessing the health of a subject. The physician would also be able to listen to the gathered sound data files, with or without a variety of filters and sound enchantment aids to further enhance the diagnosis. This work will focus on the identification of wheeze and crackle adventitious lung sounds and their sites, as they are the primary indication of lung diseases. It is anticipated that the system developed in this work would lessen the necessity and cost of using potentially harmful imaging techniques such as x-rays. Moreover, this system can provide some objectivity to the diagnostic process.

3.1.1 Overview of the Automated Auscultation System's Architecture and Design

Figure 3.1 shows a block diagram of the system with its interconnections. With reference to the figure the system consists of three major subsystems: the hardware, the core analyses and diagnostic subsystem, and the Graphical User Interface (GUI). As shown in the figure, the respiratory acoustical signals are acquired by an array of transducers (electronic stethoscopes) and converted into a digital data stream. Each microphone output is fed through an adjustable gain pre-amplifier to an audio acquisition and processing unit. Then, the sound files gathered from the auscultation process are stored on the auscultation workstation where the developed auscultation software is housed. In addition to the Graphical User Interface subsystem, the Digital Signal Processing (DSP) and filtration modules, and the identification and diagnosing NN, the auscultation software comprises an audio interface device driver. Descriptions of the different parts of the system follow.

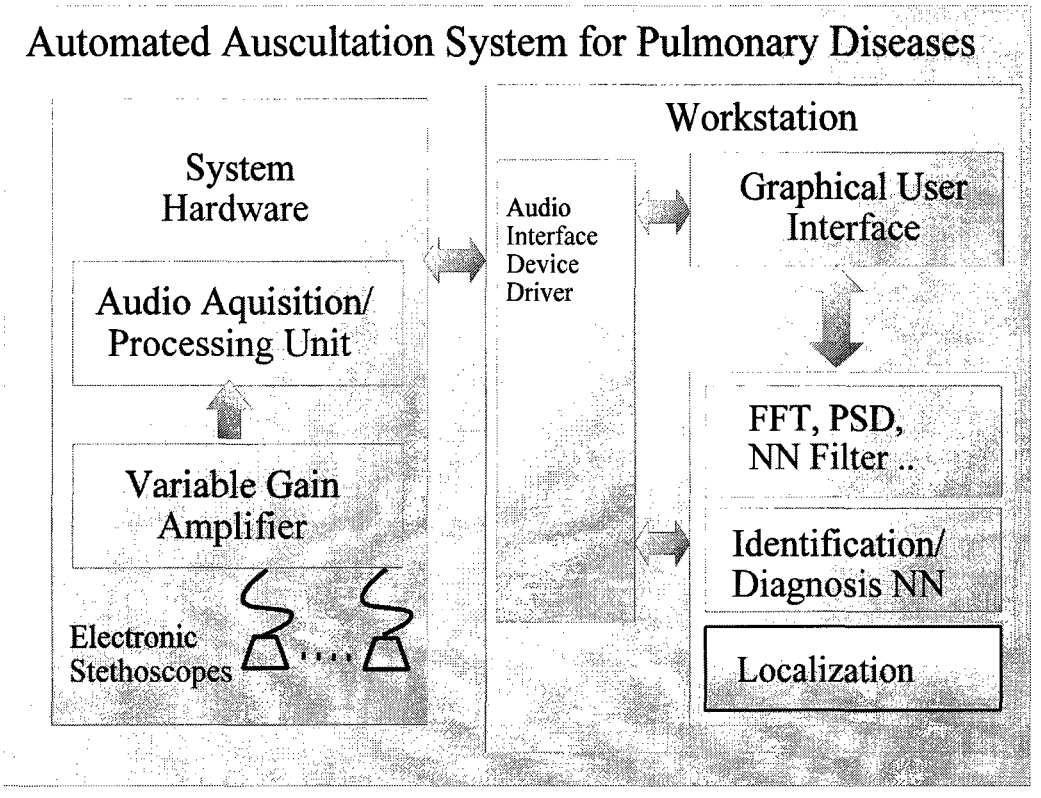

Figure 3.1: Architecture of the Automated Auscultation System

3.2 Hardware of the Automated Auscultation and Diagnostic System

With reference to Figure 3.2, the system hardware consists of the following components; a) an omni-direction electret microphones which are used to structure the chest piece of the multi-channels electronic stethoscope. These microphones have an almost flat response in the frequency range of 20 Hz-20 kHz. They are chosen to have a high sensitivity of -35 dB ± 4 (defined as the voltage generated by the microphone when the input sound pressure is 0.1 Pa at a frequency of 1 kHz) and with the signal to noise ratio (S/N) greater than 62 dB. b) an in-house designed and built array of variable gain pre-amplifiers housed in a Faraday cage with a totally isolated power source to eliminate electromagnetic noise contamination, and c) an audio acquisition and processing unit

capable of acquiring all the sound signals simultaneously with up to 24 bit resolution and up to 96 KHz sampling rate.

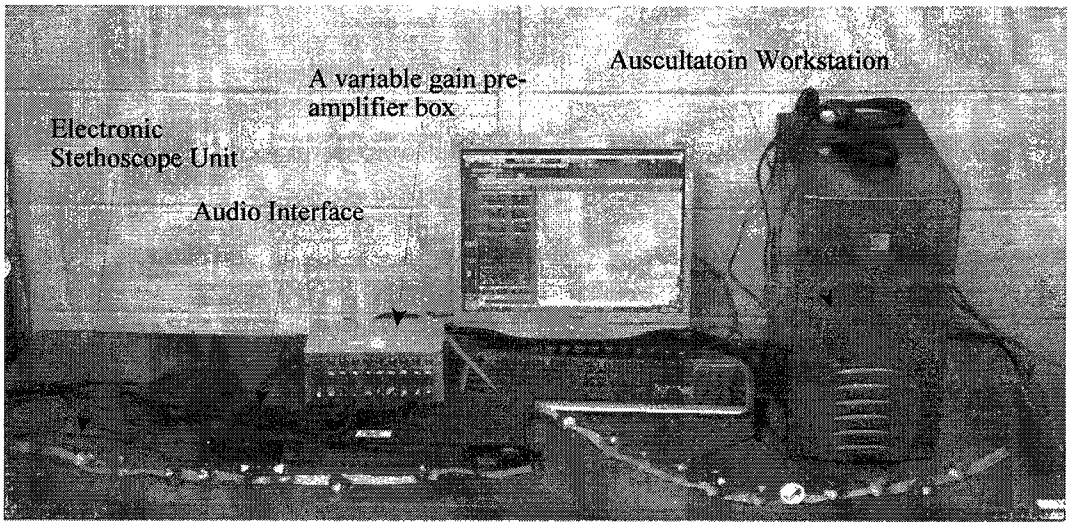

Figure 3.2: Computerized Automated Auscultation and Diagnostic Systems

With reference to Figures 3.3 -3.5 the transducers are housed in a nylon cup with a stainless steel cone-like head cover. The transducers in the chest array are strung on two elastic belts with 10 transducers each and quick buckles for easy and rapid deployment around the subject's chest. Shielded cables are used to connect the transducers to the pre-amplifier unit so as to eliminate noise picked up by wires. Figure 3.6 shows a schematic diagram of the transducer and its connection to the pre-amplifier circuit and sound acquisition system. With reference to the figure, the transducer conic head that comes into contact with the patient body is made out of stainless steel. The transducer head is held to the transducer body using a nylon cup. The microphone case is anchored into the nylon cup but does not contact the transducer stainless steel head. The microphone is connected to the pre-amplifier using a shielded cable whose ground is in common with the microphone case and the pre-amplifier and sound acquisition system ground connections.

The omni-direction electret condenser microphones form the core sensing elements of the developed multi-channel electronic stethoscope. In order to test the performance of the array of transducers (the 20 channels of the stethoscope) a sound insulated chamber is used. In that test a sine wave sound was generated using MATLAB. This sound was submitted to each and every microphone of the array of microphones in the system and the sounds picked up by the microphones are recorded and analyzed. All the microphones should exhibit the same response and show similar characteristics of the recorded sounds for the amplitude and frequency content. The microphone that did not present identical output with the other microphones' outputs was rewired or replaced. This process is repeated until identical outputs from all the microphones are obtained. Then, the array of the transducers was tested by operating the 20 channels simultaneously many times. Again the microphones' outputs were analyzed to ensure that all have identical outputs when the same input is used.

With reference to Figure 3.3, the circular edge of the stethoscopic head cover is designed to be wide and not sharp-ended in order to stretch the skin of the patient at the point where it is attached against the patient's chest for more efficient sensing of lung sounds. Such an attachment makes the patient's skin act as a flexible diaphragm across the entrance opining of the conic head cover to transmit the sound. In general, the chest piece of the manual acoustic stethoscope is made of stainless steel and generally has a bell shaped side and a diaphragm side. The bell section of the chest piece is open, has a diameter of 1.13 in. (28.7 mm), and is 0.25 in. (6.4 mm) deep with a cone angle of about 68.8°. When using the bell section of the stethoscope, the patient's skin acts as a flexible diaphragm across the mouth of the bell to transmit the sound (this is similar manner to our developed stethoscope). On the other hand, the design of the electronic stethoscope consists of a stethoscopic head that has a conic inner chamber with a 20-mm base diameter and a 5-mm depth [111], while, the stethoscopic head cover of the system developed here has a diameter of (23.8 mm), is (5 mm) deep, and the cone angle is about (67.3°).

The stainless steel conic-shaped head cover of the multi-channel electronic stethoscope has a polished hard surface which acts as a specular reflector of sound with negligible diffusion. Such

a surface will not absorb or disperse sound. The conic-shaped stethoscopic head has a cone angle so designed such that it would gather sound waves from its base and guides them to the opening at its apex where the electret microphone resides. Figure 3.4 shows a schematic of waves and their reflection from the conic surface. Furthermore, the reflected waves can interfere with incident waves, producing patterns of constructive interference.

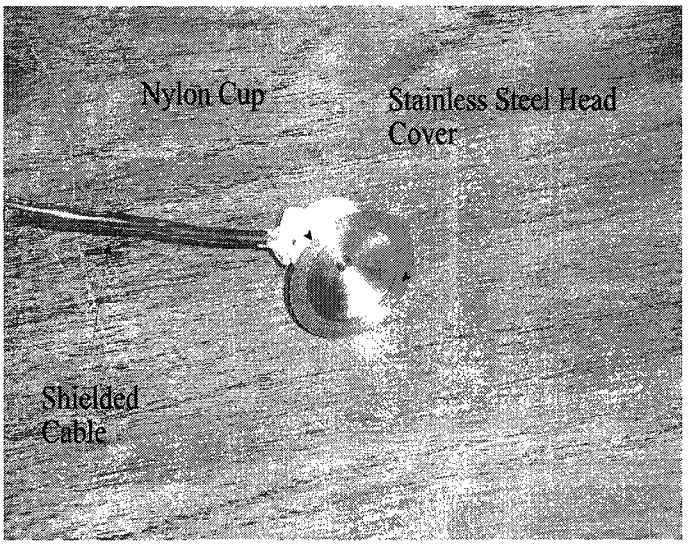

Figure 3.3: Transducer (Electronic Stethoscope)

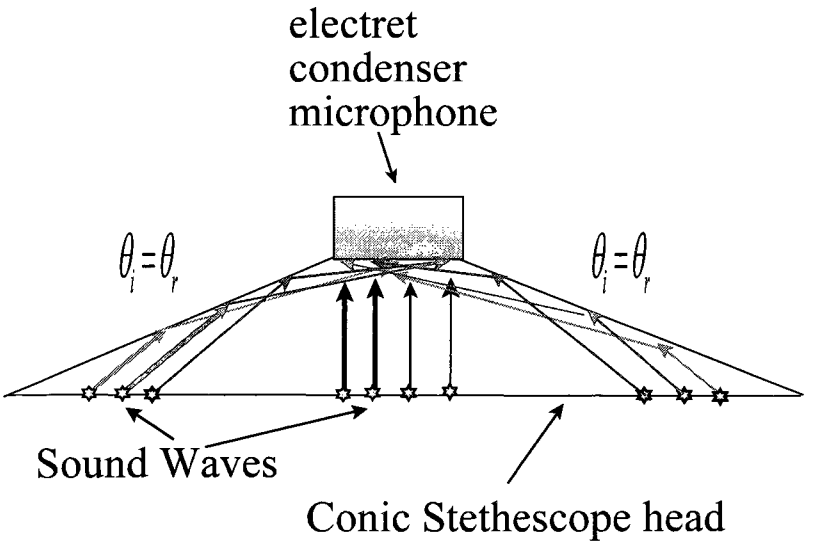

Figure 3.4: Propagation of Sound Waves Through the Conic Stethoscope Head

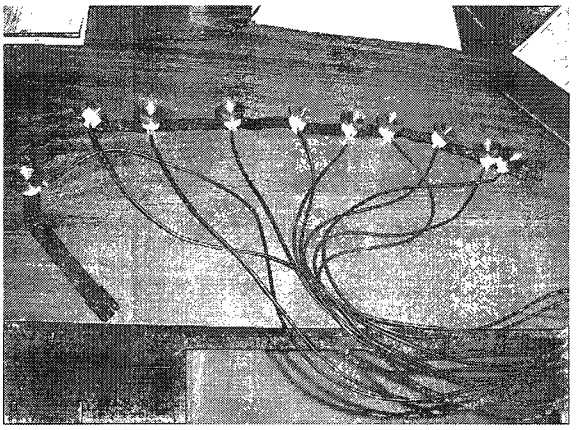

Figure 3.5: The Array of Transducers

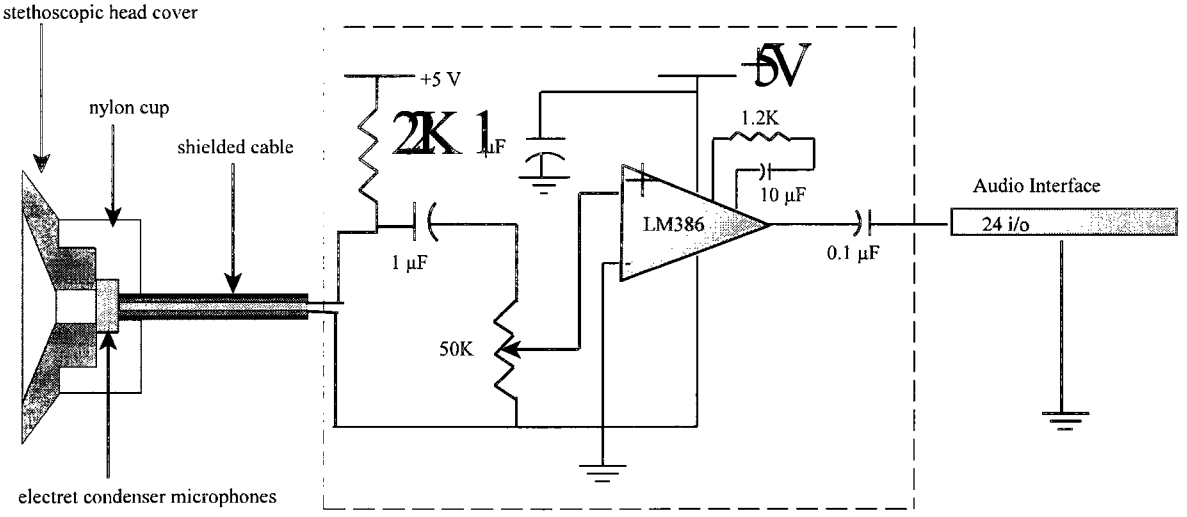

Figure 3.6: Schematic Diagram of the Microphone Circuit

The 20 channels of the electronic stethoscope are deployed around the chest in order to acquire lung sound from all the lung lobes simultaneously. Table 3.1 shows the channels distribution with respect to lung lobes:

Lung Lobe	**Channels Number**
Right Upper Lobe	1, 2, 8, 9 and 10
Left Upper Lobe	3, 4, 5, 6,and 7
Right Lower Lobe & Right Middle Lobe	11, 12, 18, 19 and 20
Left Lower Lobe	13, 14, 15, 16 and 17

Table 3.1 : Location Distribution of the Multichannel Electronic Stethoscope

Figure 3. shows the stethoscope array deployed over a subject's chest. The auscultation is performed symmetrically over the left and right lungs using the array of 20 transducers. The location of the transducers on the carriers can be adjusted to coincide with the conventional sites of auscultation, indicated in Chapter 2, on the back, front and sides.

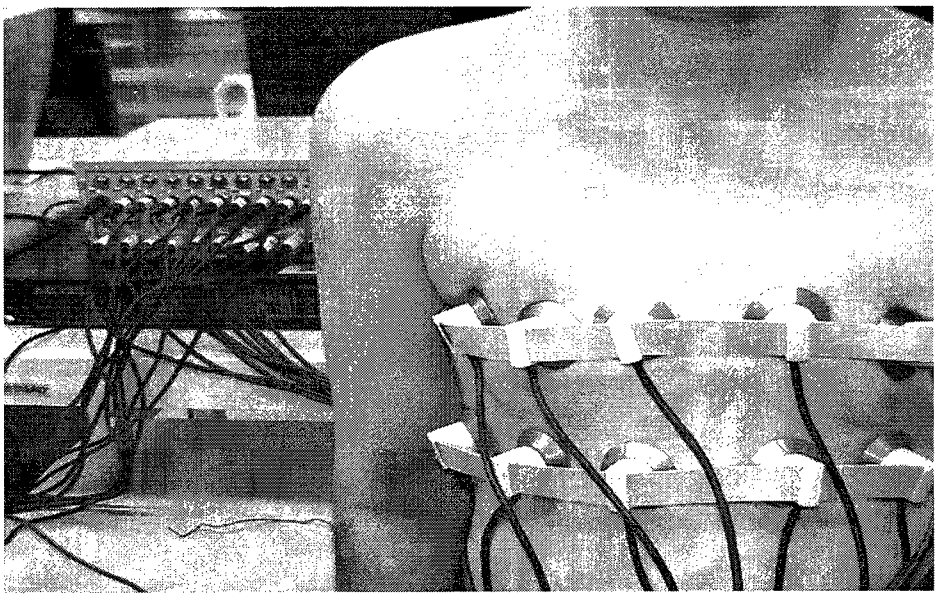

Figure 3.7: The Array of the Electronic Stethoscope Attached at the Chest

3.3 The Core Analyses and Diagnostic Subsystem of the Auscultation and Diagnostic System

The core software consist of modules for filtration, analysis, identification and diagnosis of the respiratory acoustical signals. The software is developed using a combination of C++ and MATLAB code integrated together. The design of the auscultation core software is modular to allow effective development, modification, and maintenance.

Two types of filters are implemented. The first is a targeted filter that eliminates the heart beat from the auscultation sounds. The second is a general filter that can eliminate ambient or internal organ sounds, either aided by signals from a reference microphone that monitors these sounds or unaided using general filtration algorithms based on the frequency content of these sounds. In addition, this module is responsible for processing and preparing the data in a number of formats including FFT, PSD, and time domain for subsequent presentation by the GUI or for storage.

The identification and diagnosis sub-system employs a NN specially trained to identify lung sounds from non lung sounds, normal lung sounds, and diagnose advantageous lung sounds. This subsystem can distinguish between crackle and wheeze sounds and classify these as indicative of lung ailments. Details about the core software functionality will be given in Chapters 4 and 5.

3.4 Graphical User Interface (GUI) of the Auscultation and Diagnostic system

With reference to Figure 3.8, the graphical user interface provides the auscultation physician with an easy access mechanism to monitor and control the functionality of the different system hardware and software modules. Audio inspection of the auscultation sounds, analysis and diagnosis can be practiced in real time or off line. The user can listen to each channel individually by browsing through and selecting from a drop down menu. The position of each channel is displayed on a generic upper body view. The user controls all the parameters of the low-pass, high-pass, band pass, and band stop filters, as well as the operation of the heartbeat filter. The system can be commanded to perform a diagnostic process on any one of the channels or a general diagnosis of the entire set of channels. The user can view the sound signals for any of the 20 channels in one of three formats; time base wave file, frequency, and Power Spectral Density (PSD).

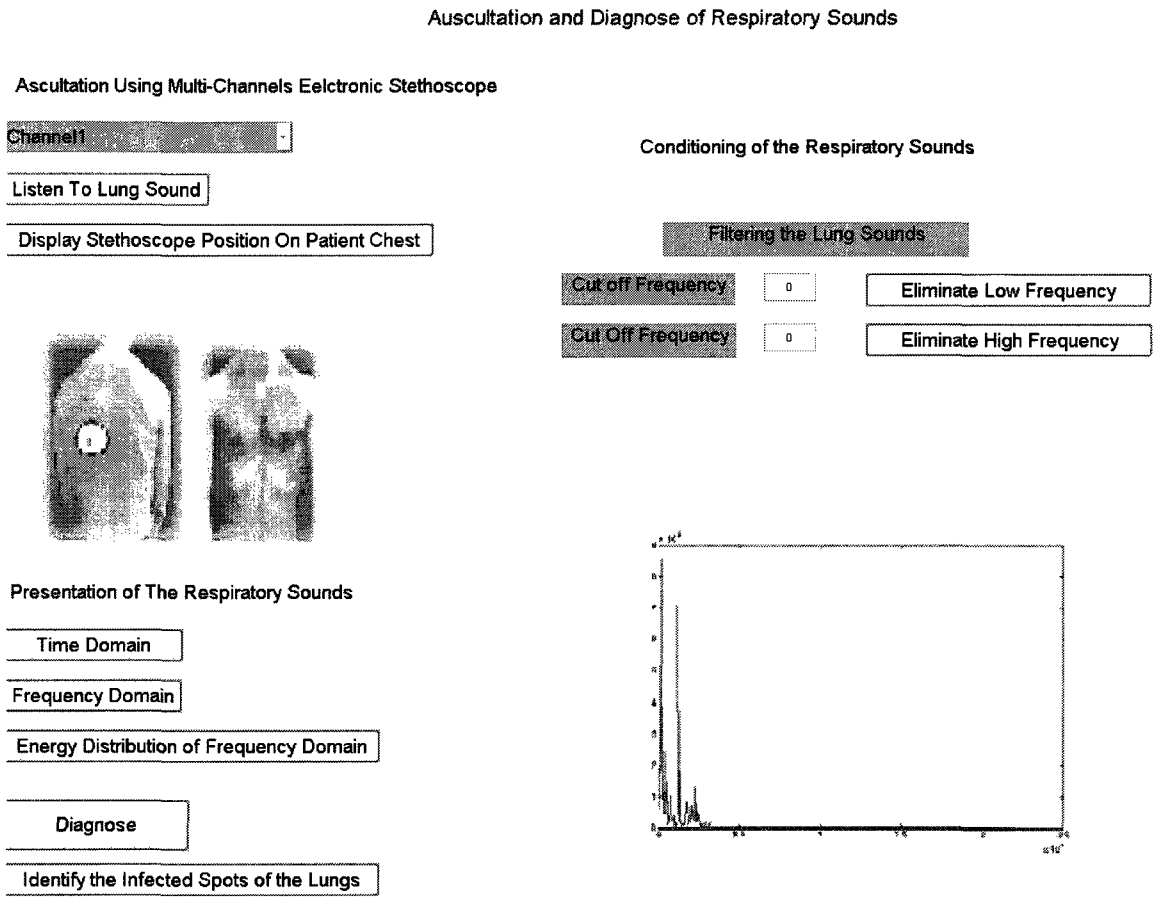

Figure 3.8: The GUI of the Auscultation and Diagnostic System

CHAPTER IV

Respiratory Acoustical Signals Filtration and Analysis

4.1 Introduction

As has been shown in the literature review, there is a major overlap between the frequency ranges of the different types of lung sounds that complicate substantially the process of separation, identification, and diagnosis of the respiratory sound signals. The problem is further aggravated by the fact that the heartbeat sound is loud, prominent and fall within the same frequency range of the lung sounds. Furthermore, unless unrealistic precautions are taken, respiratory sound signals will be polluted by sound signals from other sources including; ambient noise, and muscle sounds.

4.1.1 Filtration of the Respiratory Sound Signals

4.1.1.1 Filtration of Noises that Fall within the Bandwidth of the Respiratory Sound Signals

Filtration of noises that fall within the bandwidth of the respiratory sound signals can be performed using different techniques such as DSP and Neural Networks filters. Those alternatives will be discussed below.

4.1.1.2 Filtering the Heartbeat from Lung Sounds Using DSP Filters

Conventional filtering of noise that fall within the bandwidth of the respiratory acoustical signals will result in the loss of some useful information. For instance, the heartbeat sounds have a major frequency contribution between 40 and 100 Hz which fall within the frequency range of the lung sounds. Using band stop or high pass filters would result in removing or attenuating the heartbeat frequency as well as that band of the lung sounds. Alternatively, using adaptive filters

would reduce the heartbeat range but would not eliminate it [51]. This is because such adaptive filters need a reference signal that is exactly time aligned as the interference in the primary signal.

4.1.2 Filtering the Heartbeat from Lung Sounds Signals Using Linear Neural Networks (ADALINE)

ADALINE was first introduced by Widrow in 1960 [52]. ADALINE, architecture is similar to the perceptron neural network, but has a linear transfer function rather than the hard limiting one used in perceptron networks. Adaptive linear neural networks has been successfully used for signal noise cancellation [52]. This approach has been successfully employed in this research to overcome the problem of filtering the heart beat noise pattern from the lung sounds even with the absence of a time aligned reference signal. The MATLAB implementation of this type of filter is used here with the Least Mean Squares (LMS) learning rule. In this learning method the square of the errors between the target (desired values) and the computed values is calculated first, and then the average is taken to obtain the mean squared error. The set of values of weights that minimizes the mean squared error is what is needed for the next cycle of operation of the neural network. The least mean square error (LMS) learning algorithm is a supervised training one where the network is provided with a set of examples of time based desired network behavior tuples, $[p_1, t_1], [p_2, t_2], \ldots [p_n, t_n]$, where the $\boldsymbol{P}_q$ is an input to the network, and $\boldsymbol{T}_q$ is the corresponding target output. The details of the filter will be discussed below.

During classical auscultation, a health care practitioner hears the lung sounds as well as the heart beat and other internal body sounds of the patient. Such a practitioner is trained to mentally filter such sounds and focuses attention on the target lung sounds. The frequency content of noise emanating from within the body coincides with that of the lung sound and poses a major problem for an automated diagnosis system. As has been mentioned above, filtering techniques used so far result in either marginal reduction of these undesired sounds or a significant effect on the lung sound. However if a subject is asked to stop breathing for a few seconds, a pure heart beat can be recorded by the auscultation system. After that, a regular auscultation process would be performed and the

lung sound signal plus the heartbeat sound would be obtained and recorded. The pure heartbeat sound signal is then provided to a specially designed NN filter as the reference signal, and the combination of the lung and heartbeat sounds are presented to the NN filter as the primary signal. The pure heartbeat signal provide the NN with sufficient information it can use to predict and eliminate the heartbeat's contribution to the lung plus heart beat signal. This linear neural network adaptively learns to refine the lung sound by eliminating the heartbeat. It is important to mention that this adaptive noise cancelling usually provides a much better performance than a classical filter because the noise here is subtracted from, rather than, filtered out of the signal.

4.1.2.1 Filtration of other Noise that Fall out of the Bandwidth of the Respiratory Sound Signals

High-pass and low-pass filters are used to attenuate all sound signals that fall outside the interest bandwidth of the lung sound signals. The high-pass filter (HPF) has an adjustable cut-off frequency and is used to reduce or remove low-frequency noise from the respiratory sounds. Such noise is typically produced as a result of the relative motion between the microphone cup and the skin, by cardiovascular sounds, muscle noise, abdominal sounds and external low-frequency noise. The low pass filter also has an adjustable corner frequency and is used to reduce high frequency noise such as that produced by external sources or by electromagnetic pick up during the auscultation.

4.2 Analysis of the Respiratory Acoustical Signals

In order to improve the diagnosis process of diseases through the analysis of auscultation, breath sounds are digitized and processed in multiple forms and domains to allow insight and reveal their characteristics. One examples each of healthy breath sound and two abnormal adventitious categories (crackle and wheeze) breath sounds are analyzed. The signals were plotted in the time domain and the frequency domain (FFT, and PSD). A comparison of the different characteristics of these sound forms follows. It should be noted that the amplitude of the signals cannot be used as a measure since it depends on the recording level and the amplification applied. Rather, qualitative measures like the shape of the plots and the relative strength of the frequency content are used.

4.2.1 Time Domain Analysis

The time-domain representation of the audio signals displays each digitized sample value of the lung sound versus time, creating a plot which shows the variation of the amplitude of the sound. The breath samples exemplified for the normal, wheeze, and crackle sounds are shown below. With reference to Figure 4.1, during normal breathing, inspiration begins at low amplitude. The amplitude rises rapidly over time as the lung expands, reaching a maximum slightly before the end of inspiration. The amplitude drops gradually as the lung nears full capacity and the velocity of the in-rushing air drops. Inspiration is followed by a pause which is represented by practical silence before the start of expiration. The expiration phase looks like a downscaled and mirror image of the inspiration segment. The pause that follows exhilation is longer then the intermediate pause between inhaling and exhaling. The normal breathing graph also shows that inspiration has a longer duration then expiration.

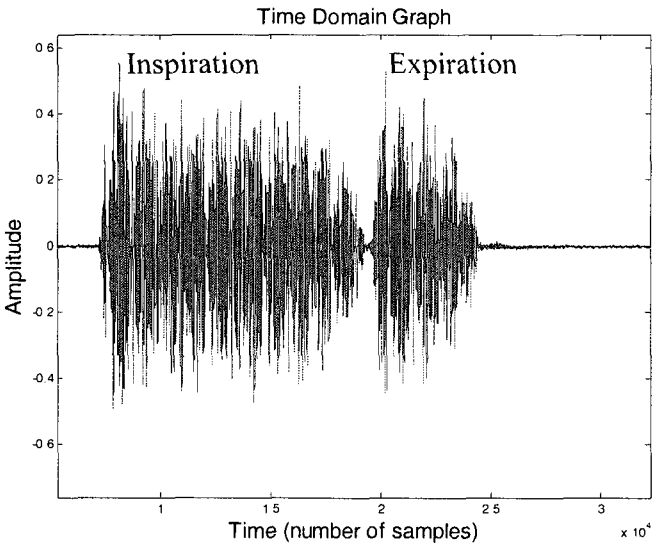

Figure 4.1 Time Domain of the Normal Lung Sounds

The steady increases in amplitude in inhalation and the decrease in exhalation is easily explained by the physiology of breathing. As air is inhaled, the lungs begin to expand creating a progressively larger cavity that acts as an amplifier. The larger the volume of the lungs is, the higher the amplification and vice versa during exhalation [57]. Hence, the amplitude of the respiratory sounds varies with the air flow.

As mentioned in Chapter 2, crackle is the result of the explosive equalization of gas pressure between two compartments of the lung when a blocked section of the airways separating them suddenly opens. With reference to Figure 4.2, a breath sound that has adventitious crackles shows again the distinct breath cycle. The exploding sound of the crackles is shown in the graph as the sharp spikes of extreme amplitude relative to the general form of the sound wave. It is apparent in the graph as the individual spikes that occur over short time intervals., In general, the major duration of crackle sound within the lung breath sound last less then 25ms [57-58]. The plot corresponds to the physiological explanation of the crackles. Crackles are associated with the presence of mucus and fluids that block some of the lung air passages. During inhalation when the diaphragm and the ribs cage expands, the pressure behind these blocked passage drops significantly below atmosphere.

Beyond a certain pressure the mucus and fluids blocking the passage dislodges suddenly resulting in the explosive sound.

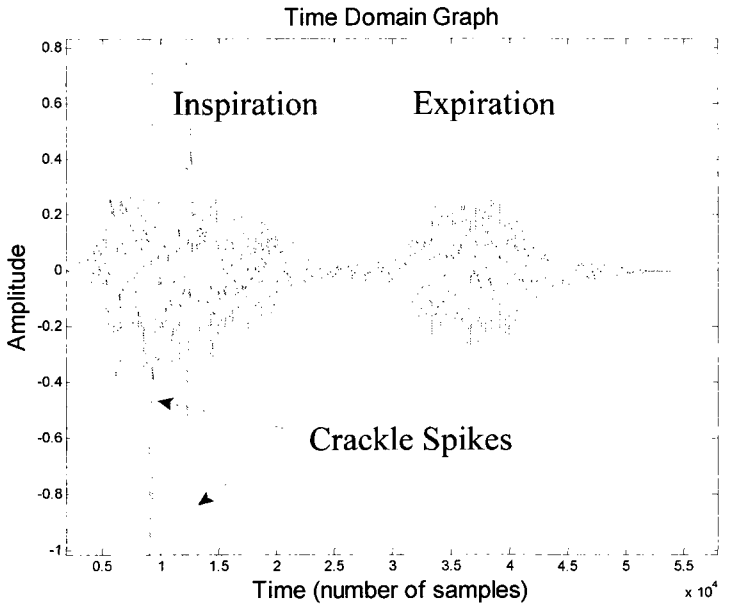

Figure 4.2: Time Domain of the Crackle Lung Sounds

With reference to Figure 4.3, a breath sound that has adventitious wheeze shows that there is a change from the expected breath intervals. While the breath cycle is easily identifiable, the inspiration phase shown is shorter than the expiration phase. Furthermore, unlike the cases of healthy breath sounds and those with crackle, the amplitude of the exhalation is higher than that of the inspiration. The apparent shorter inhalation breathing phase is a dominant feature of wheezing and is due to the fact that wheezing is predominantly an expiration adventitious sound. The wheezing sound continues late into the expiration phase as air exits constricted passages, and results in the continuous musical tone of the wheeze. In general, the wheeze duration lasts more than 250 ms [57].

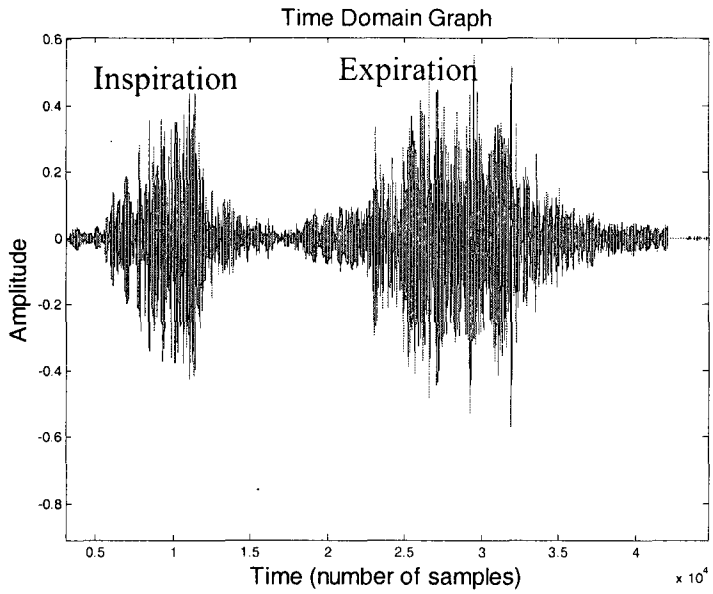

Figure 4.3: Time Domain of the Wheeze Lung Sound

4.2.2 Frequency Domain Analysis of the Lung Sound Signals

While the time domain plots are easy to visually understand and reveal the signal's duration, they do not provide information about the details of the characterizing frequencies of the lung audio signal. Furthermore, they do not lend themselves to automatic analysis. The frequency domain analyses of the signals allow for the decomposition of the complex waveform into its component frequencies. Two such frequency analyses are carried out below; the fast Fourier analysis, and the probability density function analysis. The three sound files shown in Figures 4.1 to 4.3 are used below.

4.2.2.1 Fast Fourier Transform (FFT) Analysis

Figure 4.4 shows a FFT frequency plot of a healthy lung sound. With reference to the figure, the plot of the amplitude versus frequency allows for the identification of specific frequencies of interest that would help provide a more complete view of the adventitious sounds which can then be

used for filtration and identification. The plot of the normal lung sound shows the expected high amplitude of the frequencies at the low end as has been mentioned in Chapter 2.

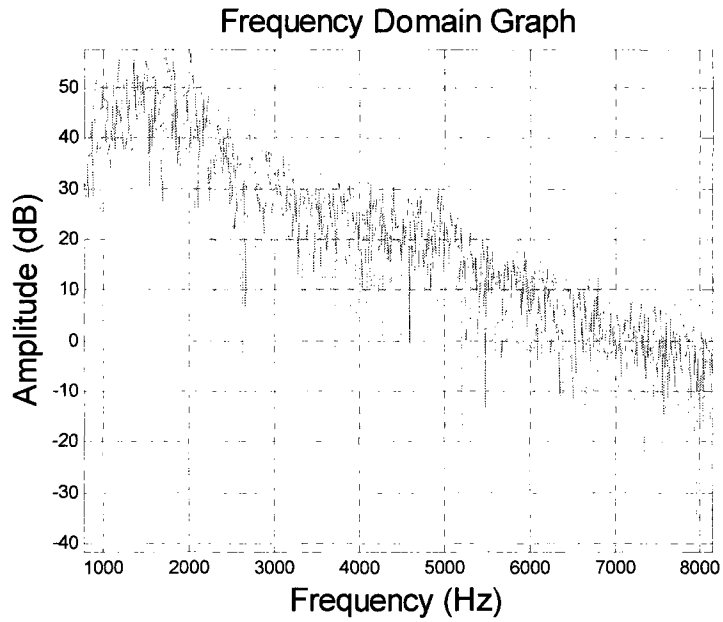

Figure 4.4: Frequency Domain of the Healthy Lung Sound

Figures 4.5 and 4.6 show the FFT plots of the inspiration and expiration phases of healthy breath cycle respectively. As can be seen from the plot the amplitudes of all the frequencies are higher during inspiration than those during expiration. However, the frequency range seem to be the same. Therefore, it is possible to characterize the normal lung sound as larger, louder sounds during inspiration than during expiration.

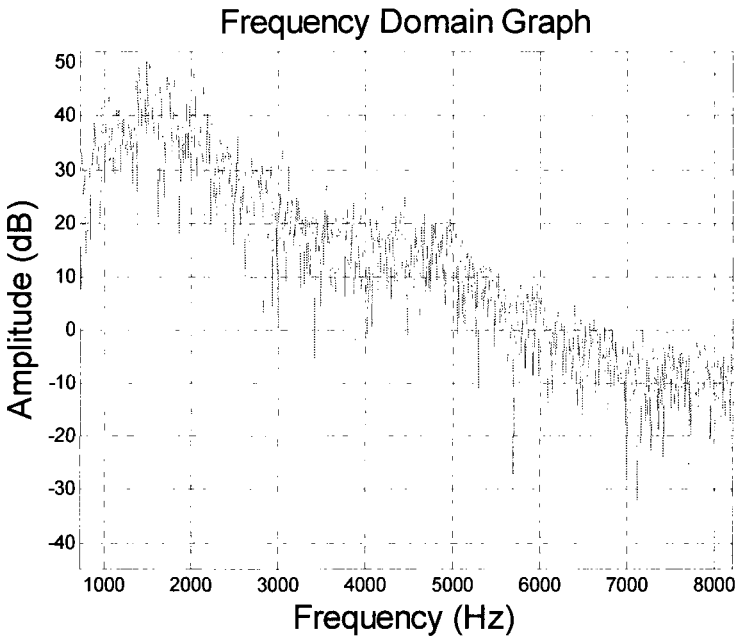

Figure 4.5: Frequency Domain of the Inspiration Phase of the Healthy Lung Sound

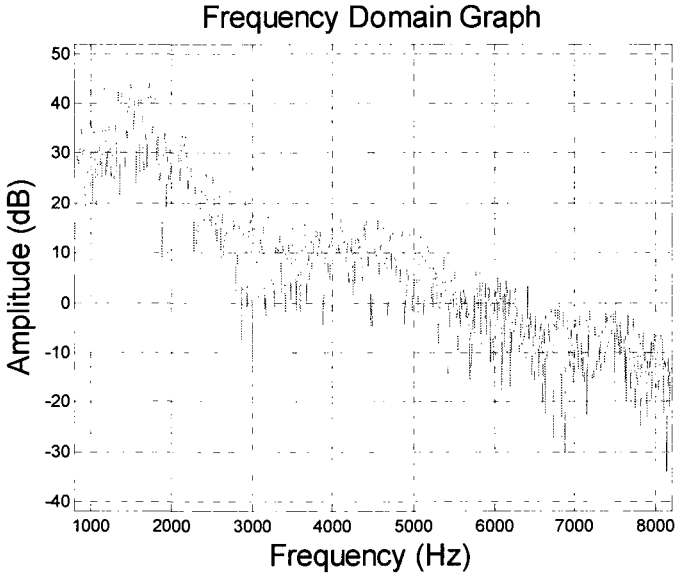

Figure 4.6: Frequency Domain of the Expiration Phase of the Healthy Lung Sound

With reference to Figure 4.7, the frequency plot of the breath sounds with crackles reveal that while the crackle duration is small, its frequency content cover a wider band than the normal sound signal. It should be noted though that the crackle frequencies and those of healthy breathing overlap in the major frequency contribution ranges.

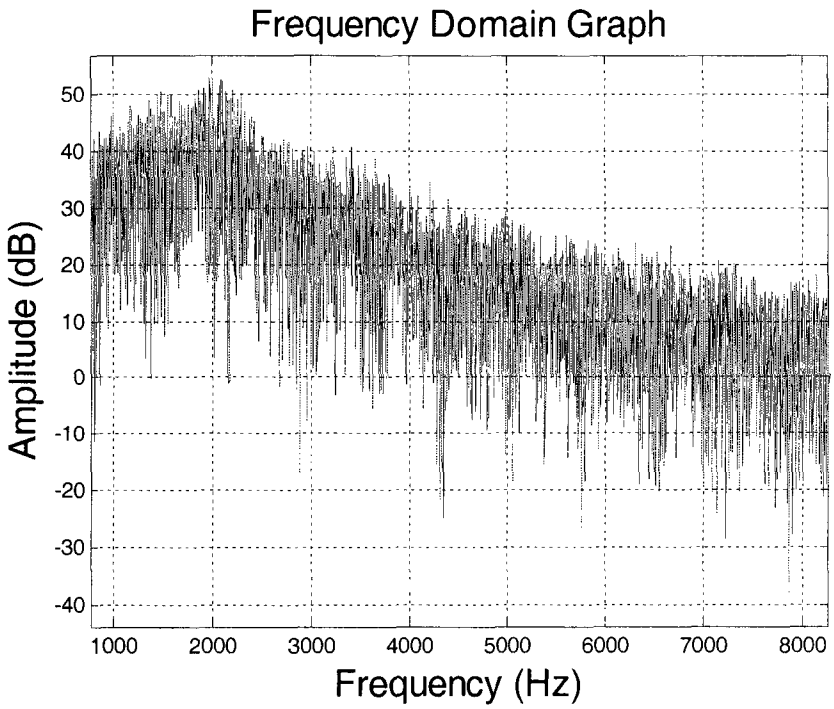

Figure 4.7 Frequency Domain of Crackle Lung Sound

Figures 4.8 and 4.9 show the FFT plots of the separated inspiration and expiration phases of the full respiration cycle shown in Figure 4.7. With reference to the figure, it is noticeable that crackle frequency content has higher magnitudes in the inspiration phase. Furthermore, the amplitude at very low frequencies is much higher than that during expiration as the phenomenon is primarily an inspiration one.

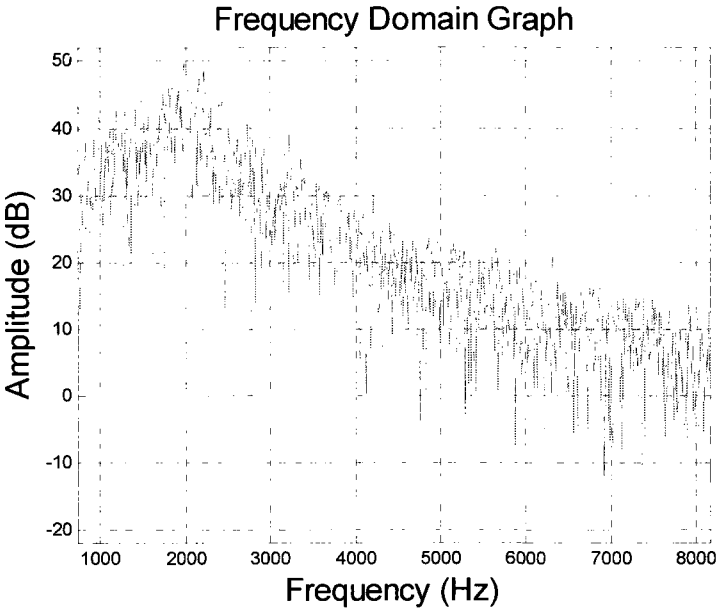

Figure 4.8: Frequency Domain of the Inspiration Phase of Crackle Lung Sound

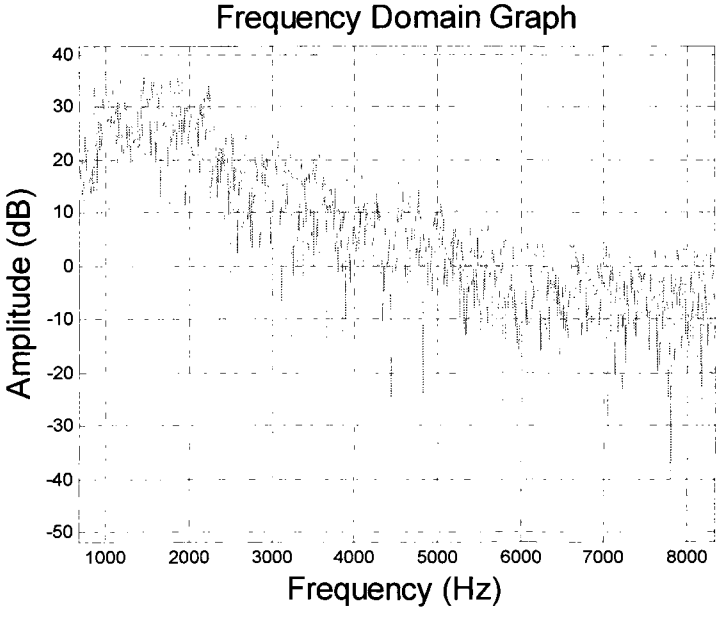

Figure 4.9: Frequency Domain of the Expiration Phase of Crackle Lung Sound

Figure 4.10 shows the frequency plot of the wheeze lung sound shown in Figure 4.3. The plot shows a distinctive pattern with a major contribution till about 3 KHz followed by an almost sudden drop in amplitude to a level higher than that of a healthy breath spectrum. This amplitude is sustained way into the high frequency range, and almost to 9 KHz.

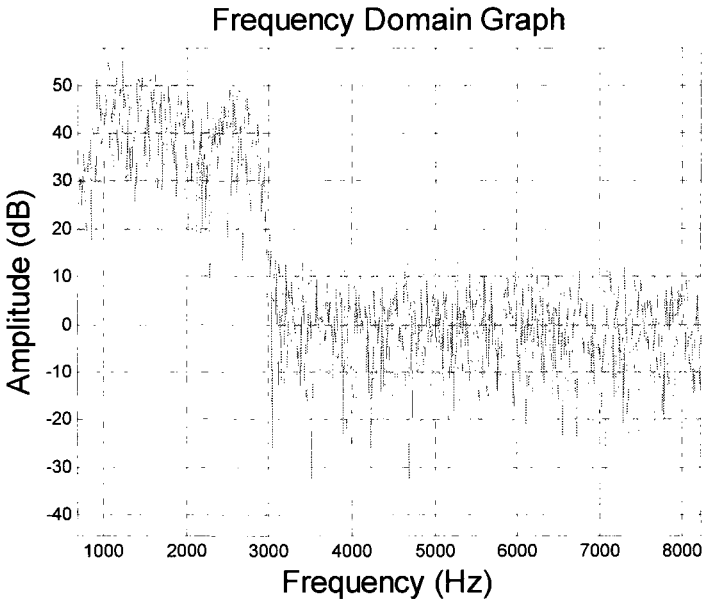

Figure 4.10: Frequency Domain of the Wheeze Lung Sound

Figures 4.11 and 4.12 show the FFT plots of the inspiration and expiration phases presented in Figure 4.10 separately. The plots show that the amplitude of different frequencies is higher in the expiration phase than in the inspiration one. This is contrary to the cases presented above for the healthy lung sound phases and those with crackles, and is attributed to the occurrence of wheezing in the expiration phase as has been mentioned above.

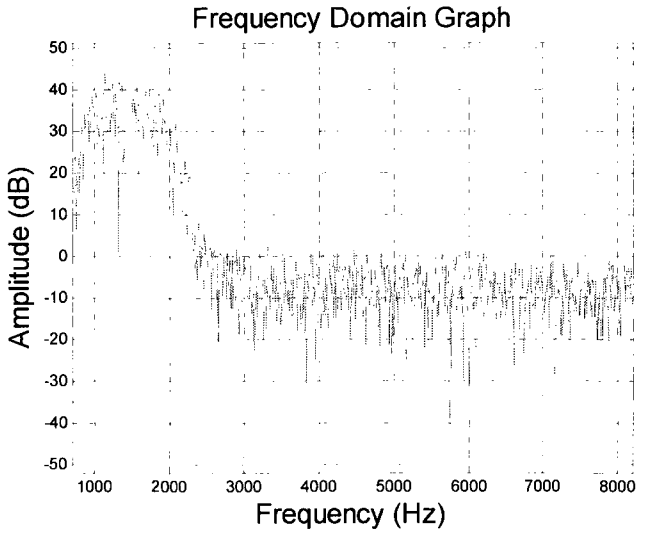

Figure 4.11: Frequency Domain of the Inspiration Phase of Wheeze Lung Sound

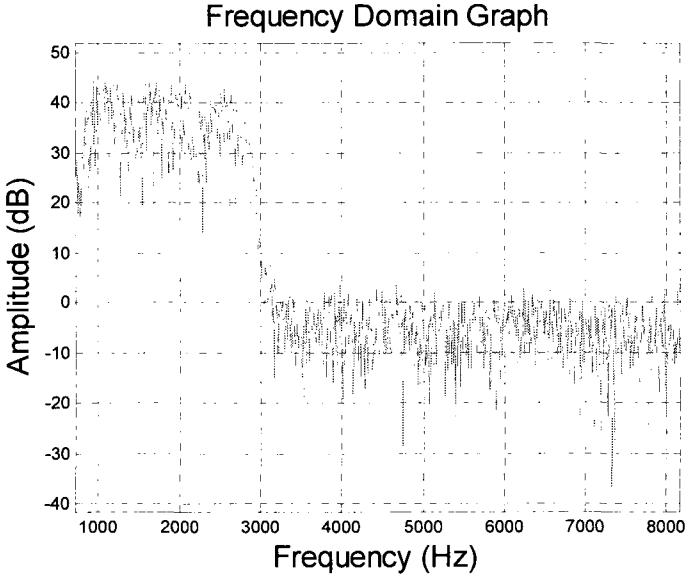

Figure 4.12: Frequency Domain of the Expiration Phase of Wheeze Lung Sound

4.2.2.2 Power Spectrum Density (PSD) of the Lung Sound Signals

Figure 4.13 shows plots of the computed average power of the lung sound signals over a given frequency (PSD). The plot shows a marked difference between the three types of lung sounds, however, as has been mentioned before, their frequency ranges overlap. The power at frequencies beyond 2 KHz is insignificant, but is higher for the case of the breath sound with wheeze.

The power spectrum plot of the healthy lung sound is highest at low frequencies, and decreases sharply beyond 100 Hz. The plot has an exponential character and decays smoothly towards its minimum. The plot also shows that there is very little acoustical contribution beyond 1.2 KHz.

The lung sound with crackle power spectrum plot again shows that most of the power is packed at low frequencies. The plot shows that the power drops fast beyond 100 Hz, be it a more gentler drop than that of the healthy lung sound. The contribution to the audible sound remains significant up to about 1.2 KHz, and continues to approximately 1.6 KHz.

Unlike the cases of the healthy lung sound and the one with crackle, the lung sound with wheeze power spectrum shows that it only after 1.4 KHz that the strength starts to decline. As has been mentioned in Section 2.4.2 the continuous music-like wheeze sound has a major tonal contribution between 600 Hz and 2 KHz. This can be observed here where the signal is still very perceptible up to 2 KHz, and can still be seen almost to 3 KHz.

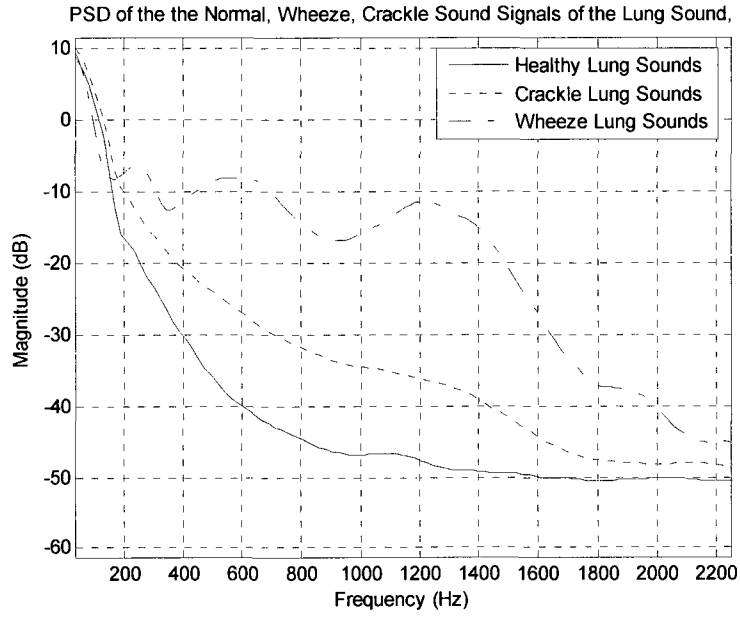

Figure 4.13: PSD of the Healthy, Crackle and Wheeze Lung Sounds

CHAPTER V

Neural Networks Based Identification of the Respiratory Acoustical Signals and Localization of Adventitious Respiratory Sounds

5.1 Introduction

A Neural Network (NN) is primarily a very complex function that maps the values of one or more inputs to a single or multiple outputs. However, it is distinguished from ordinary transfer function because the mapping is done by example rather than analytical or empirical. Specifically, one does not needs to know the analytical form of the functions governing the inputs to a NN to map them to the desired output. Rather, the network is provided with a set of inputs and corresponding desired outputs to "teach it" the expected behavior. In addition, NNs can adapt to changes in the inputs and outputs. That is, if the inputs change over time, the NN learning objective can continue to adjust its perceptron parameters to map the new inputs to the proper output. This feature of NNs creates a great potential for their application in signal processing and pattern recognition. NNs have a layout similar to the neurons in the human brain. That is, they are composed of functionally similar interconnected cells in a fashion similar to the synaptic connection of neurons to other neurons. Due to this similarity, the computational cells are often called neurons.

5.1.1 Perceptrons Neural Network Model Used for the Identification Process

A Multilayer Perceptrons (MLP) neural network with many neurons in a single hidden layer is used in this work for the identification process of lung sounds. Such a network has been constructed as a general approximation function for signal identification. A simple perceptron model consists of a single neuron with a linearly weighted network function and a threshold activation function as is shown in Figure 5.1. The input to the neuron $\boldsymbol{x} = [x_1, x_2, \ldots\ldots, x_n]$ is an element input vector weighted by a vector $\boldsymbol{w}$=[$w_1, w_2, \ldots\ldots, w_n$] where each element has a weight w_i. The network function $u(x)$ is the weighted sum of the inputs [53-55] and is given by:

$$u(x) = \sum_{i=1}^{n} x_i w_i \tag{3}$$

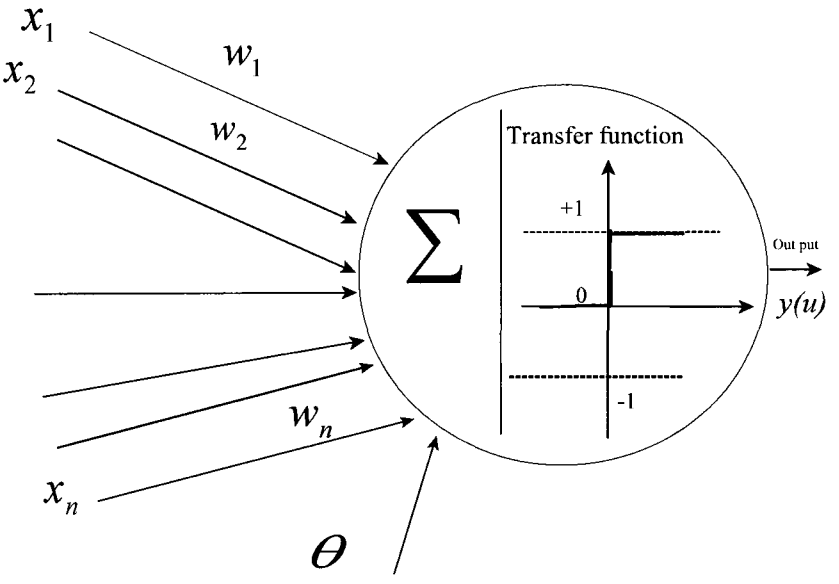

Figure 5.1: Perceptron Model

where θ is the bias, and the output $y(u)$ is obtained from $u(x)$ via a threshold activation function as follows:

$$y(u) = \begin{cases} 1 & u(x) \geq 0 \\ 0 & u(x < 0 \end{cases} \tag{4}$$

The perceptron architecture is similar to the ADALINE neural network that is used in NN filtering of the heartbeat from the lung sounds, but the ADALINE has a linear transfer function rather than the hard limiting one used in perceptron networks. Following Figure 5.2 shows the ADALINE neural network model.

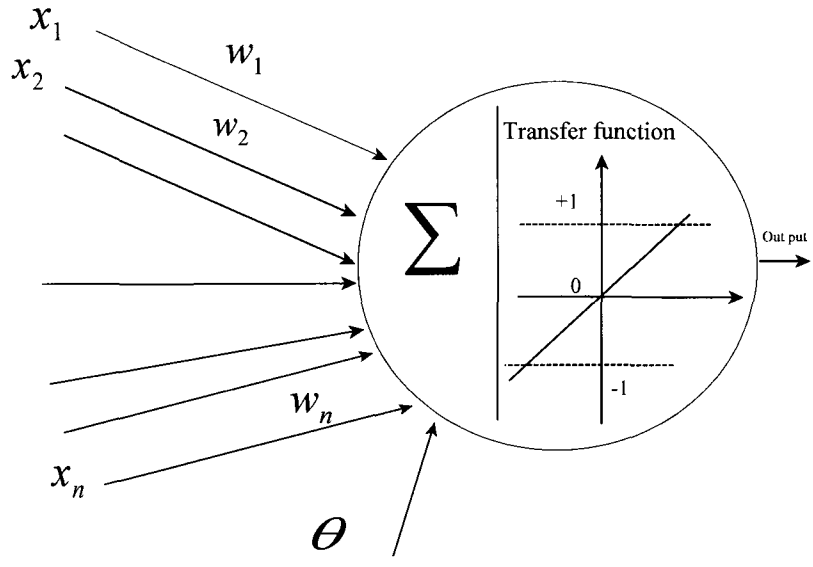

Figure 5.2: Model of the ADALINE

The perceptron neural network have been reported in the literatures to perform well for the problem of identification and classification of linearly separable signals [53].The perceptrons input feature vector x should narrowly matches the target vector through training for proper identification. This causes the inner product to exceed the threshold , and in turn causes the output to become +1 signifying the detection of a target. However, the perceptron neuron model can not be used for medical diagnosis and signal detection problems, because the respiratory sound signal patterns are not linearly separable. This difficulty can be remedied by using the Multilayer Perceptron (MLP) neural network.

5.1.2 Multilayer Perceptrons (MLP) Architecture for the Identification Process

A multilayer perceptron is a feed-forward artificial neural network model that maps sets of input data onto a set of an appropriate output. The MLP is the most effective neural network structure for identification and diagnoses applications. This network is a modified version of the standard linear perceptron network in that it uses more than one layer of neurons with nonlinear activation functions. As a result, it is more powerful than the perceptron in that it can distinguish data that is not linearly separable. The MLP was chosen for the diagnostic process for these reasons.

The architecture of a MLP network consists of an input layer, one or more hidden layers and an output layer. Each layer consists of one or more neurons. The weights of the MLP hidden and output neurons adjust adaptively throughout the course of the training process. The network's ability to identify patterns can be enhanced by increasing the number of hidden layers and/or the number of neurons in each hidden layer. The draw back, though, is an increase in the complexity of the network and the training period. Other problems like over-fitting or under-fitting may also be encountered. Under-fitting occurs when the MLP does not have enough hidden neurons and it is not effectively complex to solve the function approximation problem, and may produce excessive errors at the output. On the other hand, over-fitting occur when the MLP has too many hidden nodes, and would attempt to fit the noise.

In this research a Multilayer Perceptrons (MLP) neural network model with a feed-forward structure and a log-sigmoid activation function is used. Back propagation is used for training. Initial tests showed that the log-sigmoid activation function is able to successfully diagnose respiratory sound signals. The sigmoid function is a monotonic S-shaped one that maps values in the interval $(-\infty, \infty)$ to a finite interval, (-1,+1) or (0,1), and is given by:

$$f(u) = \frac{1}{1+e^{-u}} \tag{5}$$

Figure 5.3 shows a general MLP architecture, circles in the hidden and output layers represent individual neurons. The input layer has no neuron. The term 'hidden layer" signifying the fact that the output of these neurons will be fed forward to successor layer of neurons and not directly visible to the network output. The interconnections are provided only between neurons of consecutive layers and only feed forward patterns are used for the interconnections between neurons.

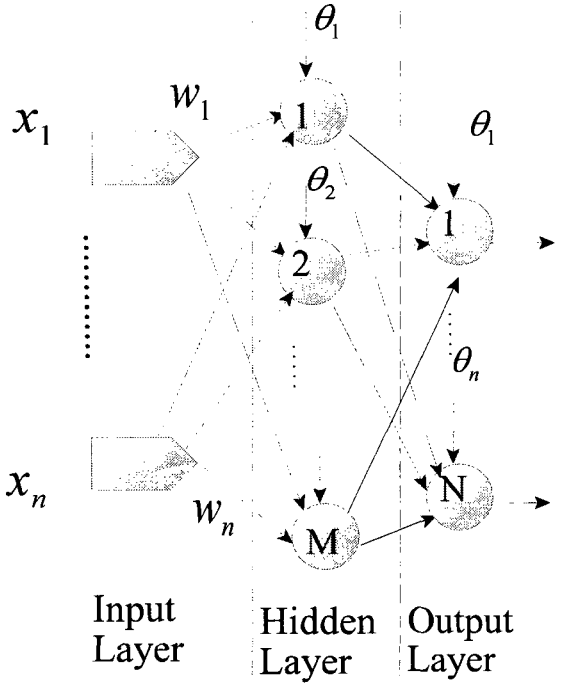

Figure 5.3 : MLP Architecture

The set of respiratory sound signals and the desired output pairs used for training are denoted by $\{(\boldsymbol{x}(k), \boldsymbol{d}(k)); 1 \leq k \leq K\}$. It should be noted that for a given $x(k)$ the corresponding output $\boldsymbol{d}(k)$ is a vector representing the desired output neurons response. Furthermore, for all members of a subset of the same type of sound (none lung sound, healthy, lung sound with crackle, and lung sound with wheeze) in the training set the desired output $\boldsymbol{d}(k)$ is the same. Training is accomplished by feeding all K inputs to the MLP network and computing the corresponding output $\{z(k); 1 \leq k \leq K\}$. Again here, $z(k)$ is the vector of actual output neurons response to the given training sample $x(k)$.

With reference to Figure 5.4 the summing junction output $u_j^l(k)$,of the j^{th} neuron in the l^{th} layer to a stimulus $z_i^{l-1}(k)$,which is the output of the i^{th} neuron in the l-1 layer, during training on the k^{th} training pair is given by:

$$u_j^l(k) = \sum_{k=1}^{K} z_i^{l-1}(k).w_{ji}^l(k) \qquad (6)$$

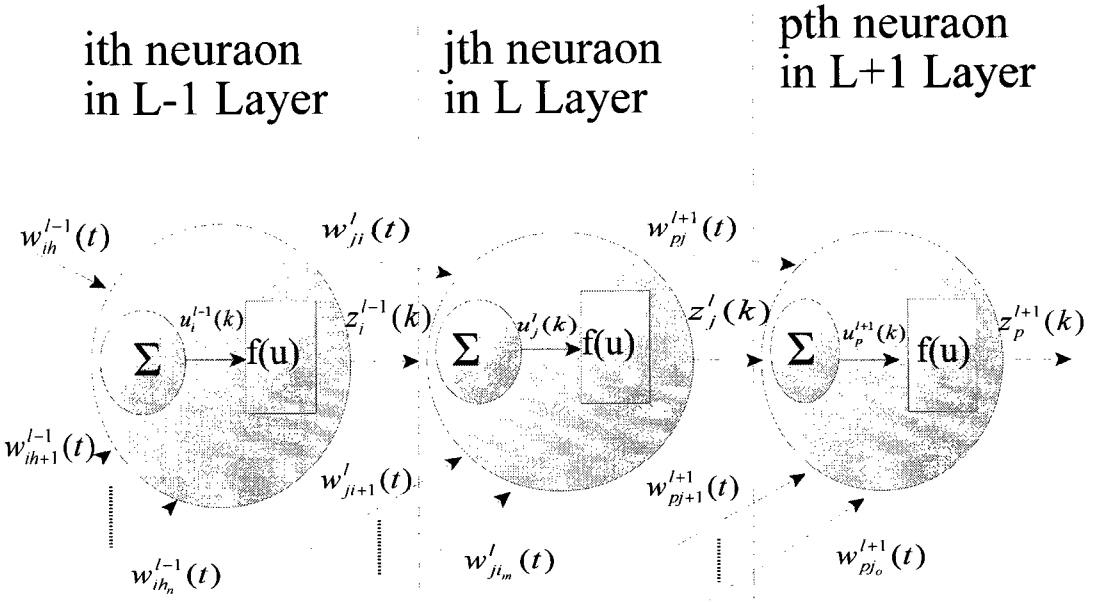

Figure 5.4: Notations Used in MLP

where j is the index of the neurons in the current layer and varies between 1 and M, i is the index of the neurons in the previous layer and varies between 1 and N, and p is the index of the neuron in the next layer and varies between 1 and O.

5.1.3 Back-Propagation in a Multiple Layer Perceptron Network for the Training of the Diagnosing Module

For the back propagation training process, the weights are determined by back-propagating the errors of the neurons of the output layer. These back-propagated errors are used as a basis for iterative adjustment of the connection weights for the entire network. The network performs the training process with a finite number of pattern pairs consisting of an input pattern and a desired output pattern. Each pass through the training pattern is called a cycle or an epoch t. The training is carried out until the outputs of two consecutive cycles of training is within a prescribed tolerance, or a maximum number of training epoches is reached. With reference to Figure 5.5, the calculation of the sum squared error E needed for the wight update is computed as follows [53-55]:

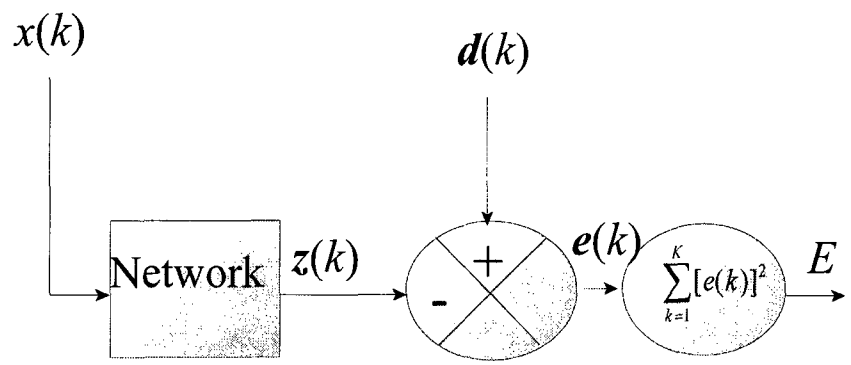

Figure 5.5: MLP Back propagation Error Calculation

$$E = \sum_{k=1}^{K} [e(k)]^2 = \sum_{k=1}^{K} [\boldsymbol{d}(k) - \boldsymbol{z}(k)]^2 \tag{7}$$

the wight update is carried out as follows:

$$\boldsymbol{W}(t+1) = \boldsymbol{W}(t) + \Delta \boldsymbol{W}(t) \tag{8}$$

where $\Delta \boldsymbol{W}(t)$ is the correction made to the current weights $\boldsymbol{W}(t)$. The objective is to adjust the weight matrix $\boldsymbol{W}$ to minimize the error E. The steepest descend gradient method is used for the calculation of the $\Delta \boldsymbol{W}(t)$ as follows:

$$\Delta \boldsymbol{W}(t) = -\eta \partial E / \partial \boldsymbol{W} \tag{9}$$

where η is the step size or the learning rate. The derivative of the error E with respect to individual weights for a given layer l in the MLP network $\partial E / \partial w_{ji}^{l}$ is given by:

$$\frac{\partial E}{\partial w_{ji}^{l}} = \sum_{k=1}^{K} \frac{\partial [e(k)]^2}{\partial w_{ji}^{l}} = \sum_{k=1}^{K} 2[d(k) - z(k)](-\frac{\partial z(k)}{\partial w_{ji}^{l}}) \quad for\ i = 0,1,\ldots n \tag{10}$$

It should be noted that $\boldsymbol{d}(k)$ in Equation 7 a constant for a given sound type $\boldsymbol{z}(k)$ as has been mentioned earlier. The partial rate of change of the actual output with respect to the weight for a given layer l shown in Equation 9 is given by:

$$\begin{aligned}\frac{\partial z(k)}{\partial w_{ji}^{l}} &= \frac{\partial f(u_j^l(k))}{\partial u_j^l}\frac{\partial u_j^l(k)}{\partial w_{ij}^l} \\ &= f'(u_j^l(k))\frac{\partial}{\partial w_{ji}^l}\left(\sum_{i=0}^{n} w_{ji}^l z_i^{l-1}\right)(k) \\ &= f'(u_j^l(k))z_i^{l-1}(k)\end{aligned} \tag{11}$$

substituting Equation 11 in 10 and rearranging gives:

$$\frac{\partial E}{\partial w_{ji}^l} = -2\sum_{k=1}^{K}\delta_j^l(k)z_i^{l-1}(k) \tag{12}$$

where $\delta_j^l = [d(k) - z(k)]f'(u_j^l(k))$, is the error signal modulated by the derivative of the activation function and hence represents the amount of correction needed to be applied to the weight w_{ji}^l for the given input $z_i^{l-1}(k)$.

Given the delta error, the weights are updated using the formulation of the general weight update and is given by Equation 5 in long form as follows:

$$w_{ji}^l(t+1) = w_{ji}^l(t) + \eta\cdot\sum_{k=1}^{K}\delta_j^l(k)z_i^{l-1}(k) \tag{13}$$

The above weight update scheme can lead to weight magnitude oscillation in some cases or to slow convergence in others. A momentum parameter μ is introduced to moderate or speed up the update rate as follows:

$$w_{ji}^l(t+1) = w_{ji}^l(t) + \eta\cdot\sum_{k=1}^{K}\delta_j^l(k)z_i^{l-1}(k) + \mu\left[w_{ji}^l(t) - w_{ji}^l(t-1)\right] \tag{14}$$

Values of μ chosen between $0 < \mu \leq 0.5$ slow down the update rate and stabilize perceptron weight update oscillation. Values of μ chosen between $0.5 < \mu \leq 1$ speeds up the update process and results in faster conversion.

The complete sets of training process and tests result of the NN's diagnosing process will be explained in the following subsection.

5.2 Training Process for the Lung Sound signals Identification Network

In this work a neural network is utilized as the core of the lung sound diagnosis system. The architecture used is that of a feed forward back propagation network explained above. This architecture includes an input layer, one hidden layer with 10 nodes, and the output layer. Such networks are trained by providing them with samples of pairs of input information and the corresponding output. They deduce, or learn, from data pair the pattern, and should be able to respond correctly to any input information within the range of the training data set. The number of hidden layers and the number of nodes in them has been selected based on extensive experimentation carried out on networks with different numbers of layers and nodes. The selected set of numbers results in the best overall diagnosing results on different lung sound signals. Furthermore, the network avoids the problems associated with over fitting and under fitting phenomenons. Under-fitting occurs when the MLP does not have enough hidden neurons and it is not effectively complex to solve the function approximation problem, and may produce excessive errors at the output. On the other hand, over-fitting occur when the MLP has too many hidden nodes, and would attempt to fit the noise.

5.2.1 Data Set Preparation and Usage

The network is trained using three sources of data; data recorded using the developed automatic auscultation system, data from clinically recorded lung sounds used for training medical students [57- 59], and data synthesized by injecting various noise sounds with different loudness to the previously mentioned two sets of data. The noise polluted set is used to train the system on correctly diagnosing adventitious pulmonary sounds irrespective of the noise level present in the

surrounding environment. A total of 120 sound samples were used for the training and testing. 60 of these samples are noiseless lung sounds, while 60 are noisy with varying noise loudness.

The 60 noiseless samples contain 20 normal lung sounds, 20 with wheezes, and 20 with crackles. The noisy samples are again equally divided into normal lung sounds, ones with wheezes, and ones with crackles. The format of all sound data samples is that of digital WAVE files. The WAVE format is a time based one which contains uncompressed audio in the pulse-code modulation (PCM) format. PCM audio is the standard audio file format for CDs, containing two channels of 44,100 samples per second, 16 bits per sample. While that format is suitable for audio listening it is not very suitable for signal analysis, processing and identification. For this work the PSD of the sound files was used for training and testing. For diagnosing purposes, however, the subject lung sounds are digitized and stored in WAVE format for audio inspection by the physician and technician or for subsequent analysis.

5.2.2 The Training Process

The philosophy of training adopted here involves a primary training phase, a secondary phase, and a reinforcement phase. During the primary phase the network is trained to recognize noiseless data of none lung sound, healthy lung sound, lung sound with wheeze, and lung sound with crackle. As has been mentioned earlier, the heartbeat was filtered out of all sound data. Figure 5.6 shows the progression of the network training during the primary phase. The target, or acceptable Sum Square Error (SSE) was set at 0.1, the allowable number of epochs was set to 5000, and the momentum constant was set to 0.95. The figure shows that the SSE starts at about 13 and monotonically decreases to below the target (0.0906).

In the secondary phase, the network is trained on recognizing noisy sound files. Again here, none lung sound, healthy lung sound, lung sound with wheeze, and lung sound with crackle together with the appropriate response in each case is fed to the network. The target SSE is set in this case to 0.6 due to the presence of the noise, and so as not to unduly prolong the learning time for this

secondary phase. The maximum number of epochs allowed was set to 1000, again to reduce the time spent in this phase, and the momentum constant was set to 0.95. Figure 5.7 shows the training progression of the network. With reference to the figure, and as expected, the SSE shoots high to 13.8 at the beginning of training due to signal contamination. However, it takes less epochs than previous phase to drop monotonically below the target to 0.5756.

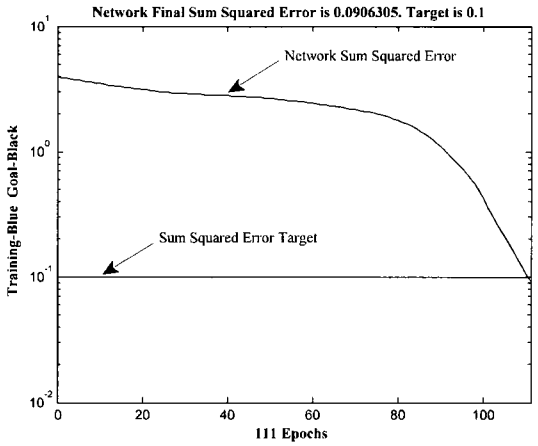

Figure 5.6: Progression of Primary Training with Noiseless Breathing Sounds.

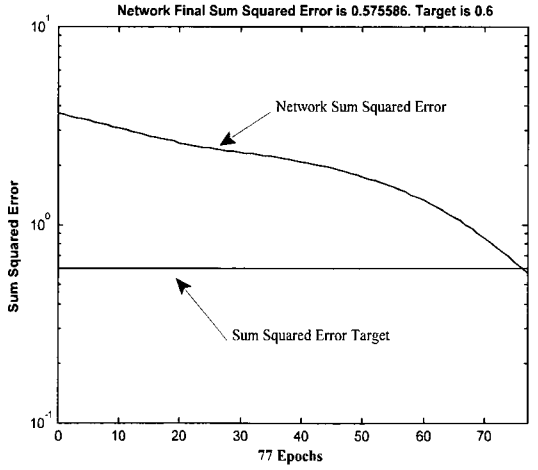

Figure 5.7: Progression of Secondary Training with Noisy Breathing Sounds

The third reinforcement phase is critical in the sense that it attempts to correct some of the "unlearning" that occurred due to the presence of noise. In this phase, the network is trained again on a complete set of noiseless data. The target SSE is again set low to 0.1, the maximum number of epochs allowed for this training was set to 500, and the momentum constant was set to 0.95. Figure 5.8 shows the results of training the neural network during the reinforcement phase. The figure shows that at the inception of learning, the SSE is very low, at 0.12, and slides monotonically downward to the 0.0997 level with less number of epochs.

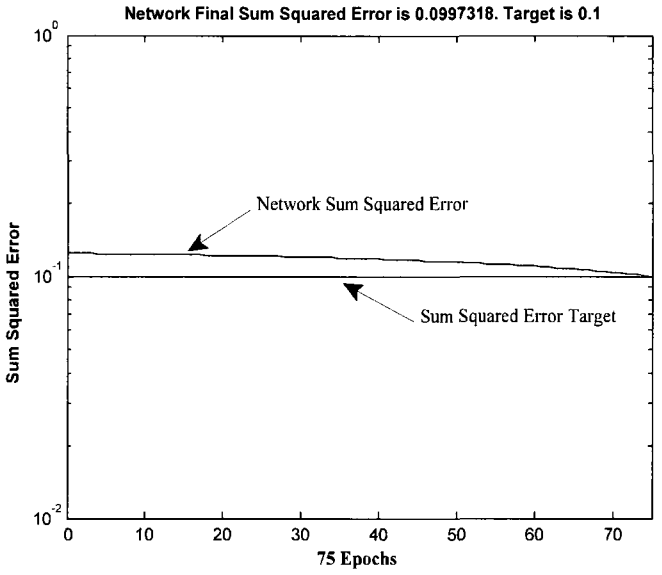

Figure 5.8: Progression of Reinforcement Training with Noiseless Breathing Sounds

5.2.3 Test Results

The ability of the network to identify the different lung sounds for which it was trained was tested using data files that the network was not trained on. These sound files were reserved specifically for testing. During testing the network learning algorithms were turned off, and the network is considered to be mature at this stage. The input to be identified is effectively presented to all the network inputs. The network responds by placing a normalized confidence level on its outputs corresponding to the lung sounds it was trained to identify. On any of the four outputs the maximum confidence levels are 1 if the sound is deemed to positively belong to this output, and 0 if the output is deemed to positively does not belong to this output.

Figures 5.9 to 5.11 show the test results for files of healthy lung sounds, lung sounds with wheezes, and lung sounds with crackles respectively. Each of the bar graph sets in a figure correspond to one of ten test results. Each of the color bars in a set corresponds to a network output. The confidence levels on these outputs are proportional to the length of the bars, and are tabulated numerically below each graph. With reference to Figure 5.9, when the network was presented with ten healthy lung sounds, it was able to identify them correctly with a very high confidence level that varied between 0.977 and 0.98. The maximum output on any of the network's other output was 0.136, which signifies that the network identifies the sound as not belonging to these outputs. When the network was presented with lung sounds with wheezes, it identified these with confidence levels between 0.82 and 0.933 as shown in Figure 5.10. For the case of lung sounds with crackles, the confidence level for the identification ranged between 0.777 and 0.999. It should be noted that the variation in identification confidence level is primarily due to the presence of noise in the signal, and the relative amplitude of that noise.

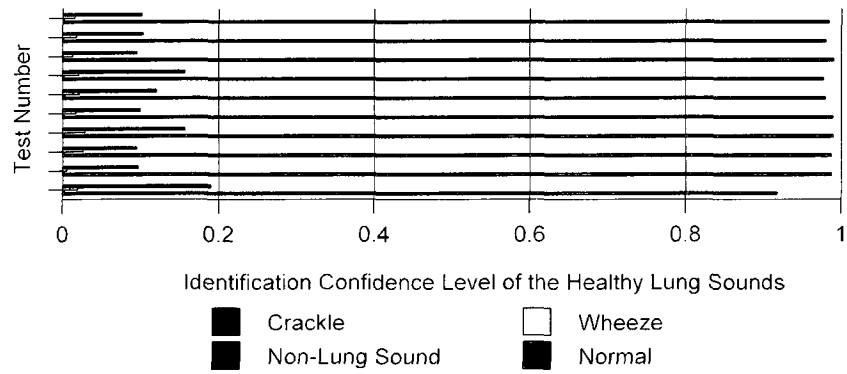

Normal	0.9177	0.9871	0.9866	0.9891	0.9887	0.9792	0.9773	0.9904	0.9805	0.9839
Non-Lu>	0.0017	0.0017	0.0023	0.0022	0.0019	0.0029	0.0017	0.0021	0.0021	0.0016
Wheeze	0.0191	0.0052	0.0262	0.0284	0.0168	0.0211	0.0209	0.013	0.0178	0.0152
Crackle	0.1895	0.0966	0.0947	0.1566	0.0994	0.1201	0.1565	0.0954	0.1033	0.1009

Figure 5.9: Confidence Level when NN is asked to Identify Healthy Lung Sounds

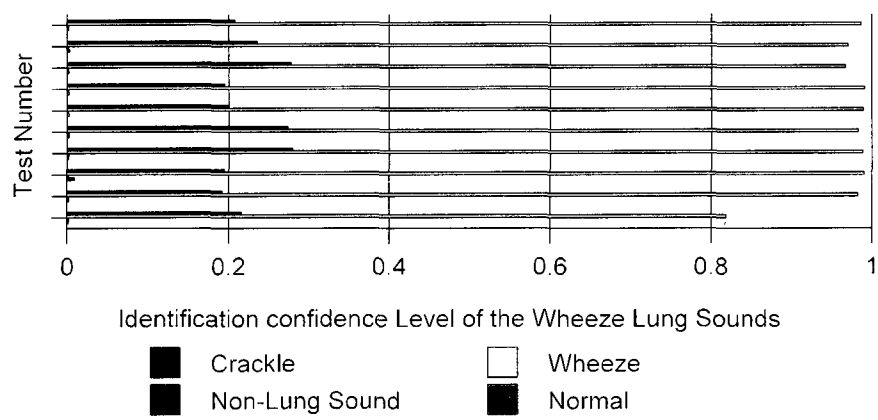

Normal	0.0013	0.0019	0.0094	0.0014	0.0023	0.0026	0.0024	0.0018	0.0028	0.0023
Non-Lu>	0.0019	0.0014	0.0017	0.0021	0.0019	0.0014	0.0017	0.0014	0.0016	0.0019
Wheeze	0.8189	0.9829	0.9908	0.9885	0.9827	0.9892	0.9908	0.9672	0.9699	0.9862
Crackle	0.2161	0.192	0.1955	0.2795	0.2734	0.1994	0.1955	0.2776	0.2361	0.208

Figure 5.10: Confidence Level when NN is Asked to Identify Wheeze Lung Sounds

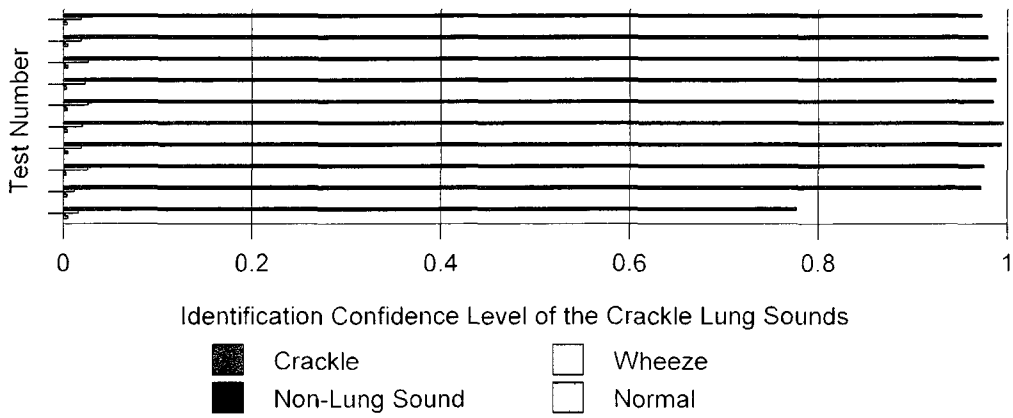

Normal	0.0048	0.0039	0.0036	0.0045	0.0038	0.0042	0.0031	0.0049	0.0047	0.0042
Non-Lung>	0.0019	0.0022	0.0019	0.0014	0.0021	0.0026	0.0019	0.0018	0.0018	0.0026
Wheeze	0.0157	0.0119	0.0257	0.0187	0.0199	0.0262	0.0227	0.0266	0.0189	0.0192
Crackle	0.7771	0.9722	0.9745	0.9936	0.9957	0.9851	0.9875	0.9908	0.9791	0.9728

Figure 5.11: Confidence Level when NN is Asked to Identify Crackle Lung Sounds

5. 3 Identification of Different Infected Sites of the Diseased Lungs

While one of the major objectives of the identification and differentiation among healthy lung sounds, wheezes, and crackles is done in the previous sections, this section will achieve the other major objective of the identification of the different infected sites in the lungs.

A wheeze or crackle detected in only one channel indicates that there is only one source of the adventitious sound signals, which means only one infected site in the lungs. However, adventitious sound signals (wheeze or crackle) detected in multiple channels indicate two possibilities. Either the channels represent one source of adventitious sound (one infected site), or they represent different infected sites. Lung sound signals with almost identical characteristic signatures are coming from the same source of infected site and vice versa.

A preliminary study of correlation analysis of advantageous sounds concluded that any two of the same type of the lung infection sound signals seem to be related. However, due to the

listening to the signals. In addition, the existence of any pulmonary infections at different sites add to the complexity of the pulmonary acoustical signals. It is apparent that these signals have highly related patterns and that some of the acoustical signals acquired by the multi-channel electronic stethoscope are very similar and cannot be discerned audibly. Hence statistical techniques like cross correlation are being investigated here as a means of localization.

The correlation process is a mathematical one that uses statistical techniques to identify similarities between signals. In general, the correlation is carried out on two signals to produce a third; if a signal is correlated with itself the resulting signal is an auto-correlation; otherwise it is a cross-correlation. The amplitude of each sample in the resulting correlation signal is a measure of how much the two correlated samples are similar. This means that the correlation value is maximized when one sound signal resembles the other. Hence, how identical the lung sound signals are can be ascertained quantitatively through this process.

5.3.1 Cross-Correlation of the Lung Sound Signals Acquired by the Multichannel Stethoscope

The cross-correlation of the identified adventitious lung sound signals acquired by the multi-channel electronic stethoscope will be used to map the mutual relationships among them. This will help in locating the sources of these adventitious sounds in the lungs. The strength of the cross-correlation function (CCF) resulting from the correlation process is an excellent indicator of the degree of similarity between the adventitious lung sounds identified.

The correlation process involves cross-correlating channels diagnosed with the adventitious sounds with all other channels diagnosed as having adventitious lung sound of the same type to check if they represent the same source of infection or not. Signals that are highly related and produce strong correlation signals will be categorized as having the same source of infection.

In general, the CCF has the property of being in the range [-1, 1] with 1 indicating perfect correlation. That means the signals exactly overlap. If the two adventitious lung sound signals vary together (that is, when one of them is above its expected value [arithmetic means] and the other variable is above its expected value as well), then the correlation between the two lung sound signals will be positive. On the other hand, when one of them is above its expected value and the other variable is below its expected value, then the correlation between the two lung sound signals will be negative.

The cross correlation coefficient in statistics is defined as the arithmetic mean of the products of the standardized form of two variables X and Y, which is $X - \mu_x / \sigma_x$ and $Y - \mu_x / \sigma_x$. Then the correlation can be calculated as follows:

$$\rho = E\left[\left(\frac{X-\mu_x}{\sigma_x}\right)\left(\frac{Y-\mu_y}{\sigma_y}\right)\right] \tag{15}$$

where E is the expected value which is the arithmetic mean. X and Y are variables, and are the two adventitious sound signals of the same type under correlation consideration. The μ_y & μ_x are the expected value (arithmetic mean) of the two adventitious sound signals X and Y, and the σ_y & σ_x are the standard deviation of the two signals X and Y respectively. The standard deviation is the squar root of the variances of the X and Y. The variance of X and Y can be measured from averaging the squares of the deviations of its possible values from its expected value (mean). When a random variable X has an expected value $\mu = E(X)$, then the variance σ^2 of X is given by:

$$\sigma_x^2 = E[(X-\mu)^2] \tag{16}$$

Equations 15 can hence be written as :

$$\rho = \frac{E[(X - \mu_x)(Y - \mu_y)]}{\sigma_x \sigma_y} \tag{17}$$

As explained above, ρ can take any value from -1 to 1, and $\rho = 1$ indicates a complete correlation between X and Y.

The numerator is called is cross covariance of the two variables X and Y

$$\sigma_{xy} = E[(X - \mu_x)\,(Y - \mu_y)] \tag{18}$$

and is calculated as follows:

$$\sigma_{xy} = \frac{\sum_{i=1}^{n} (x_i - \bar{x})(y_i - \bar{y})}{n} \tag{19}$$

The positive average of the product $(x_i - \bar{x})(y_i - \bar{y})$ implies that most of the individual samples with locations in the same direction against the means $\bar{x}$ and $\bar{y}$ are such that the X and Y considered to be positively correlated. Similarly, a negative average of the product $(x_i - \bar{x})(y_i - \bar{y})$ implies that most of the individual samples with locations in a different direction against the means $\bar{x}$ and $\bar{y}$ are such that the X and Y are considered to be negatively correlated.

5.4 Detecting the Repeated Occurrence of Lung Sound Patterns.

With reference to Figure 5.12, a source of infection may broadcast its sound signal to different channels in the electronic stethoscope array. Furthermore, multiple infections may also broadcast sound to the same channel. In order to identify the locations of the infections, it is necessary to identify the recurring presence of specific waveforms emanated from the different sources and compare them together.

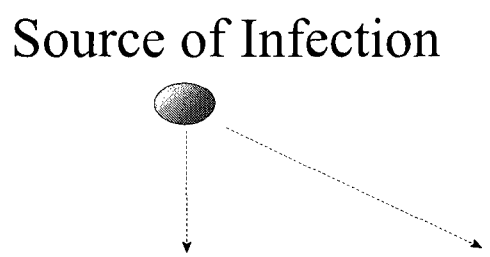

Figure 5.12: One Source of Infection Detected by Two Different Channels of the Stethoscope

To do so, the correlation values between two or more detected adventitious lung sound signals of the same type should be calculated. Through the experiments carried on in this research on healthy lung sounds, wheezes and crackles from different patients, it was concluded that the correlation values of the same type of lung sound signals that exceed the 90 percent confidence limits indicate statistically significant correlation. In other words, when the correlating signal of two adventitious sound signals acquired by different channels has a value of 90% or higher, this will be taken to indicate that those signals represent the same source of infection.

5.4.1 Verification of the Lung sound Signals Using Cross-Correlation

Adventitious sound signals from the database of the clinically recorded lung sounds used for training medical students [57- 59] are going to be used in a novel process for hypothetical patient generation in Chapter 6 . Table 5.1 summarize such adventitious lung sound signals and present the index of the patients, the type of the anomalous lung sound signals (wheeze and crackle), and the number of adventitious sounds acquired from the patient. For example, patient number 1 has one adventitious sound signal of a wheeze, while patient number two has two adventitious sound signals of crackle that are being referenced as signals 2A and 2B, and so on. These sound signals of the same type are correlated together in order to verify the resemblance among them. For example, wheeze lung sounds from all the patients in Table 5.1 are cross-correlated, and the results are presented in Figure 5.13. The same process was used for the correlation of the crackle sound signals and the results are presented in Figure 5.14.

Patients Index	Number of Signals	Type of Lung Sounds
1	1	Wheeze
2	2 Signal A Signal B	Crackle Crackle
3	1	Wheeze
4	1	Wheeze
5	1	Wheeze
6	1	Crackle
7	1	Crackle
8	1	Crackle
9	1	Wheeze
10	2 Signal A Signal B	Wheeze Wheeze

Table 5.1: Source of Adventitious Lung Sounds

The following figures present the cross-correlation process output of the wheeze and crackle of the different patients in Table 5.1. With reference to Figures 5.13 and 5.14, the correlation signals of any two of the lung sound signals of the same type can be associated, however, non of them are identical and the degree of similarity varies depending on the nature of the lung signals. This can be concluded since none of the CCF values come close to the 90% value and none are low enough to declare them totally dissimilar.

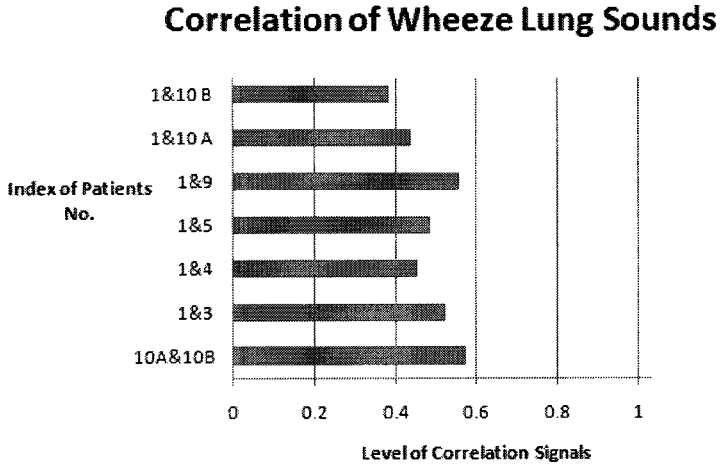

Figure 5.13: Cross-Correlation of Different Wheeze Lung Sound Signals

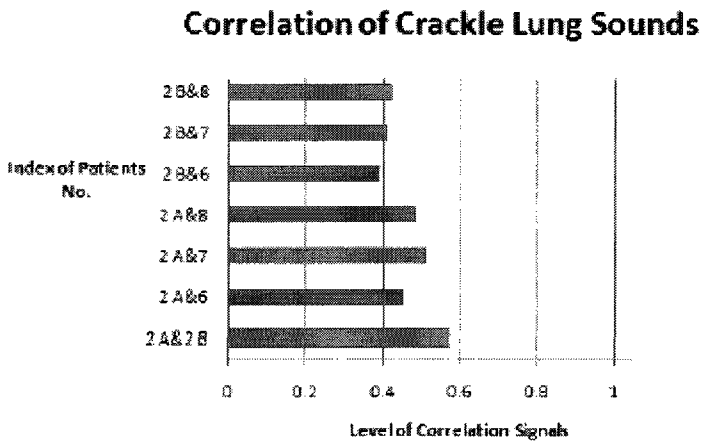

Figure 5.14: Cross-Correlation of Different Crackle Lung Sound Signals

CHAPTER VI

Testing the Identification and Localization of Different Infected Sites of the Diseased Lungs

6.1 Introduction

The process and methodology of lung sound acquisition, analysis, identification, differentiation and localization among healthy lung sounds, wheezes, and crackles were developed and presented in the previous chapters. The remaining work of assessing and testing the performance of the identification and localization modules of the computerized automated system will be reported in this chapter. The process consists of three major steps. Firstly, due to the difficulty and length of the procedures to acquire approval for a clinical trial, virtual patients were generated from the available database that was summarized in Table 5.1 and the recorded healthy lung sound signals acquired from different healthy individuals. Secondly, the efficacy of the identification module of the system is tested using the lung sound signals of the generated patients in order to diagnose different types of lung sounds (healthy lung sounds, wheezes, and crackles). Thirdly, the efficacy of the localization module of the system is tested using the diagnosed adventitious lung sound signals from the generated patients to localize the source of infection.

6.1.1 The Process of Generating Virtual Patients

Virtual patients are generated by extracting adventitious sounds from the lung sound files of sick patients, modifying them and superimposing them on lung sound files of healthy patients.

Let wave form w of the lung sound signals that consist of healthy and adventitious sounds be denoted as follows:

$w\{H_m^n \ \lambda A_m^n\}$;

where H represents the healthy part of the lung sound, A represents the adventitious part, λ represent the adventitious sound intensity level ($\lambda = 1$ for original intensity), subscripts (e.g. n) represent the patient number in the database, and

superscripts (e.g. m) represent the channel number.

In this process for generating virtual patients, the original lung sound signals such as $w\{H_1^1\ 1A_1^1\}$ and $w\{H_1^2\ 1A_1^2\}$ are processed to extract the adventitious part such as ($w\{A_1^1\}$ and $w\{A_1^2\}$). The intensity of this adventitious parts are modified to produce another set of signals such as $w\{\lambda A_1^1\}$ and $w\{\lambda A_1^2\}$. The following Table 6.1 presents all the adventitious sounds that were extracted from the patients in Table 5.1, and are used in generating virtual patients.

Patient Number	**Channel Number**	**Symbols of the Adventitious Sounds**	**Type of The Adventitious Sounds**
1	**1**	$w\{A_1^1\}$	**Wheeze**
2	**1**	$w\{A_1^2\}$	**Crackle**
2	**2**	$w\{A_2^2\}$	**Crackle**
3	**1**	$w\{A_1^3\}$	**Wheeze**
4	**1**	$w\{A_1^4\}$	**Wheeze**
5	**1**	$w\{A_1^5\}$	**Wheeze**
6	**1**	$w\{A_1^6\}$	**Crackle**
7	**1**	$w\{A_1^7\}$	**Crackle**
8	**1**	$w\{A_1^8\}$	**Crackle**
9	**1**	$w\{A_1^9\}$	**Wheeze**
10	**1**	$w\{A_1^{10}\}$	**Wheeze**
10	**2**	$w\{A_2^{10}\}$	**Wheeze**

Table 6.1: Adventitious Sounds Used in Generating Patients

Lung sounds recorded from healthy individuals are recorded and are used as base signals for generating virtual patients. These carrying signals will be referred to as *Gx*, where *x* is the generic individual number. The extracted adventitious sounds presented in Table 6.1 and modifications thereof are superimposed on some of the 20 channels of the lung sound signals recorded from the healthy individuals to generate virtual patients with different infections and locations of infections. The symbolic representation of this process follows:

$$w\{H_y^{Gx}\} \oplus w\{\lambda A_z^v\} \Rightarrow w\{H_y^{Gx} \lambda A_z^v\}$$

Examples of virtual lung sound signals produced follow:

$$w\{H_1^{G1}\} \oplus w\{\lambda A_1^1\} \Rightarrow w\{H_1^{G1} \lambda A_1^1\} \ ;$$

$$w\{H_2^{G1}\} \oplus w\{\lambda A_1^1\} \Rightarrow w\{H_2^{G1} \lambda A_1^1\} \ ;$$

$$w\{H_3^{G1}\} \oplus w\{\lambda A_1^1\} \Rightarrow w\{H_3^{G1} \lambda A_1^1\} \ ;$$

$$w\{H_4^{G1}\} \oplus w\{\lambda A_1^1\} \Rightarrow w\{H_4^{G1} \lambda A_1^1\} \ ;$$

Lung sounds attenuate as they propagate through the parenchyma (the lung tissue). This attenuation is properly taken into consideration when generating the virtual patients. The lung sounds attenuation is frequency dependent [99-101]; (refer to Chapter 2 for details). In fact, the attenuation varies based on the frequency, the propagation distance, and the different level of lung inflation as well [102]. In their work, Berger et al [102] produced a lung sound attenuation chart for frequencies between 1500 Hz and 3000 Hz, and for different lung inflations. With reference to Figure 6.1, using extrapolation methods (MATLAB toolbox), the results reported by Berger et al are extended to cover two additional frequencies of 500 Hz and 1000 Hz.

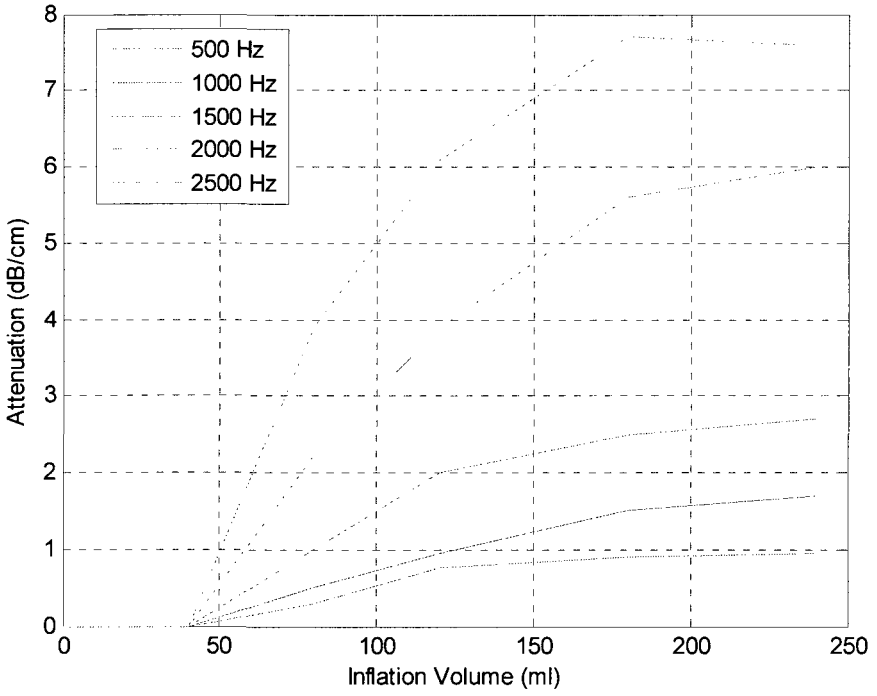

Figure 6.1 Extrapolation of the Attenuation dB/cm vs Frequency and Inflation

The lung sounds propagate through different distances to reach different elements of the stethoscope array deployed at different sites on the upper torso. Based on a sound speed of 30 m/s in the lung parenchyma [101] a delay of 4.0×10^{-4} s/cm is added to the adventitious sound signals (wheeze and crackle). The attenuation of the adventitious lung sounds has been calculated and added based on the difference in the propagation distance, frequency, and inflations. The difference in the propagation distance depends on the location of the lung infection and the position of the stethoscope channel.

As has been discussed before, the elements of the stethoscope array of the computerized auscultation system are deployed around the upper torso in order to auscultate all the lung lobes simultaneously. The five lung lobes and their subdivisions (the segments) have been identified and named in Chapter 2. When an auscultated patient is suspected of having a lung infection, it is common to confirm the finding through radiographic means. If an infection is revealed, the radiologist

would normally identify the infection site relative to the lung lobes and their segments. Accordingly, the distribution of infection spots are set within selected segments of the different virtual patients. Furthermore, it is assumed that the infection always occur at the center of the segment.

The sound propagation distance is calculated mainly using the straight line length between the position of the assumed infection and the position of the receiving element of the stethoscope array on the body of the subject from which the lung sounds were auscultated. The detailed discussion on the lung's lobes position with respect to the chest's ribs, their segments physiology and positions, the auscultation process, and positions of the stethoscope channels was presented in Chapters 2 and 3. The sound propagation distance in the parenchyma is used to calculate the appropriate attenuation of the adventitious lung sound based on the frequency and a lung inflation level. In addition to the attenuation, different severity levels of infection are assumed as well. The infection severity levels are assumed to correspond to different adventitious sounds SPL, and are categorized as follows: 0.75 - 0.90 of the original SPL for low infection, 0.90 - 1.0 of the original SPL for the medium infection, and 1.0 - 1.2 of the original SPL for high infection.

The lung inflation scale presented in Berger et al work [102] is mapped here to the lung inflation levels commonly reported during auscultation. The residual lung capacity is 1200 ml, and the normal tidal volume (the volume of air inhaled during inspiration and exhaled during expiration) is measured to be 500 ml. However, during the medical auscultation procedure, a patient is asked to ``take a deep breath`` which results in a tidal volume much larger than the normal 500 ml and can go up to the inspiratory capacity which is about 3500 ml. This tidal volume depends largely on the age of the patient and their medical condition among other factors. The attenuation filter used here is designed to work on different ranges of frequencies and on different sections of the inspiration and expiration cycles, each with its assigned lung inflation level. In general, the lung inflation is sorted into three different segments: low, medium, and high levels of inflation. Such inflation segments have been applied to both the inspiration and expiration parts of the respiration cycle. Therefore, to add the attenuation to the adventitious signals, a multi-band FIR filter is designed with the following passband edges specifications: [0, 500, 1000, 1500, 2000, 2500] Hz. The FIR transfer function H(z) of length N+1 is a polynomial in z^{-1}:

$$H(z) = \sum_{n=0}^{N} h[n] z^{-n} \tag{20}$$

The corresponding frequency response is given by:

$$H(e^{jw}) = \sum_{n=0}^{N} h[n] e^{-jwn} \tag{21}$$

Where N represents the order of the filter, $H(e^{jw})$ is the desired magnitude in the passband edges of the filter at the specified frequency w . This frequency is specified in the chart of the attenuation in Figure 6.1, and *h[n]* are the filter coefficients that will produce the desired output. With reference to Figure 6.1, the magnitude is varying based on the propagation distance , frequency, and inflation level. For instance, the attenuations per 1 centimetre at different level of inflations [100, 150, 200] ml, are provided to the filter by the following matrix of attenuation in dBs: [0.0, 0.4, 0.65 , 1.3, 2.8, 4.9; 0.0,0.8, 1.3, 2.2, 4.8, 6.9; 0.0,0.9, 1.6, 2.6, 5.8, 7.6]. These corresponds respectively to the passband edges of this filter in Hz: [0, 500, 1000, 1500, 2000, 2500].

Figures 6.2 and 6.3 illustrate the attenuation suffered by the adventitious sound signal before and after presented to the attenuation filter. The figures show clearly that the adventitious lung sounds suffer different degrees of attenuation at different frequencies of this wheeze sound.

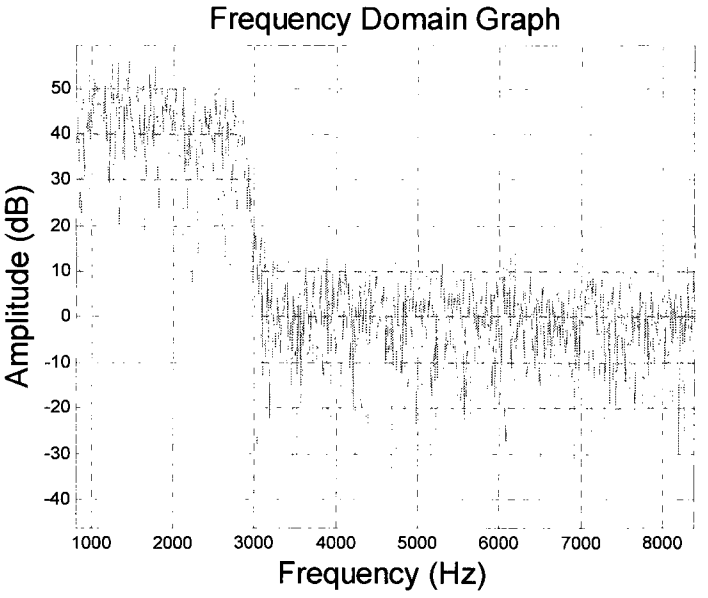

Figure 6.2: FFT of the Wheeze Sound before Presented to the Attenuation Filter

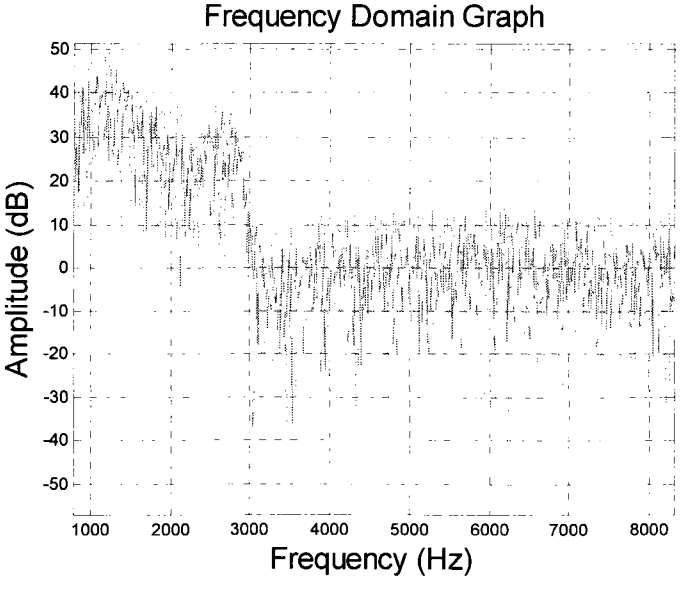

Figure 6.3: FFT of the Wheeze Sound After Presented to the Attenuation Filter

6.1.2 Generated Virtual Patients

Applying the process explained in the previous subsection, 40 distinct patients have been generated from the adventitious lung sounds presented in Table 6.1 and the 20 recorded channels of the healthy lung sound recordings obtained using the developed auscultation system. Table 6.2 presents all the generated virtual patients. This table lists the index of the generated patient, the source of the adventitious sound signal as per Table 6.1, the type of the adventitious sound, the level of the infection imposed, and the site of the infection relative to the segment and its lobe.

Patient Number	**Source of Sound Signals**	**Type and Number of Infections**	**Level of Infection**	**Infected Lobes**	**Infected Segment of the Lung's Lobe**
1	$A_1^1 \oplus$ G1	Wheeze; #1	Low	Right Upper Lobe	Posterior Segment
2	$A_1^3 \oplus$ G2	Wheeze; #1	Low	Left Upper Lobe	Anterior Segment
3	$A_1^3 \oplus$ G3 $A_1^4 \oplus$ G3	Wheeze; #2	Medium	Right Lower Lobe & Left Lower Lobe	Apical Segment & Subapical Segment
4	$A_1^4 \oplus$ G4	Wheeze; #1	High	Left Upper Lobe	Posterior Segment
5	$A_1^3 \oplus$ G1 $A_1^1 \oplus$ G1	Wheeze; #2	Medium	Right Upper Lobe & Left Lower Lobe	Posterior Segment & Anterior Basal Segment
6	$A_1^5 \oplus$ G2	Wheeze; #1	Low	Right Middle Lobe	Lateral Segment
7	$A_1^9 \oplus$ G3	Wheeze; #1	low	Left Lower Lobe	Apical Segment
8	$A_1^{10} \oplus$ G4	Wheeze; #1	Low	Right Lower Lobe	Lateral Basel Segment

9	$A_2^{10} \oplus$ G1 $A_1^{10} \oplus$ G1	Wheeze; #2	High	Right Middle Lobe & Left Upper Lobe	Lateral Segment & Superior Segment
10	$A_1^1 \oplus$ G2	Wheeze; #1	low	Right Upper Lobe	Anterior Segment
11	$A_1^{10} \oplus$ G3	Wheeze; #1	Low	Right Middle Lobe	Lateral Segment
12	$A_1^9 \oplus$ G4	Wheeze; #1	Low	Left Upper Lobe	Anterior Segment
13	$A_1^3 \oplus$ G1 $A_1^5 \oplus$ G1	Wheeze; #2	Low	Right Lower Lobe & Left Lower Lobe	Apical Segment & Subapical Segment
14	$A_1^3 \oplus$ G2	Wheeze; #1	Medium	Right Upper Lobe	Posterior Segment
15	$A_1^4 \oplus$ G3	Wheeze; #1	Medium	Left Lower Lobe	Apical Segment
16	$A_1^5 \oplus$ G4 $A_1^1 \oplus$ G4	Wheeze; #2	low	Right Upper Lobe & Left Lower Lobe	Posterior Segment & Anterior Basal Segment
17	$A_1^5 \oplus$ G1	Wheeze; #1	High	Left Lower Lobe	Posterior Segment
18	$A_1^3 \oplus$ G2	Wheeze; #1	Low	Right Lower Lobe	Lateral Basel Segment
19	$A_1^3 \oplus$ G3 $A_1^9 \oplus$ G3	Wheeze; #2	Low	Right Middle Lobe & Left Upper Lobe	Lateral Segment & Superior Segment
20	$A_1^4 \oplus$ G4	Wheeze; #1	Medium	Right Upper Lobe	Anterior Segment
21	$A_1^5 \oplus$ G1	Wheeze; #1	Low	Right Middle Lobe	Lateral Segment

22	$A_1^9 \oplus$ G2	Wheeze; #1	High	Left Upper Lobe	Anterior Segment
23	$A_1^{10} \oplus$ G3 $A_1^4 \oplus$ G3	Wheeze; #2	Medium	Right Lower Lobe & Left Lower Lobe	Apical Segment & Subapical Segment
24	$A_1^3 \oplus$ G4	Wheeze; #1	low	Right Upper Lobe	Posterior Segment
25	$A_1^1 \oplus$ G1	Wheeze; #1	Low	Left Lower Lobe	Apical Segment
26	$A_1^2 \oplus$ G2 $A_1^6 \oplus$ G2	Crackle; #2	Medium	Right Upper Lobe & Left Lower Lobe	Posterior Segment & Anterior Basal Segment
27	$A_1^6 \oplus$ G3	Crackle; #1	Low	Left Lower Lobe	Posterior Segment
28	$A_1^7 \oplus$ G4	Crackle; #1	High	Right Lower Lobe	Lateral Basel Segment
29	$A_1^8 \oplus$ G1 $A^6 \oplus$ G1	Crackle; #2	Medium	Right Middle Lobe & Left Upper Lobe	Lateral Segment & Superior Segment
30	$A_2^2 \oplus$ G2	Crackle; #1	low	Right Upper Lobe	Anterior Segment
31	$A_1^2 \oplus$ G3	Crackle; #1	Low	Right Middle Lobe	Lateral Segment
32	$A_1^6 \oplus$ G4	Crackle; #1	High	Left Upper Lobe	Anterior Segment
33	$A_1^7 \oplus$ G1 $A_2^2 \oplus$ G1	Crackle; #2	low	Right Lower Lobe & Left Lower Lobe	Apical Segment & Subapical Segment
34	$A_1^8 \oplus$ G2	Crackle; #1	Low	Right Upper Lobe	Posterior Segment

35	$A_2^2 \oplus$ G3	Crackle; #1	Low	Left Lower Lobe	Apical Segment
36	$A_1^7 \oplus$ G4 $A_1^2 \oplus$ G4	Crackle; #2	Low	Right Upper Lobe & Left Lower Lobe	Posterior Segment & Anterior Basal Segment
37	$A_1^8 \oplus$ G1	Crackle; #1	Medium	Left Lower Lobe	Posterior Segment
38	$A_1^2 \oplus$ G2	Crackle; #1	Medium	Right Lower Lobe	Lateral Basel Segment
39	$A_1^7 \oplus$ G3 $A_1^6 \oplus$ G3	Crackle; #2	low	Right Middle Lobe & Left Upper Lobe	Lateral Segment & Superior Segment
40	$A_1^8 \oplus$ G4	Crackle; #1	Low	Right Upper Lobe	Anterior Segment

Table 6.2: The Generated Virtual Patients

For testing purpose all the 40 generated virtual patients are used. First all the channels with adventitious lung sound signals are identified. If there is only one channel exhibiting an adventitious sound, lung segment and the lobe it monitors is declared as the site of the infection. If multiple channels are exhibiting adventitious sounds, then all of these are cross-correlated two at a time. The outputs of the cross-correlation process are compared to identify the channels that echo the same adventitious sound, if any. Among these channels, the segment and lobe monitored by the channel with the highest SPL is declared to be the site of the infection.

The results of the identification and localisation processes will be presented in the next sections

Figure 6.4 depicts graphically the process of generating virtual patients, testing these patients to diagnose the adventitious sounds, and cross-correlating the diagnosed signals to localize the source of infection.

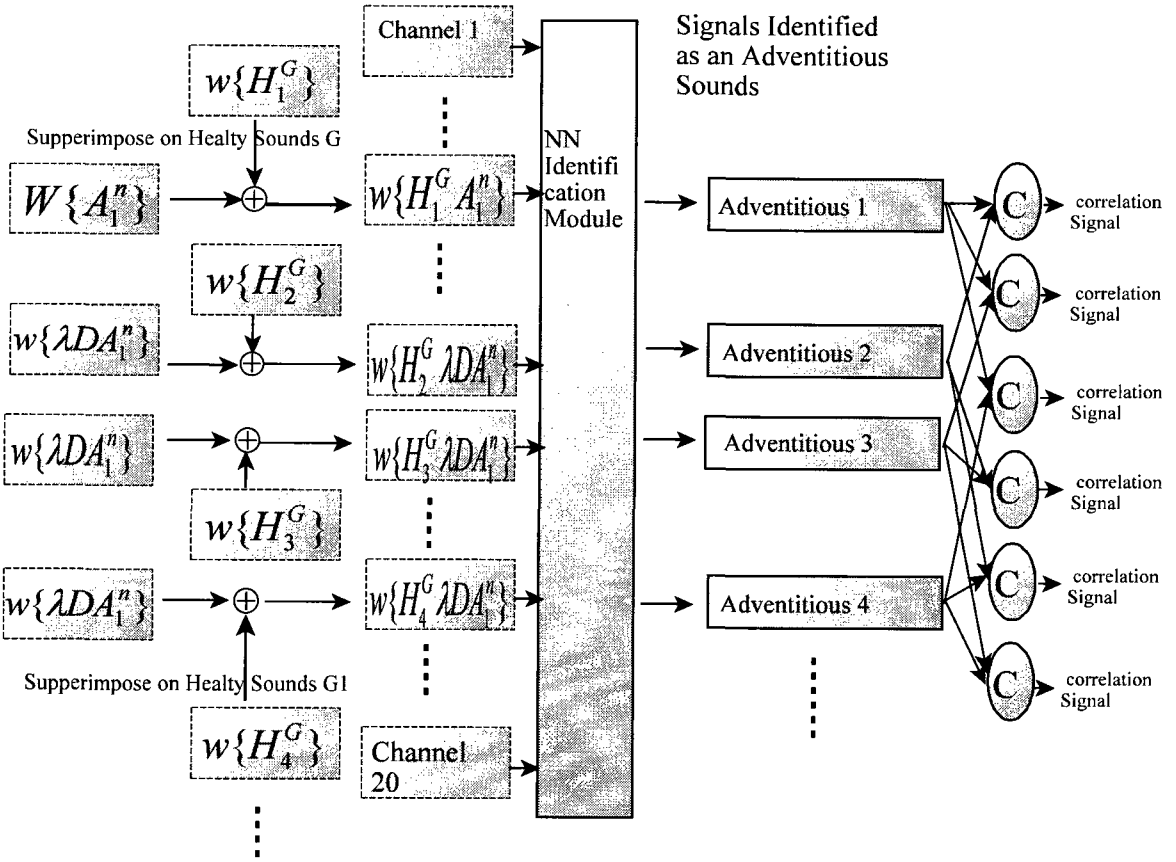

Figure 6.4: Block Diagram of Generating Virtual Patients and Testing the Identification and Localization of the Adventitious Lung Sounds

6.2 Test Cases

6.2.1 Testing the Generated Virtual Patients for Diagnosing the Adventitious Sounds

The capability of the identification module of the computerized automated auscultation and diagnostic system for the classification and differentiation of the diverse lung sound types is tested using the generated patients presented in Table 6.2. The 20 channels of each patient are presented to the identification module inputs. The module generates a normalized confidence level corresponding to the lung sounds it was presented with and the adventitious sounds it was trained to identify. On any of its four outputs the maximum confidence level is 1 if the sound is deemed to positively belong to this output, and 0 if the output is deemed to positively do not belong to this output (refer to Section 5.2.4). Figures 6.5 to 6.9 present the identification outputs for patients 1-5 respectively. The 20 channels of the electronic stethoscope are deployed and distributed with respect to the lung's lobes as follows: channels 1, 2, 8, 9 and 10 cover the Right Upper Lobe; channels 3, 4, 5, 6,and 7 cover the Left Upper Lobe; channels 11, 12, 18, 19 and 20 cover the Right Upper Lobe & Right Middle Lobe; and channels 13, 14, 15, 16 and 17 cover the Left Lower Lobe (for more details on the auscultation process and position with respect to the lung lobes and segments see Chapter 2 and 3). Figures 6.5 to 6.9 showed that in all the cases the identification module was extremely successful in diagnosing the adventitious and healthy lung sound signals. The confidence level of the identification varies depending on the attenuation of the adventitious sound signals which depends mainly on the propagation distance before reaching the electronic stethoscope. With reference to Figures 6.5 to 6.9, each of the bar graph sets in the figures corresponds to one of twenty test results of the 20 different stethoscope's channels. Each of the colour bars in a set corresponds to a network output. The confidence levels of these outputs are proportional to the length of the bars. After the identification of the lung sounds is completed, signals are presented to the localization module. The results of the identification process of the remaining test cases for patients 6 to 40 are presented in Appendix A.

Figure 6.5 shows the test results for patient #1 which is generated from one source of wheeze infection assumed to be located in the middle of the posterior segment of the right upper lobe. With reference to the figure, the network was able to identify the wheeze on channels 8, 9, and 10 and healthy lung sounds in the rest of the channels correctly with a high confidence level that varied

between 0.78 and 0.91. The verity of the identification confidence level comes from the fact that the adventitious lung sounds suffer different degrees of attenuation depending on the propagation distance, before reaching different auscultation channels. The maximum output on any of the network's other outputs was 0.18, which signifies that the network identifies the sound as not belonging to these outputs.

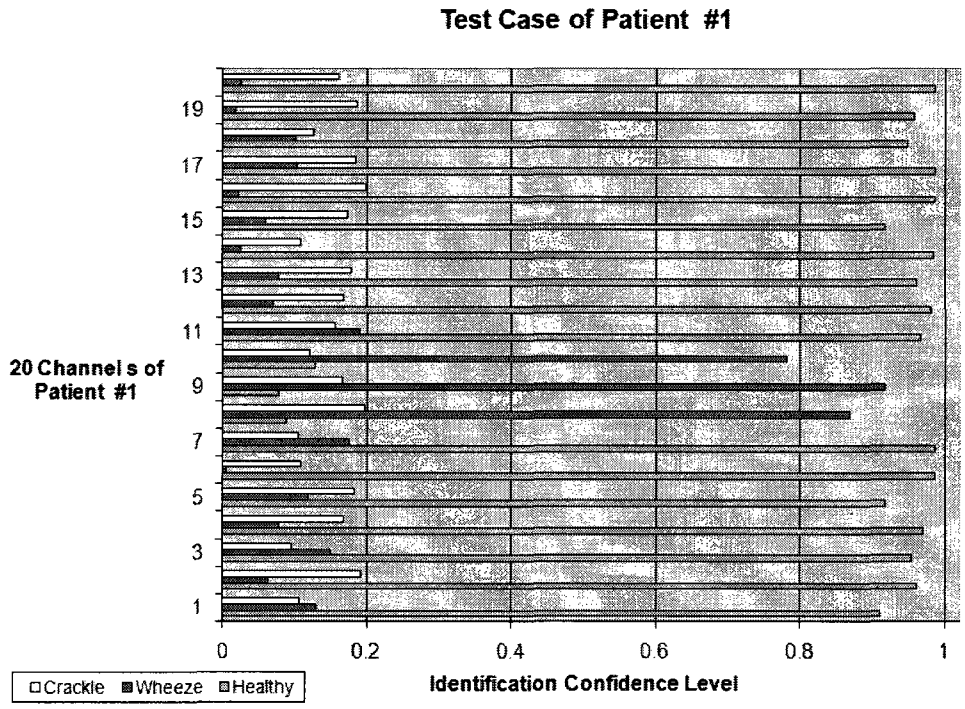

Figure 6.5: Test Case Patient #1 - Identification of Lung Sounds

Figure 6.6 shows the test results for patient #2, which is generated from another source of wheeze infection assumed to be located in the middle of the anterior segment of the left upper lobe. With reference to the figure, the network is able to identify the wheeze in channels 3, 4, and 5 and healthy lung sounds in the rest of the channels correctly with a high confidence level that varied between 0.82 and 0.93. Again, as explained in the previous case, the verity of the identification confidence level comes from the fact that the adventitious lung sounds suffer different degrees of attenuation depending on the propagation distance, before reaching different auscultation channels. The maximum output on any of the network's other outputs was 0.17, which signifies that the network identifies the sound as not belonging to these outputs.

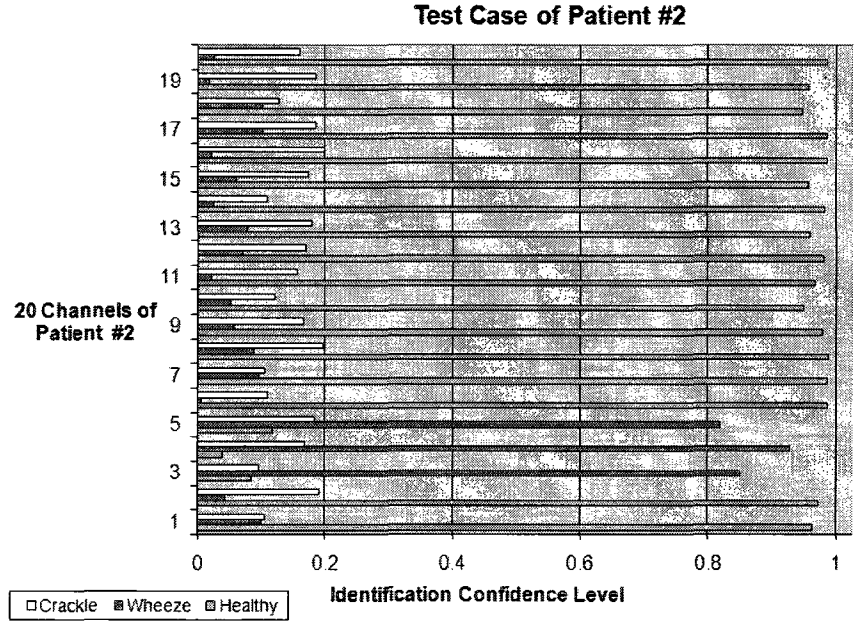

Figure 6.6: Test Case Patient #2 - Identification of Lung Sounds

Figure 6.7 shows the test results for patient #3 which is generated from two different source of wheeze sound signals, these signals assumed to be in the middle of the apical segment and subapical segment of the of the right lower lobe and left lower lobe respectively. With reference to the figure, the network is able to identify the wheeze in channels 8, 9, 10, 13, 14, and 15 and healthy lung sounds in the rest of the channels correctly with a high confidence level that varied between 0.79 and 0.92. Such a variation in the identification confidence level comes from same reason explained above. The maximum output on any of the network's other outputs was 0.19, which signifies that the network identifies the sound as not belonging to these outputs.

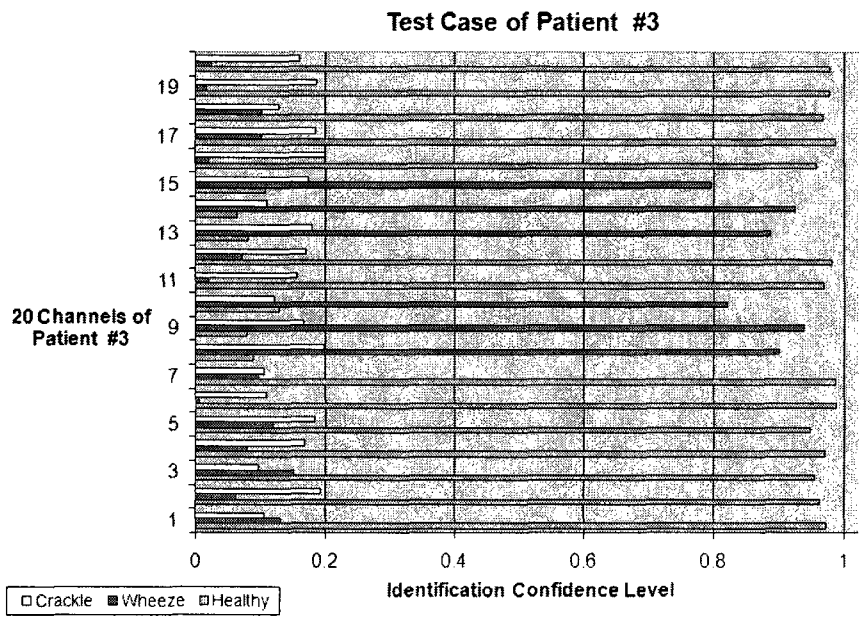

Figure 6.7: Test Case Patient #3 - Identification of Lung Sounds

Figure 6.8 shows the test results for patient #4 which is generated from one source of wheeze infection assumed to be located in the middle of the posterior segment of the left upper lobe. With reference to the figure, the network was able to identify the wheeze in channels 3, 4, 5, 6, and 7 and healthy lung sounds in the rest of the channels correctly with a high confidence level that varied between 0.71 and 0.95. The maximum output on any of the network's other outputs was 0.27, which signifies that the network identifies the sound as not belonging to these outputs.

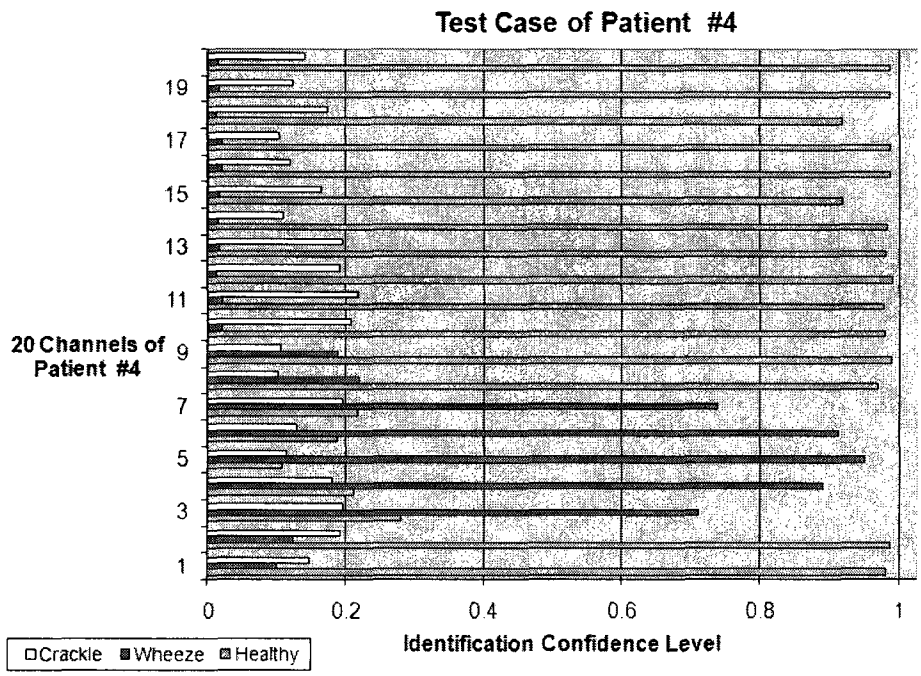

Figure 6.8: Test Case Patient #4 - Identification of Lung Sounds

Figure 6.9 shows the test results for patient #5 which is generated from two different sources of wheeze infections assumed to be located in the middle of the posterior segment & anterior basal segment of the right lower lobe and left lower lobe respectively. With reference to the figure, the network was able to identify the wheeze in channels 15, 16, 17, 18, 19, and 20 and healthy lung sounds in the rest of the channels correctly with a high confidence level that varied between 0.75 and 0.96. The maximum output on any of the network's other outputs was 0.23, which signifies that the network identifies the sound as not belonging to these outputs.

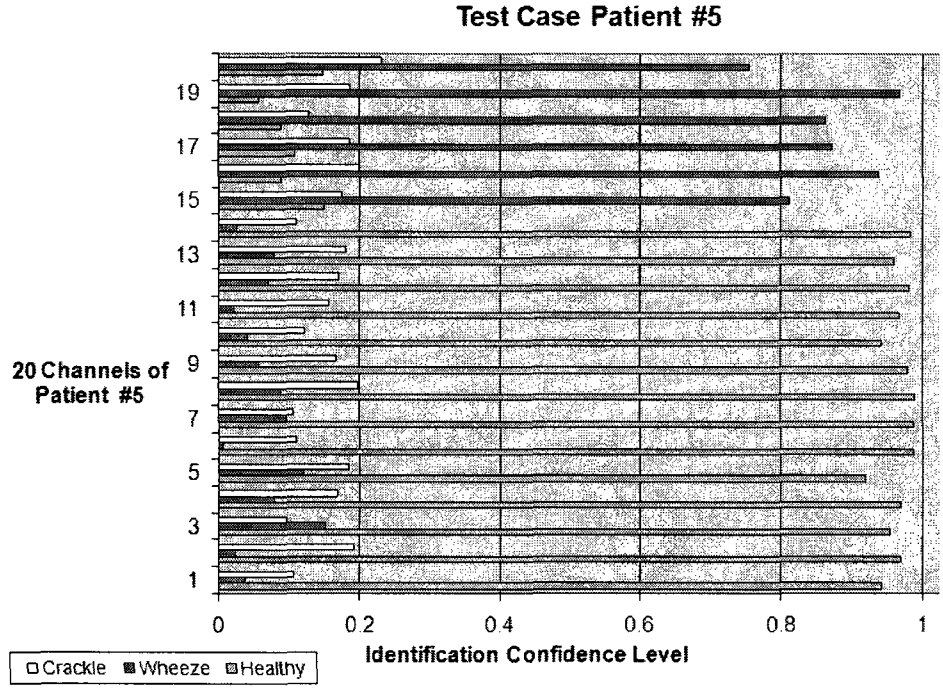

Figure 6.9: Test Case Patient #5 - Identification of Lung Sounds

Table 6.3 summarizes the results of the above five test cases of the virtual patients. Refer to Chapters 2 and 3 for the detailed description of the auscultation position and corresponding channel location.

Patient Number	Type and Number of Infections	Level of Infection	Detected Infected Channels	Infected Segment of the Lung's Lobe
1	Wheeze; #1	Low	8, 9, & 10	RUL; Posterior Segment
2	Wheeze; #1	Low	3, 4 & 5	LUL; Anterior Segment
3	Wheeze; #2	Medium	8, 9, 10, 13, 14, & 15	RLL & LLL; Apical Segment & Subapical Segment
4	Wheeze; #1	High	3, 4, 5, 6, & 7	LUL; Posterior Segment
5	Wheeze; #2	Medium	15, 16, 17, 18, 19, & 20	RUL & LLL Posterior Segment & Anterior Basal Segment

Table 6.3: Summary of The Identified Adventitious Signals of the Generated Patients

6.2.2 Testing the Generated Virtual Patients for the Localization of the Source of the Adventitious Sounds

Out of the 20 channels of every test case of the generated virtual patients, those identified as exhibiting adventitious sounds (wheeze or crackles) are fed to the site localization module. Cross-correlation between each two of these is carried out. Figures 6.10 to 6.14 show the outputs of the localization module of the diagnosed adventitious lung sound signals of the five test cases presented. The results of the remaining cases (case 6 to 40 shown in Table 6.2) are presented in Appendix B.

The results presented in Figures 6.10 to 6.14 show that the statistical features of the lung sounds examined have varying degrees of similarities though they are not identical. Even in cases where it is known that the same adventitious lung sound was used to generate a primary signal and its echo in two different channels, the frequency differentiation of the attenuation filter results in a of correlation values less than one. With reference to the figures, the bars represent the degree of the cross-correlation between the channels.

Figure 6.10 shows the correlation signals between wheeze lung sound signals for virtual patient #1. The identification module was successfully able to diagnose three different channels with wheeze sound signals. The output values of the correlation among these adventitious sound signals ranges between 0.94 and 0.97. These relatively high correlation values indicate that the adventitious lung sound signals are from the same source of infection. The difference between these signals are the result of the differential frequency attenuation they suffered as they propagated to the different elements of the stethoscope array through the parenchyma. Since the SPL of level of channel number 9 is the highest one , it is concluded that the segment of the lung lobe underneath this channel is the site of infection.

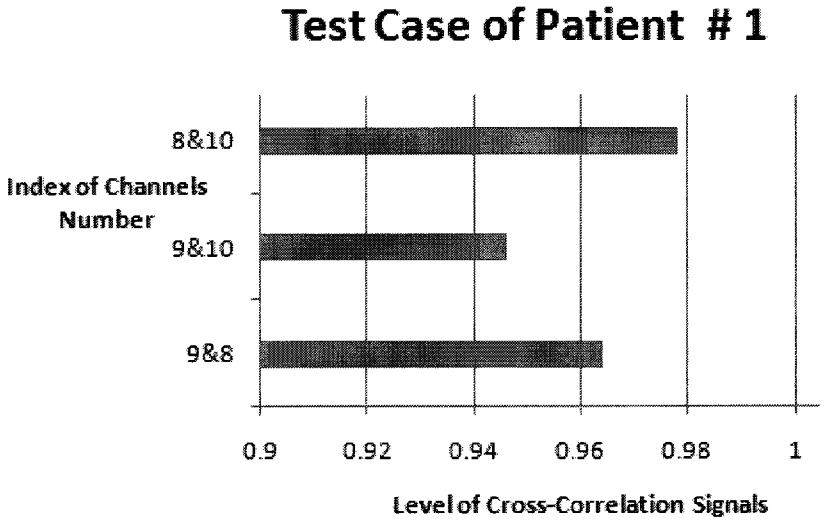

Figure 6.10: Test Case Patient #1 Localization of the Source of Infection

Figure 6.11 shows the results of the correlations between the channels identified with wheezes in lung sounds of virtual patient #2. The identification module was successfully able to diagnose three channels with wheeze sounds on them. The output values of the correlations carried out between these are high. And ranges between 0.95 and 0.97. This indicates that the adventitious lung sound signals are from the same source of infection. Again here, the lower than perfect correlation is due to the signal propagation filter used during the virtual patient generation process. The primary site of infection is identified as segment of lobe based on its higher SPL wheeze signal.

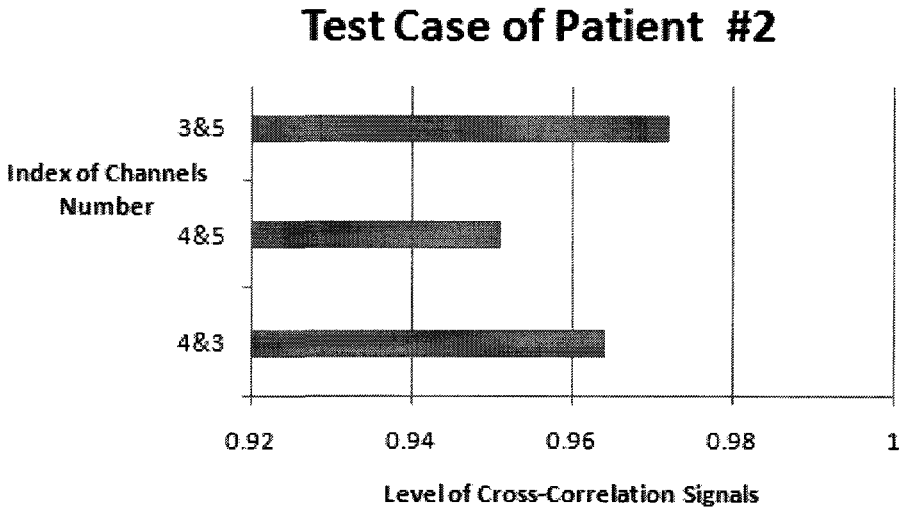

Figure 6.11: Test Case Patient #2- Localization of the Source of Infection

Figure 6.12 shows the correlation outputs carried out on between the channels identified with wheeze lung sound for patient #3. The identification module was able to successfully diagnose six channels with wheeze sounds. The outputs of the correlation process carried out on the identified channels ranged from 0.92 to 0.98. The high correlation signals indicate that the adventitious lung sound signals of channels 8, 9 and 10 are from the same source of infection, and the same thing is true for signals of channels 13, 14, and 15. The correlation signals between signals such as 8 &13, 9 & 14 and 10 & 15 are low and in the range of 0.46 to 0.52 and this indicate that these signals are from different sources of infection.

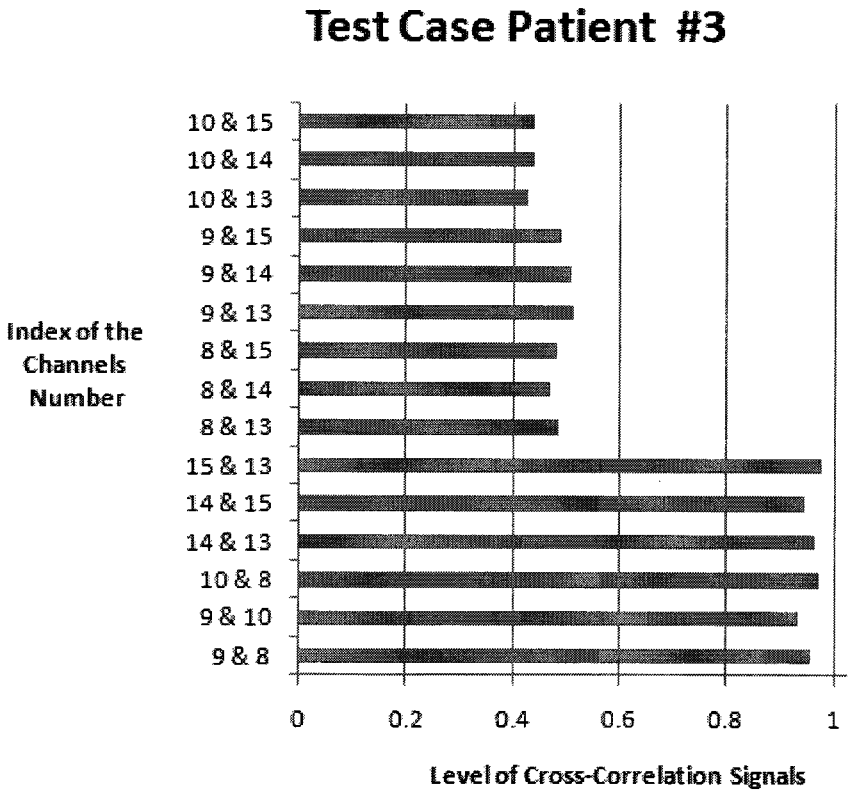

Figure 6.12: Test Case Patient #3 Localization of the Source of Infection

Figure 6.13 shows the results of the correlations between the channels identified with wheezes in lung sounds of virtual patient #4. The identification module was successfully able to diagnose five channels with wheeze sounds on them. The output values of the correlations carried out between these are high. And ranges between 0.93 and 0.97. This indicates that the adventitious lung sound signals are from the same source of infection. Again here, the lower than perfect correlation is due to the signal propagation filter used during the virtual patient generation process. The primary site of infection is identified as segment of lobe based on its higher SPL wheeze signal.

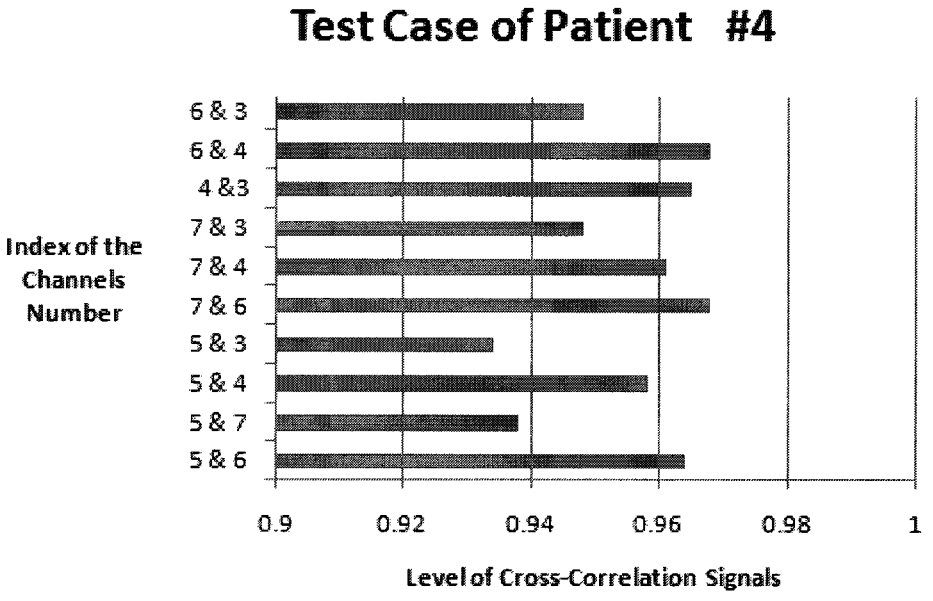

Figure 6.13: Test Case Patient #4 Localization of the Source of Infection

Figure 6.14 shows the correlation outputs carried out on between the channels identified with wheeze lung sound for patient #5. The identification module was able to successfully diagnose six channels with wheeze sounds. The outputs of the correlation process carried out on the identified channels ranged from 0.92 to 0.97. The high correlation signals indicate that the adventitious lung sound signals of channels 15, 16 and 17 are from the same source of infection, and same thing is true for signals of channels 118, 19, and 20. The correlation signals between signals such as 15 & 18, 16 & 19 and 17 & 20 are low and in the range 0.37 to 0.43 and this indicate that these signals are from different source of infection.

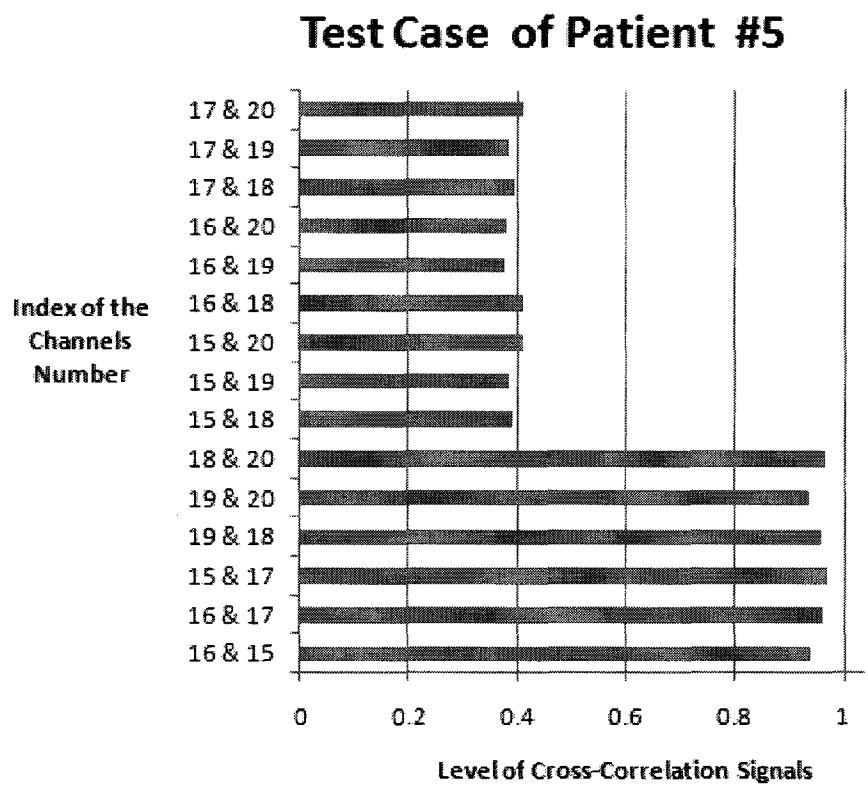

Figure 6.14: Test Case Patient #5- Localization of the Source of Infection

CHAPTER VII

Conclusion

7.1 Conclusion of the Thesis

Lung auscultation is recognized as the primary means of identifying lung diseases. However, traditional auscultation techniques depend on the training and experience of the medical personnel performing it. This research aims to develop an automated auscultation system capable of reliably and accurately diagnosing lung diseases using electronic auscultation signals. The developed system is intended as an adjunct to physician auscultation, rather than a replacement for it. The work focused for the time being on the identification of wheezes and of crackles in lung sounds.

An electronic stethoscope system capable of acquiring auscultation signals with the fidelity required for subsequent use in the system has been developed. The system has an array of 24 individual stethoscopes and is capable of auscultating all channels simultaneously, however, at this time only 20 channels of these are used to acquire lung sounds. The remaining 4 channels are reserved for future developments, for instance, one would be used for monitoring the sounds from the oesophagus, a second would be used for monitoring abdominal sounds, a third would be used for monitoring ambient noise for cancellation, and the fourth one would be used to acquire respiratory sound from trachea. Hardware signal conditioning modules and general software filters were developed to attenuate ambient noise. A unique and innovative approach that employs a clinical procedure and a specialized adaptive linear NN (ADALINE) are used to filter out the heartbeat and can be used to eliminate other noise like abdominal ones.

A special neural network is developed and appropriately trained to identify and distinguish between healthy lung sounds, wheezes, and crackles. A large number of healthy lung sounds and lung sounds with wheezes and crackles were collected for training the network. Tests on the ability of the trained network to identify different lung sounds were conducted. The results shown in this thesis

prove that the hardware and network architecture developed, coupled with the specific training methodology, is very effective as a diagnostic tool.

A localization module is also developed in order to pinpoint the site or sites of the adventitious sounds to the lung and segment and lobe level. After the identification and differentiation among healthy lung sounds, wheezes and crackles is done, then the localization module is used on channels of the auscultation array that are identified as having adventitious lung sounds. This module uses the mathematical technique of the cross-correlation as a signal processing and analyzing function. The amplitude of each sample in the cross-correlation signal is a measure of how much one of the adventitious sound signals resembles the other. Hence, how identical these lung sound signals is ascertained quantitatively with the cross-correlation function.

Due to the length of time it has taken to develop and perfect the system, a clinical trial was deemed too lengthy to perform during the course of this work and was left for future work. This election, however, was an impetus for developing a novel approach for generating virtual patients. Forty such patients were synthesized using this approach.

The automated auscultation system was tested using the generated forty virtual patients in lieu of the clinical trials. Results of identification, differentiation, and localization of adventitious lung sounds carried out on these forty patients where remarkable. The system accuracy was 100% and was able to pinpoint all the sites of adventitious lung sounds with very high confidence level.

7.2 Contribution Summary

1. Study and develop the concept for a multi-channel electronic stethoscope array for acquiring and recording respiratory sound signals from 24 channels simultaneously.
   Develop a digital filter system consisting of conventional filters and a clinical assisted ADALINE NN filter for removing heart beat sound and other identified noise signals with no effect on the auscultated lung sound.

2. Structure and train a Neural Network such that it is able to successfully identify and classify the conventional classes of adventitious lung sounds, crackles and wheezes, used as indicator of lung ailments.

   Implement and evaluate the performance of an innovative localization system capable of pinpointing the lung segments and lobes that are the sites of the adventitious sounds

3. Develop a unique approach for generating virtual patients with the ability to locate adventitious lung sounds anywhere in the lung and echoing these to any site of auscultation accurately taking into account the effects of frequency, distance and lung inflation on the attenuation. Such a method can be helpful for training health care professionals, as an adjunct for clinical trials, and for validating auscultation systems.
4. Develop and program a Graphical User Interface (GUI) for managing and controlling the entire system hardware and software. The system is user friendly and can be used for a both an automated diagnosis mode or in an adjunct to a health care practitioner mode.

7.3 Future Work

While the efficacy of the developed system was proven using clinically auscultated lung sounds used for training physicians and virtual patients generated using DSP techniques, it still need to be proven through a properly structured and controlled clinical trial. It is envisioned that such a trial would involve at least 60 subjects to make it statistically relevant at this stage. Half the subject would be patients with adventitious lung sounds and the other would be subjects with healthy lung sounds. X-ray would be used to confirm and localize the infection sites. A control mechanism would be set in place to hide the physician diagnosis and the results of the x-ray examinations from the developed auscultation system operator. The results from the developed system and those from the clinical and radiographic test would be compared to evaluate the accuracy of the system.

The heart beat sound filter developed as part of the automated auscultation system should be extended to filter other internal sounds like air such in the oesophagus and abdominal sounds. The system currently has the capacity and capabilities to allow for that at present. The auscultation array was consciously designed with 24 electronic stethoscopes.

While the system was developed at this stage to identify and classify crackles and wheezes, the same techniques can be used to diagnose other adventitious lung sounds. Extending the capability of the system would render it a more complete automated diagnosis system, and may result in reducing the use and reliance on expensive and invasive radiographic confirmation as is currently practiced.

The method of generating virtual patients developed in this work can be used in a patient simulator for training and testing health care personnel, much like a flight simulator is used for training of pilots.

At present, the system configuration is that of a fully functional and complete laboratory prototype, it is hoped that it would be reformatted as a pre-production portable prototype in the very near future so as to use it in the planned clinical trials.

REFERENCES

[1] Frederic H. Martini, and Edwin F. Bartholomew, "Essentials of anatomy & physiology", Publisher San Francisco ; London : Pearson/Benjamin Cummings, Page(s): 483-502, 2007.

[2] Steven Lehrer, " understanding Lung Sounds", Third Edition, W.B.Saunders Company, An Imprint of Elsevier Science, New York, 2002.

[3] Zahra Moussavi, "Fundamentals of Respiratory Sounds and Analysis", Department of Electrical and Computer Engineering, University of Manitoba, 2004.

[4] Statistics Canada. Selected leading causes of death, by sex. 1997. http://www.statcan.ca/english/Pgdb/People/Health/health36.htm

[5] Thoracic diaphragm, http://en.wikipedia.org/wiki/Diaphragm_(anatomy).

[6] World Health Organization (WHO), http://www.who.int/en/

[7] David J. Spiegelhalter, "Computer aided decision making in medicine", British Medical Journal, London, September 1984.

[8] J. Zar, MD, and Kim Mulholland, "Global Burden of Pediatric Respiratory Illness and the Implications for Management and Prevention Heather" , American Thoracic Society Meeting, San Francisco, CA, 2001.

[9] Andrew Davies, Carl Moores "The Respiratory System: Basic science and Clinical Conditions", Churchill Livingstone; Spain , 2003.

[10] Respiratory System and Lung Images, . www.ama-assn.org/ama/pub/category/7166.html

[11] Jeremy P.T. Ward, Jane Ward, Richard M. Leach & Charles M. Wiener; "The Respiratory System at a Glance", Second Edition, Blackwell Publishing, USA, 2006.

[12] Lung Image, http://www.utmem.edu/mlrp/IMAGES/illustrated-lung.gif.

[13] West, JB. Respiratory Physiology-The Essentials (4th Ed.), Chapter 7. Mechanic of Breathing

[14] Diaphragm Image Function, http://www.tooter4kids.com/HumanBody/respiratory3.jpg

[15] Robert L. Wilkins, John E. Hodgkin, and Brad Lopez, " Lung Sounds a Practical Guide" Second Edition; Mosby, USA, 1996.

[16] Noam Gavriely and David W. Gugell, "Airflow effects on amplitude and spectral content of normal breath sounds", Journal of applied physiology, vol. 80, 1996.

[17] George R. Wodicka, Kenneth N. Stevens, Howard L. Golub and Danel C. Shannon, "Spectral Characteristics of Sound Transmission in the Human Respiratory System", IEEE Transactions on Biomedical Engineering, Vol.37, No.12, December 1990.

[18] A. H. Leung and S. Sehati, "Sound transmission through normal and diseased human lungs", Engineering Science and Education Journal, February 1996.

[19] Stethoscope, http://en.wikipedia.org/wiki/Stethoscope;

[20] A.R.A. Sovijärvi , L.P. Malmberg , G. Charbonneau , J. Vanderschoot , F. Dalmasso , C. Sacco , and M. Rossi , J.E. Earis, "Characteristics of Breath Sounds and Adventitious Respiratory Sounds", European Respiratory Society Journals, 2000.

[21] H. Pasterkamp, G.R. Wodicka, and S.S. Kraman, "Effect of ambient respiratory noise on the measurement of lung sounds", Medical & Biological Engineering & Computing, Vol. 37, 1999.

[22] Giuliana Gendetto, Filiberto Dalamasso, and Renato Spagnolo, "Surface Distribution of Crackling Sounds", IEEE Transactions on Biomedical Engineering, VOL. 35, NO. 5, May 1988.

[23] P. Piirilä, and A.R.A. Sovijärvi, "Crackles: recording, analysis and clinical significance", European Respiratory Society Journal, January 1995.

[24] Hiroshi Kiyokawa, Matthew Greenberg, Kazuhiko Shirota, and Hans Pasterkamp, "Auditory Detection of Simulated Crackles in Breath Sounds", CHEST , Vol, 119, No. 6, 200.

[23] Pulmonary Concepts In Critical Care Breath Sounds http://rnbob.tripod.com/breath.htm.

[26] Huseyin Polat and Inan G uler, "A Simple Computer-Based Measurement and Analysis System of Pulmonary Auscultation Sounds", Journal of Medical Systems, Vol. 28, No. 6, December 2004

[27] F. Schuttler, T. Penzel, P. Von Wiichert, " Digital Recording and Computer-Based analysis of Lung Sounds", 18th Annual lnternational Conference of the IEEE Engineering in Medicine and Biology Society, Amsterdam 1996.

[28] H. A.Mansy, T.J. Royston, R.A. Balk and R.H. Sandier, "Pneumothorax detection using computerized analysis of breath sounds", Medical & Biological Engineering & Computing , Vol. 40, 2002

[29] Children Hospital, http://www.providence.org/alaska/tchap/glossary/P.htm

[30] Sameer S. Alsmadi, and Yasamin P. Kahya, "Online classification of lung sounds using DSP", Proceeding of the Second Joint EMBS/BMES Conference, Houston, TX, USA, October 2003.

[31] Yasemin P. Kahyq Ugur Cini and Omer Cerid, "Real-time Regional Respiratory Sound Diagnosis Instrument", Proceedings of the 25th Annual International Conference of the IEEE EMBS, Cancun, Mexico, 2003.

[32] Yasemin P. Kahya, E. Cagatay Guler, and Serdar Sahin, " Respiratory Disease Diagnose Using Lung Sounds", Proceedings 19th International Conference , IEEE EMBS, Chicago, IL. USA, 1997

[33] Zahra .K. Moussavi, Mary T. Leopando, Hans Pasterkamp, and Gina Rempel, "Computerized Acoustical Respiratory Phase Detection without Airflow Measurement", Medical & Biology Eng. & comp. Vol 38 (2):198:203, 2000.

[34] M. Yeginer, K. Ciftci, U. Cini, I. Sen, G. Kilinc, and Y. P. Kahya, " Using Lung Sounds in Classification of Pulmonary Diseases According to Respiratory Sub-phases", Proceedings of the 26th Annual International Conference of the IEEE EMBS, San Francisco, CA, USA, 2004

[35] Mazic, S. Sovilj, R. Magjarevic, "Analysis of Respiratory Sounds in Asthmatic Infants", Measurement Science Review, Volume 3, Section 2, 2003.

[36] V. Gross, Th. Penzel, L. Hadjileontiadis, U. Koehler and C. Vogelmeier, "electronic Auscultation based on WAVELET Transformation in Clinical use", Proceedings of the Second Joint EMBS/BMES Conference, Houston, TX, USA, 2002.

[37] Noam Gavriely, Youampalti, and Gideon Alroy, "Spectral characteristics of normal breath sounds", American Physiology Society 1991.

[38] Volker Gross, Anke Ditomar, Thomas Penzel, Frank Schuttler, and Peter von Wichert, "The Relationship between Normal Lung Sounds, Age, and Gender", American Journal of Respiratory and Critical Care Medicine, Vol. 162, 2000.

[39] Paivi Piirta, "Changes in Crackle Characteristics during, the Clinical Course of Pneumonia", CHEST, Vo. 102, No.1, 1992.

[40] Azadeh Yadollahi, Zahra Moussavi ,"Measuring Minimum Critical Flow for Normal Breath Sounds", Proceedings of the 2005 IEEE, Engineering in Medicine and Biology 27th Annual

[41] George R. Wodicka, Kenneth N. Stevens, Howard L. Golub, Ernest G. Cravalho, and Daniel C. Shannon, "A model of Acoustic Transmission in the Respiratory system", IEEE Transactions of Biomedical Engineering. VOL, 36, NO. 9, September 1989.

[42] Leabentur Raphaeal Beck, Charles Irving, and Simon Godfrey, "Nocturnal Wheeze Measurement in Young Asthmatics", Pediatric Asthma Allergy and Immunology, Volume 17, Number 3, Mary Ann Liebert, Inc, 2004.

[43] A. H. Leung and S. Sehati , "Sound transmission through normal and diseased human lungs", Engineering Science and Education Journal, February 1996.

[44] T. Rosqvist, E. Paajanen, K. Kallio I H.-M. Rajala, T. Katila, P, Piirili, P. Malmberg, A. Sovijrvi ,"Toolkit for lung sound analysis", Medical & Biological Engineering & Computing March 1995,

[45] P. Piirilä, A.R.A. Sovijärv ,"Crackles: recording, analysis and clinical significance", European Respiratory Journal, 1995, UK.

[46] H. Pasterkamp I G.R. Wodicka 2 S.S. Kraman ,"Effect of ambient respiratory noise on the measurement of lung sounds", Medical & Biological Engineering & Computing 1999, Vol. 37,

[47] Noam Gavriely and David W. Cugell, "Airflow effects on amplitude and spectral content of normal breath sounds", the American Physiological society, 1996

[48] Georger Wodicka, Kenneth Stevens and Daniel Shannon, "Spectral Characteristics of Sound Transmission in the Human Respiratory System" , IEEE Transactions on Biomedical Engineering,, VOL. 37. NO. 12, December 1990.

[49] J.S. Chuah and Z.K. Moussavi, "Automated Respiratory Phase Detection by Acoustical Means", Cybernetics & Informatics (SCI) Conference, July 2 000, pp. 228-231.

[50] J. E. Earis, J. E., and B.M. Cheetham, B. M. "Future perspectives for respiratory sound research", European Respiratory Review, 10(77), 641-646.

[51] A.S. Brown, D.M. Harvey, Dr. G.Jamieson, Dr. D.R. Graham, "ALow Cost Medical System for the Observation of Respiratory Dysfunction", The Institution of Electrical Engineers, Printed and Published by the IEE, Savoy Place, London WC2R OBL, UK, 2002

[52] JanC , JosC Antonio Fiz, JosC Morera, Antoni Homs-Corbera Raimon, "Algorithm for Time-Frequency Detection and Analysis of Wheezes", Proceedings of the 22nd Annual EMBS International Conference, July 23-28,2000, Chicago IL.

[53] Hong Wang Le Yi Wang, " Continuous Intro-Operative Respiratory Auscultation in Anesthesia", Proceedings of IEEE on Sensors, Volume: 2, On page(s): 1002- 1005, October 2003.

[54] Meng-Lun Hsueh1, Jen-Chien Chien,Feng-Chia Chang, Huey-Dong Wu, Fok-Ching Chong, "Respiratory Wheeze Detection System", Proceedings of the 2005 IEEE Engineering in Medicine and Biology 27th Annual Conference, Shanghai, China, September 1-4, 2005

[55] Yang-sheng Lu, Wen-hui Liu and Guang-xia Qin, "Removal Heart Sound Noise from Breath sound", IEEE Engineering In Medicine & Biology Society 10th Annual International Conference.

[56] Zahra Moussavi, Lung Sounds A Practical Guide, CD, lung sounds library.

[57] Lehrer, Steven. " Understanding lung sounds" , Publisher Philadelphia : W.B. Saunders, c2002.

[58] R.L.H. Murphy and M.A. Murphy, " Learning Lung Sounds", Westborough, Stethographics, Inc., c2001.

[59] Publisher Philadelphia "Auscultation skills : breath & heart sounds" , Lippincott Williams and Wilkins, c2006.

[60] Lung Sounds Auscultation Trainer, http://www.kyotokagaku.com/products_medi_lung.html

[61] Canada Health Network, http://www.canadian-health-network.ca

[62] Respiratory System and, Lung Images, www.trine-metcalf.com/asbestos/respiratory.html.

[63] The Respiratory System, http://www.fi.edu/biosci/systems/respiration.html.

[64] Fenton, T. Richard Pasterkamp, Hans Tal, A. Chernick, Victor, "Automated Spectral Characterization of Wheezing in Asthmatic Children" ,IEEE Transactions Biomedical Engineering, Jan. 1985 Volume: BME-32, Issue: 1,On page(s): 50-55

[65] A.H. Leung and S. Sehati, "Sound transmission through normal and diseased human lungs", Engineering Science and Education Journal, February 1996.

[67] Electronic Stethoscope, http://www.allheart.com/littmann4000.html

[68] Pulmonary Auscultation, http://sprojects.mmi.mcgill.ca/mvs/RESP01.HTM

[69] Pulmonary Concepts In Critical Care Breath Sounds, http://rnbob.tripod.com/breath.htm

[70] Mussel MJ, "The need for Standard in Recording and Analyzing Respiratory Sounds", Med Biol Eng comput 1992.

[71] Robert Dinwiddie, "The Diagnosis and Management of the Pediatric Respiratory Disease", Churchill Livingstone, UK, 1990

[72] Hans Pasterkamp, Steve Kraman, and Georger Wodicka, "Respiratory Sounds Advances beyond the Stethoscope", American Journal of Respiratory and Critical Care Medicine, Volume 156, Number 3, September 1997, 974-987,

[73] I. Hossain, and Z. Moussavi, " Relationship Between Airflow and Normal Lung Sounds", Proc. IEEE Canadian Conf. Elec. Comp. Eng. (CCECE) , May 2002.

[74] Golabbakhsh M., and Moussavi Z., Relationship between Airflow and Frequency-Based Features of Tracheal Respiratory Sounds, Proc. IEEE CCECE , pp. 751-4, May 2004.

[75] Yee Leng Yap and Zahra Moussavi, " Respiratory onset detection using variance fractal dimension", Engineering in Medicine and Biology Society, 2001. Proceedings of the 23rd Annual International Conference of the IEEE, Volume: 2, Page(s): 1554- 1556, 2002.

[76] Medical Diagnosis Using Neural Networks, University Utara Malaysia,Sintok,Kedah, http://www.generation5.org/content/2004/MedicalDiagnosis.asp

[77] Y. Toyoda, Jie Huang, Shuxue Ding and Yong Liu, "Environmental sound recognition by multilayered neural networks," Computer and Information Technology ", CIT '04. The Fourth International Conference on 14-16 Sept. 2004 Page(s):123 - 127, 2004

[78] V. Golovko, L. Grandinetti, V. Kochan, T. Laopoulos, A. Sachenko, and V. Turchenko, "Sensors signal processing using neural networks", AFRICON, 1999 IEEE , Volume 1, 28 Page(s):339 - 344, Sept.-1 Oct. 1999.

[79] Xin Yao and Yong Liu, "Neural networks for breast cancer diagnosis", Evolutionary Computation, Proceedings of the 1999 Congress on Volume 3, 6-9 July 1999.

[80] Mazic, 2S. Sovilj, 2R. Magjarevic, "Analysis of Respiratory Sounds in Asthmatic Infants", Measurement Science Review, Volume 3, Section 2, 2003,

[81] R. Jane, S. Cortes, A. Fiz, and J. Morera, "Analysis of Wheezes in Asthmatic Patients during Spontaneous Respiration", Engineering in Medicine and Biology Society, Conference

Proceedings of 26th Annual International Conference of the IEEE, Volume 2, Page(s):3836 - 3839, 2004.

[82] A. Homs-Corbera, R. Jane, J. Fiz, J. Morera, "Algorithm for time-frequency detection and analysis of wheezes", Engineering in Medicine and Biology Society, 2000. Proceedings of the 22nd Annual International Conference of the IEEE Volume 4, Page(s):2977 - 2980, July 2000.

[83] Jane, R.; Salvatella, D.; Fiz, J.A.; Morera, J., "Spectral analysis of respiratory sounds to assess bronchodilator effect in asthmatic patients", Engineering in Medicine and Biology Society, Proceedings of the 20th Annual International Conference of the IEEE, Volume 6, Page(s):3203 - 3206 vol.6, 29 Oct.-1 Nov. 1998

[84] H. Pasika and D. Pengelly, "Lung sound crackle analysis using generalized time-frequency representations", Medical & biological engineering & computing, vol. 32, Page(s) 688-690, 1994.

[85] Respiratory System, http://www.imaios.com/en/e-Anatomy/Thorax-Abdomen-Pelvis/Thorax-CT

[8] Anterior and posterior lung viewhttp://fitsweb.uchc.edu/ctanatomy/chest/review/lobes-anterior.html.

[87] James A. Freema, David M. Skapura, "Neural Networks Algorithms, Applications, and Programming Techniques", Addison-Wesley Publishing Company, 1991.

[88] Clifford Lau, "Neural Networks: Theoretical Foundations and Analysis", IEEE Press, 1992, Page(s) 26-53, 211-221.

[89] Donna L. Hudson, Maurice E. Cohen, "Neural Networks and Artificial Intelligence for Biomedical Engineering", IEEE Press Series in Biomedical Engineering, Page(s) 29-74.

[90] James A. Freeman ,David M. Skapura, "Neural Networks Algorithms, Applications, and Programming Techniques" , Addison-Wesley Publishing Company, 1991.

[91] N. Gavriely, M. Nissan, D.W. Cugell, and A.H.E. Rubin, "Respiratory health screening using pulmonary function tests and lung sound analysis", Eur Respir J, 7, 35–42, 1994

[92] Taketoshi Orihasi, Hayaru Shouno, and Shoji Kido, "Discrimination of Lung Sounds using a Statistics of Waveform Intervals", IPSJSIG Technical Reports, Vol.2006, No68(MPS-60), Pages(1-4), Japan, 2006.

[93] Bentur, L. And et al, "Wheeze monitoring in children for assessment of nocturnal asthma and response to therapy". European Respiratory Journal. Vol 21,pg 621-626, 2003.

[94] Tejman-Yarden, S. and et al. "Acoustic Monitoring of Lung Sounds for the Detection of One-Lung Intubation". International Anesthesia Research Society. Vol 105, No.2, pg 397-404, August 2007.

[95] A. Yadollahi, Z. Moussavi, P. Yahampath, "Adaptive Compression of Respiratory and Swallowing Sounds", Proceedings of the 28th IEEE, EMBS, New York City, USA, Aug 30-Sept 3, 2006.

[96] U. Frey, and et al "High-Frequency Respiratory Impedance Measured by Forced-Oscillation Technique in Infants"Am J Respir Crit Care Med Vol 158. pp 363–370, 1998.

[97] Hiroshi Kiyokawa,, Matthew Greenberg; Kazuhiko Shirota, and Hans Pasterkamp,"Auditory Detection of Simulated Crackles in Breath Sounds", CHEST, 119, 6 , JUNE, 2001.

[98] Takeo Kawamura, Tsuneo Matsumoto, Nobuyuki Tanaka, Shoji Kido, Zhongwei Jiang,and Naofumi Matsunaga "Crackle Analysis for Chest Auscultation and Comparison with High-resolution CT Findings", Radiation Medicine: Vol. 21 No. 6, 258–266 p.p., 2003.

[99] A. I. D'yachenko and G. A. Lyubimov, " Propagation of Sound in Pulmonary Parenchyma", Izvestiya Akademii Nauk SSSR, Mekhanika Zhidkosti i Gaza, No. 5, pp. 3-15, September-October, 1988.

[100] U. H. Cegla, "Some aspects of pneumosonography," Prog. Respir. Res. Karger, Basel, Vol. 11, 235 (1979).

[101] GEORGE R. WODICKA, KENNETH N. STEVENS, HOWARD L. GOLUB, AND DANIEL, SHANNON, "Spectral Characteristics of Sound Transmission in the Human Respiratory System", IEEE TRANSACTIONS ON BIOMEDICAL ENGINEERING, VOL. 37. NO. 12, DECEMBER 1990.

[102] Philip J. Berger, Elizabeth M. Skuza, C. Andrew Ramsden,and Malcolm H. Wilkinson1 "Velocity and attenuation of sound in the isolated fetal lung as it is expanded with air", J Appl Physiol 98: 2235–2241, 2005.

[103] N. Gavriely, M. Nissan, D.W. Cugell, and A.H.E. Rubin, "Respiratory health screening using pulmonary function tests and lung sound analysis", Eur Respir J, 7, 35–42, 1994

[104] Taketoshi Orihasi, Hayaru Shouno, and Shoji Kido,"Discrimination of Lung Sounds using a Statistics of Waveform Intervals",IPSJSIG Technical Reports, VOL.2006;NO.68(MPS-60);Pages(1-4), Japan, 2006.

[105] Bentur, L. And et al, "Wheeze monitoring in children for assessment of nocturnal asthma and response to therapy". European Respiratory Journal. Vol 21,pg 621-626, 2003.

[106] Tejman-Yarden, S. et al. "Acoustic Monitoring of Lung Sounds for the Detection of One-Lung Intubation". International Anesthesia Research Society. Vol 105, No.2, pg 397-404, August 2007.

[107] A. Yadollahi, Z. Moussavi, P. Yahampath, "Adaptive Compression of Respiratory and Swallowing Sounds", Proceedings of the 28th IEEE, EMBS Annual International Conference, New York City, USA, Aug 30-Sept 3, 2006.

[108] U. Frey, and et al "High-Frequency Respiratory Impedance Measured by Forced-Oscillation Technique in Infants"Am J Respir Crit Care Med Vol 158. pp 363–370, 1998.

[109] Hiroshi Kiyokawa,, Matthew Greenberg; Kazuhiko Shirota, and Hans Pasterkamp,"Auditory Detection of Simulated Crackles in Breath Sounds", CHEST, 119, 6 , JUNE, 2001.

[110] Takeo Kawamura, Tsuneo Matsumoto, Nobuyuki Tanaka, Shoji Kido, Zhongwei Jiang,and Naofumi Matsunaga "Crackle Analysis for Chest Auscultation and Comparison with High-resolution CT Findings", Radiation Medicine: Vol. 21 No. 6, 258–266 p.p., 2003.

[111] V. I. Korenbaum, A. A. Tagiltsev, A. E. Kostiv,S. V. Gorovoy, I. A. Pochekutova and G. N. Bondar, "Acoustic equipment for studying human respiratory sounds", Instruments and Experimental Techniques, Physical Instruments for Ecology, Medicine, and Biology , Vol. 51, No. 2, pp. 296-303, 2008.

[112] Trevor J Cox, Peter D'Antonio, " Acoustic Absorbers and Diffusers, Theory, Design and Application", ISBN: 0-415-29649-8, Pub: Spon Press: Taylor and Francis, NY, 2004, Pages 276-311.

[113] Heirnich Kuttruff, "Acoustics: An Introduction", ISBN: Pub: Taylor and Francis, NY, 2007, Pages:94-117.

[114] Michael Savic, "Computer Aided Diagnosis of Lung Disease", US Patent Issued on January 20, 2009, Patent 7479115.

APPENDIX A

Test Cases of the Classification and Identification Module

A.1 Identification Test Results of the Generated Virtual Patients

The ability of the identification module of the developed computerized automated auscultation and diagnostic system for the classification and differentiation of the various lung sound types is tested using the generated virtual patients presented in Table 6.2. The 20 channels of each patient are presented to the identification module inputs. Figures A.1 to A.40 present the identification outputs for the virtual patients 1-40 respectively. The figures show that in all the cases the identification module was very successful in diagnosing the different types of adventitious sounds (wheeze and crackle) and healthy lung sound signals.

With reference to Figures A.1 to A.40, each of the bar graph sets in the figures corresponds to one of twenty test results of the 20 stethoscope array channels. Each of the colour bars in a set corresponds to a network output. The confidence levels of these outputs are proportional to the length of the bars. Results of identification and differentiation of adventitious lung sounds carried out on these forty patients where significant. The performance of the identification module and its precision was perfect as it was able to identify all the adventitious lung sounds with very high confidence level. The test results conclude that the identification module is able to successfully identify and classify the conventional classes of adventitious lung sounds, crackles and wheezes.

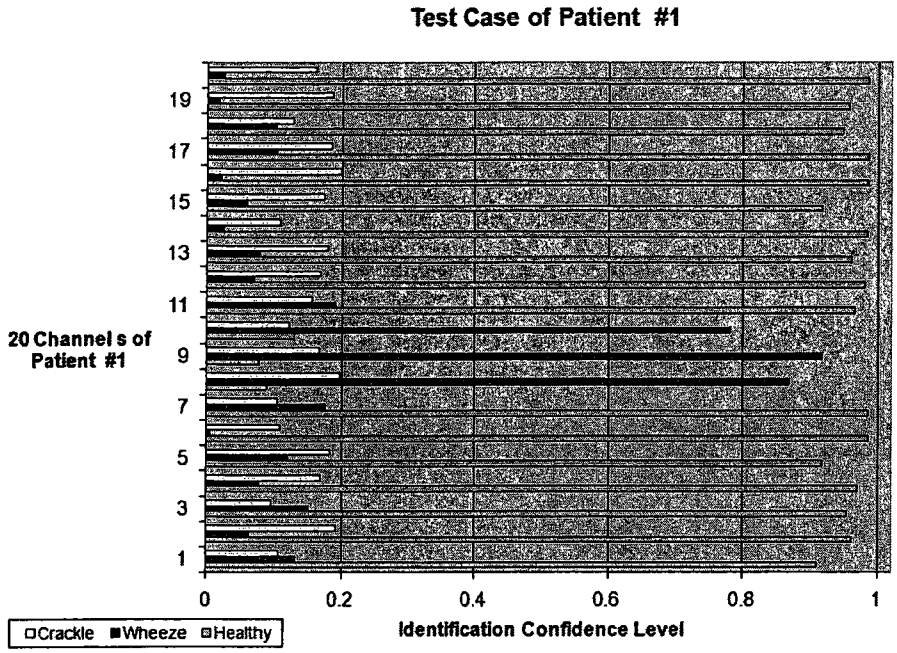

Figure A.1: Test Case Patient #1 - Identification of Lung Sounds

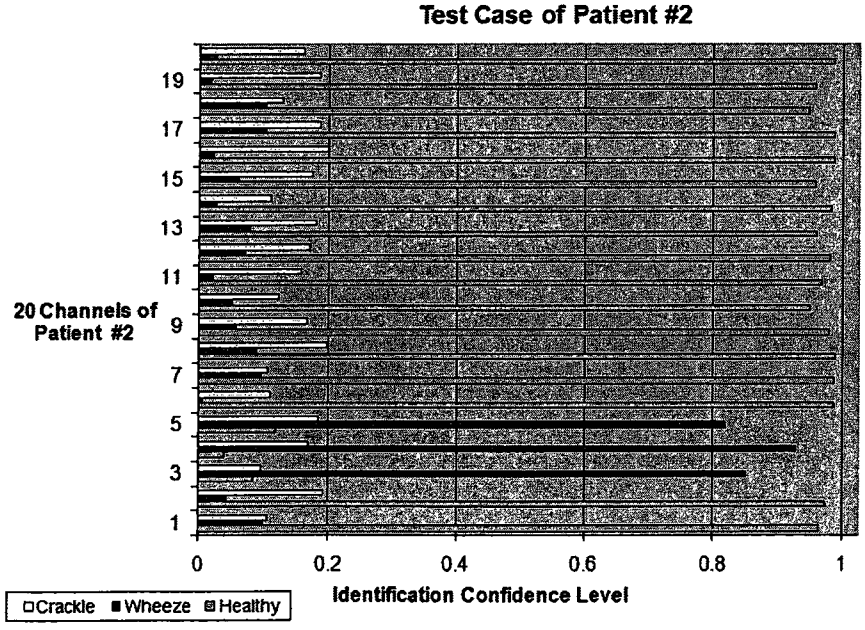

Figure A.2: Test Case Patient #2 - Identification of Lung Sounds

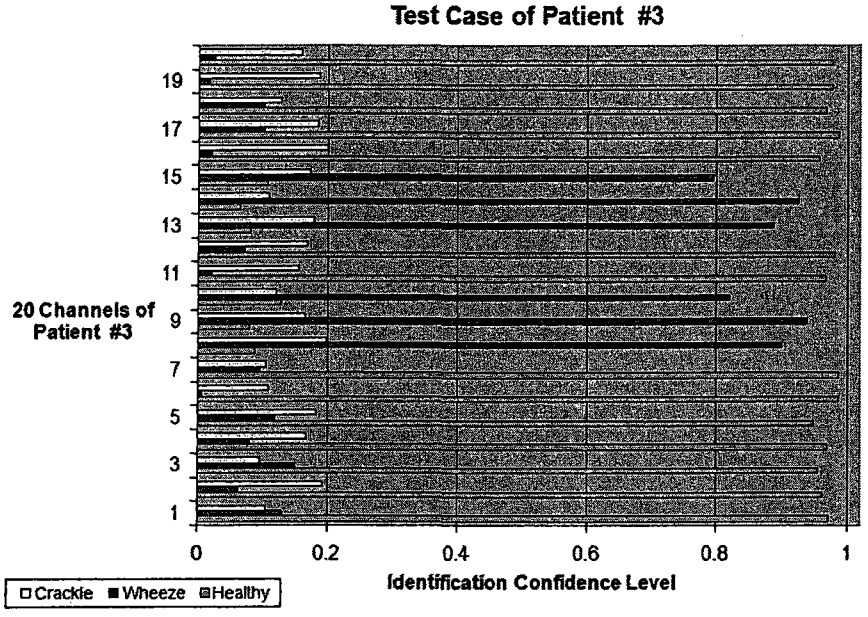

Figure A.3: Test Case Patient #3 - Identification of Lung Sounds

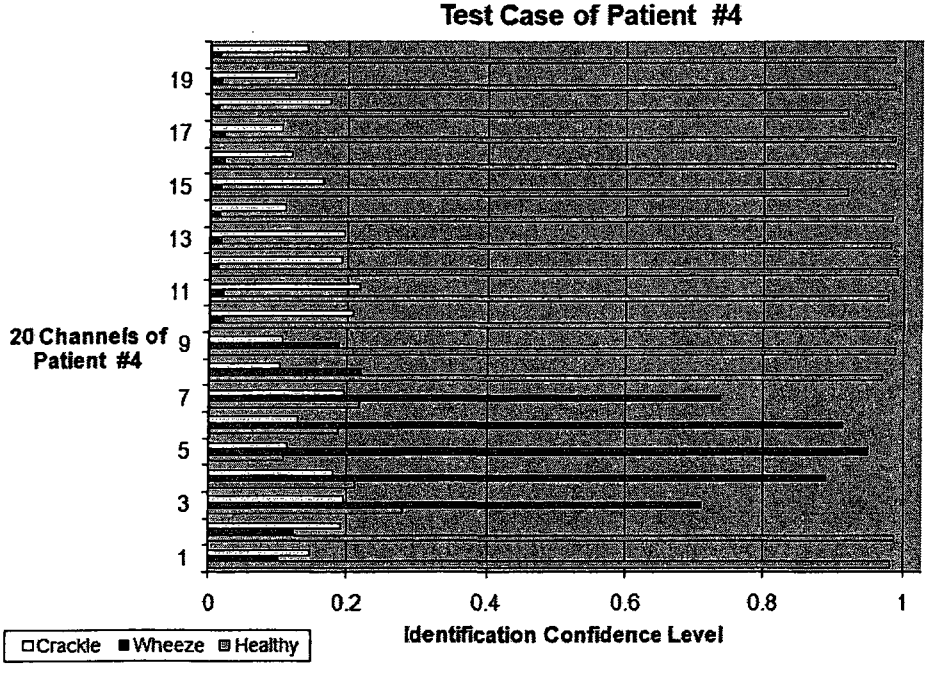

Figure A.4: Test Case Patient #4 - Identification of Lung Sounds

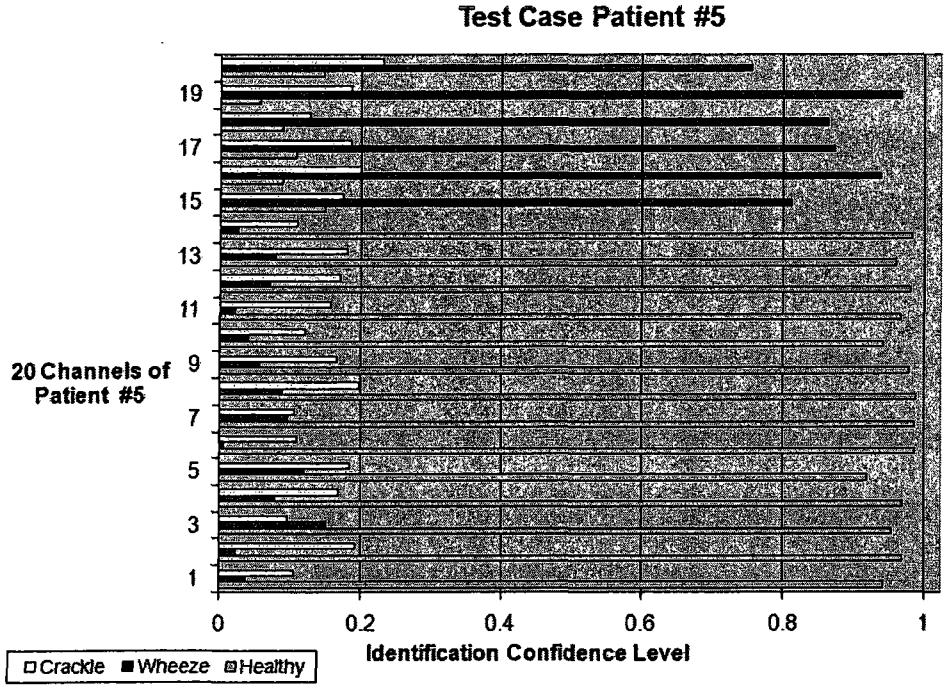

Figure A.5: Test Case Patient #5 - Identification of Lung Sounds

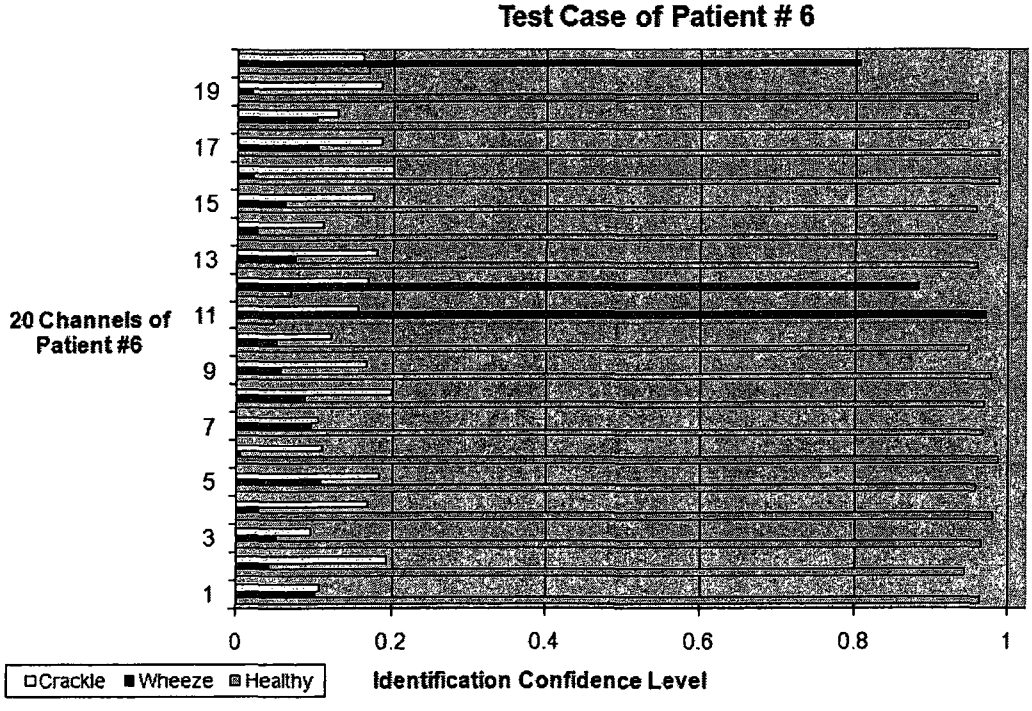

Figure A.6: Test Case Patient #6 - Identification of Lung Sounds

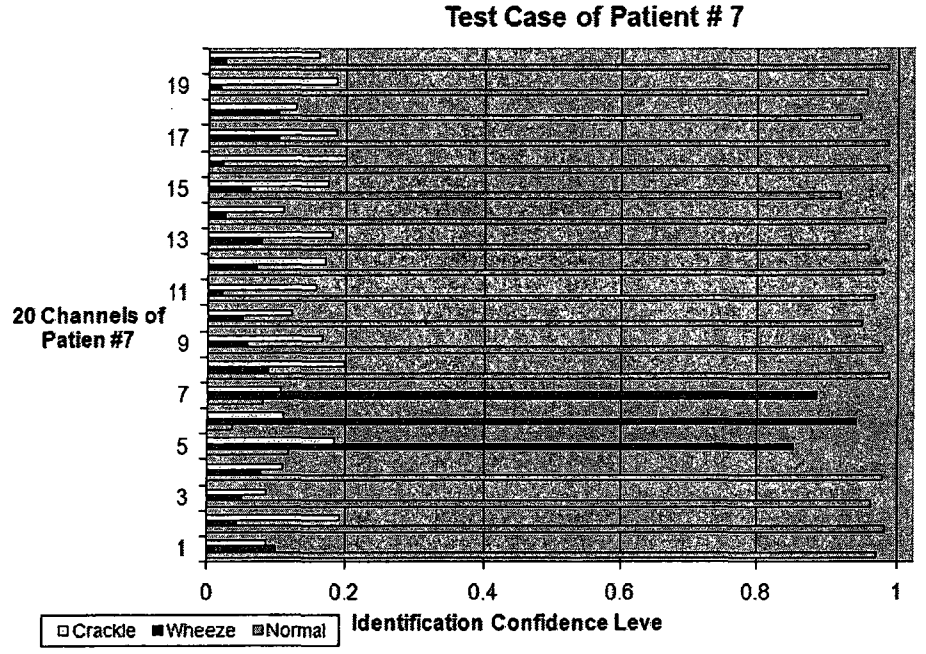

Figure A.7: Test Case Patient # 7 - Identification of Lung Sounds

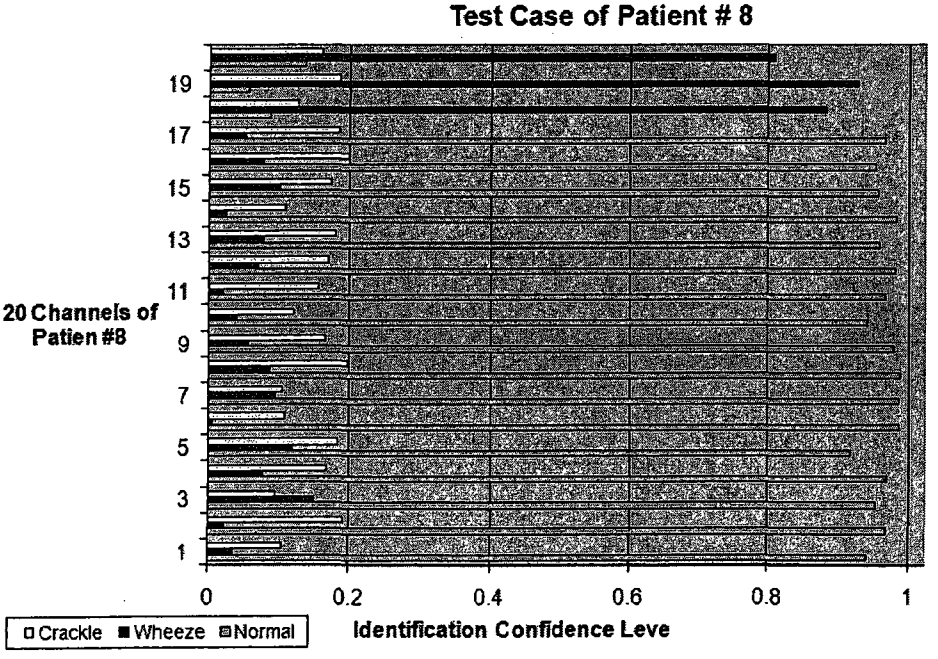

Figure A.8: Test Case Patient # 8 - Identification of Lung Sounds

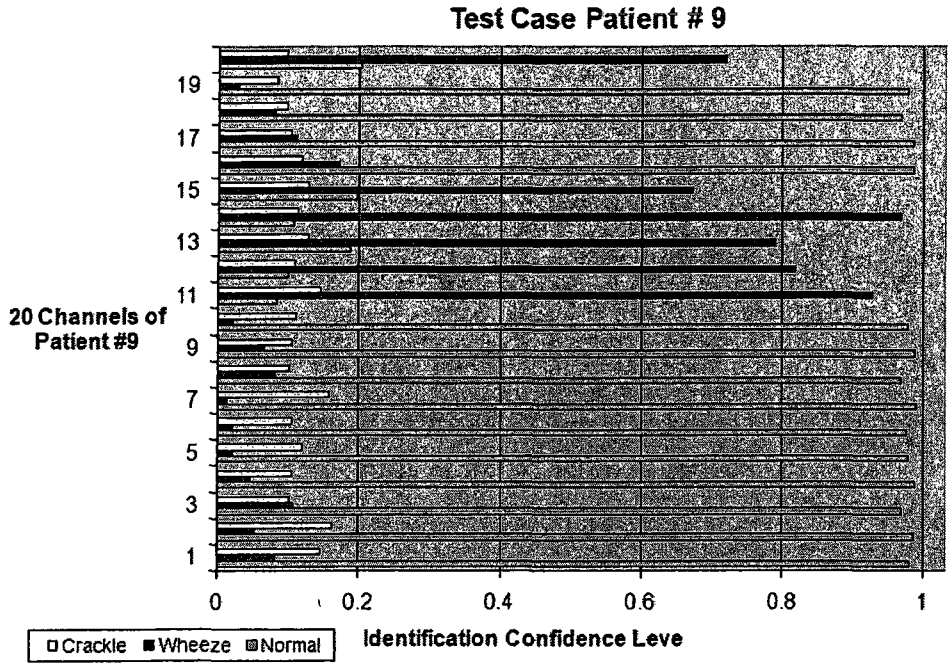

Figure A.9: Test Case Patient # 9 - Identification of Lung Sounds

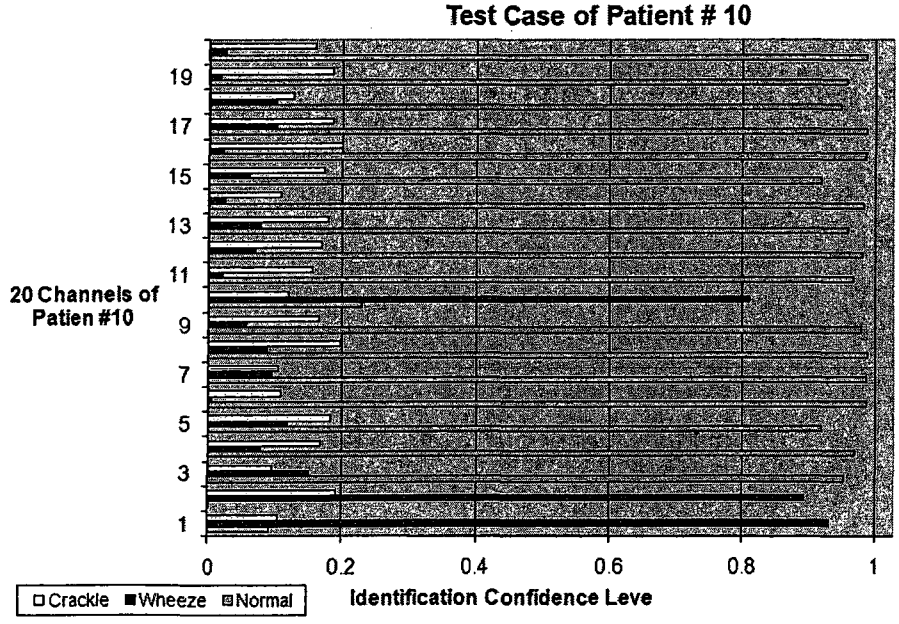

Figure A.10: Test Case Patient # 10 - Identification of Lung Sounds

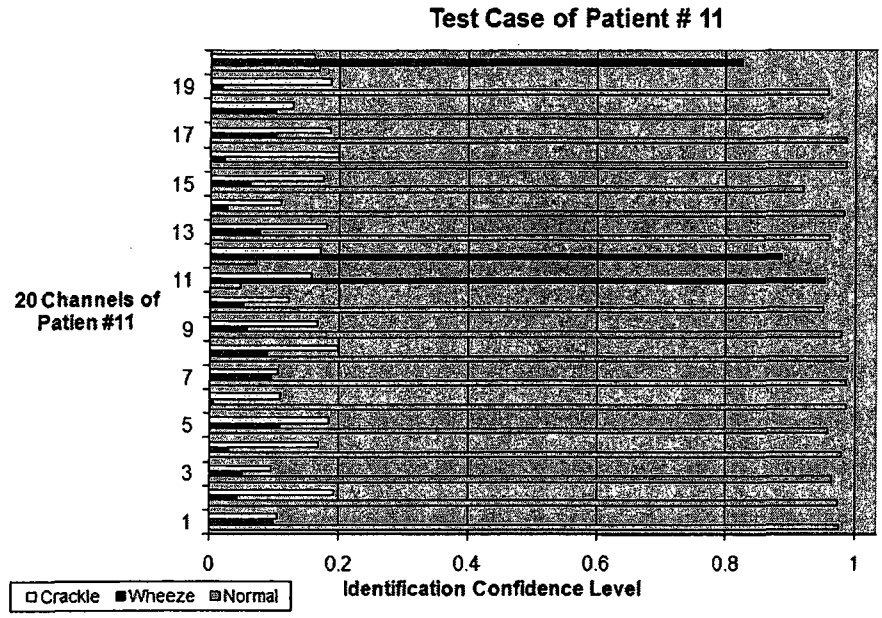

Figure A.11: Test Case Patient # 11 - Identification of Lung Sounds

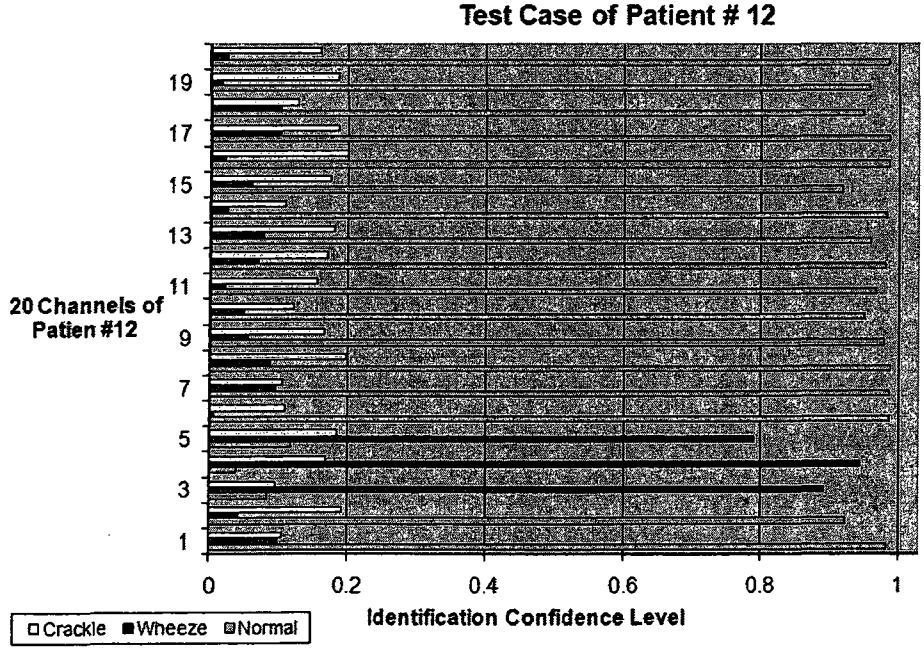

Figure A.12: Test Case Patient # 12 - Identification of Lung Sounds

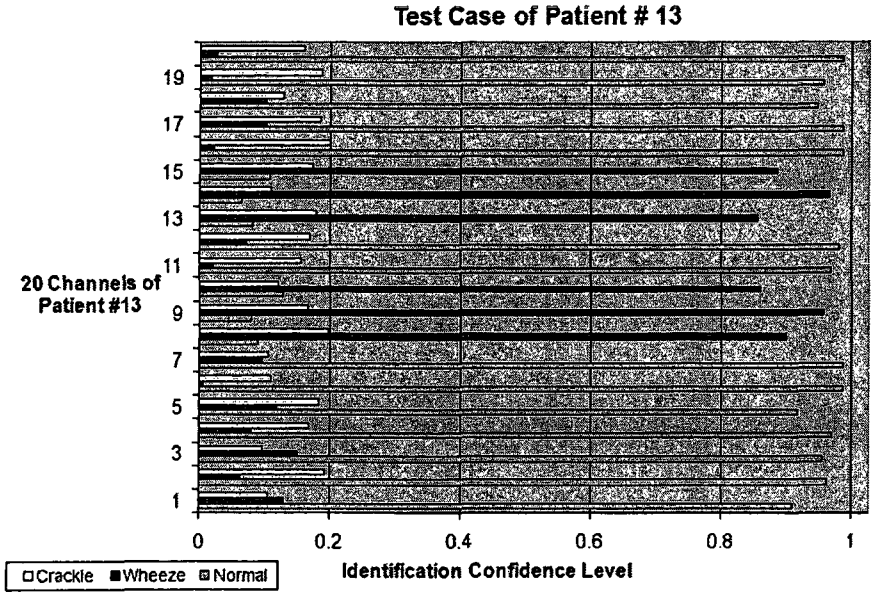

Figure A.13: Test Case Patient # 13 - Identification of Lung Sounds

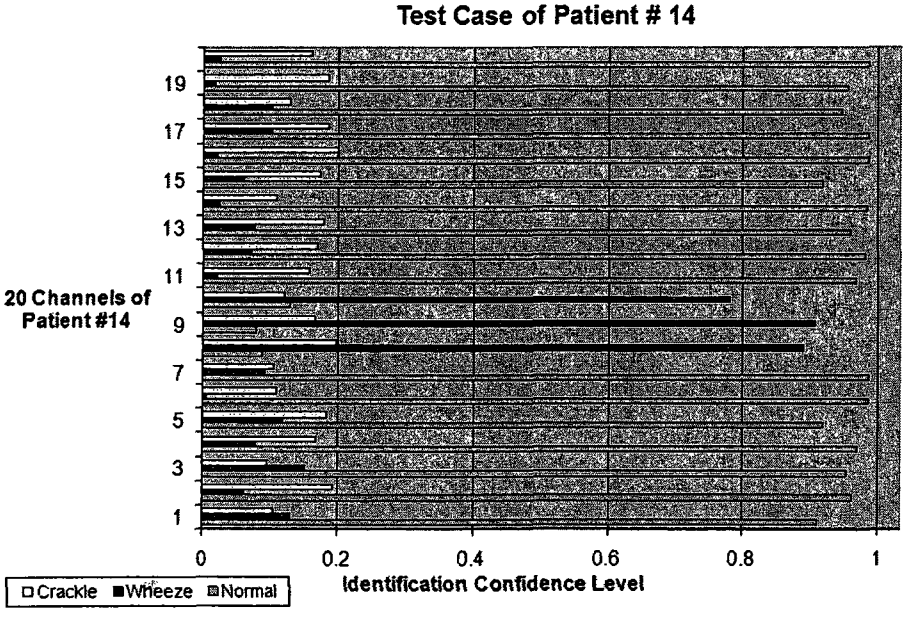

Figure A.14: Test Case Patient # 14 - Identification of Lung Sounds

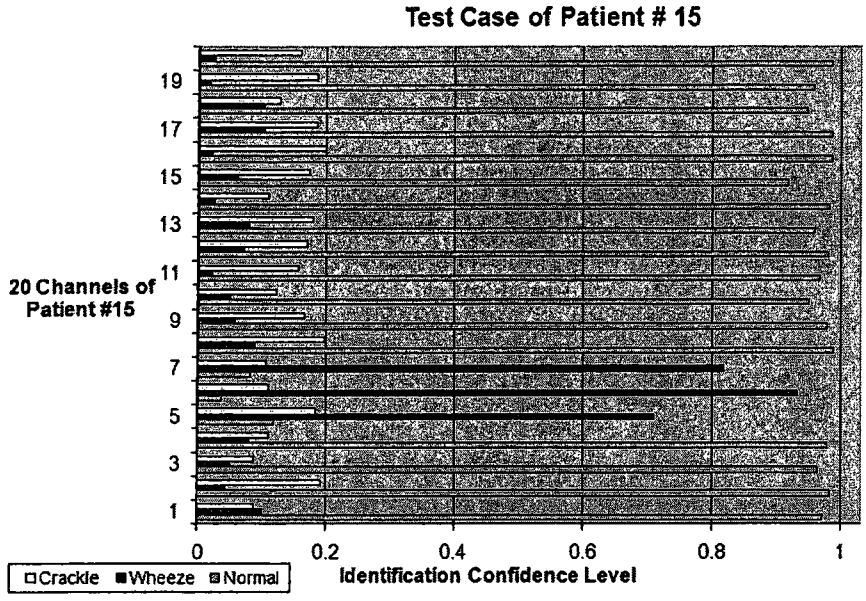

Figure A.15: Test Case Patient # 15 - Identification of Lung Sounds

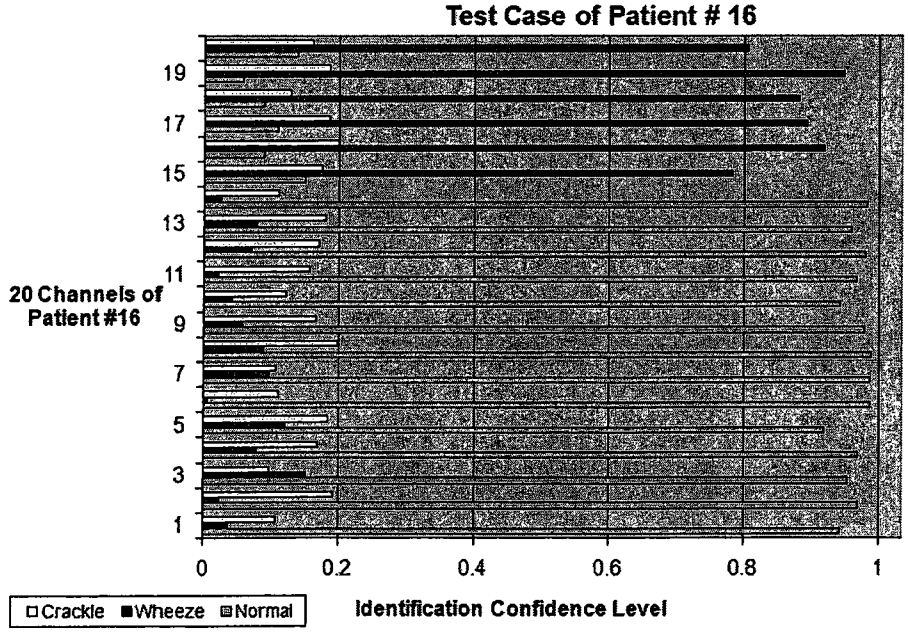

Figure A.16: Test Case Patient # 16 - Identification of Lung Sounds

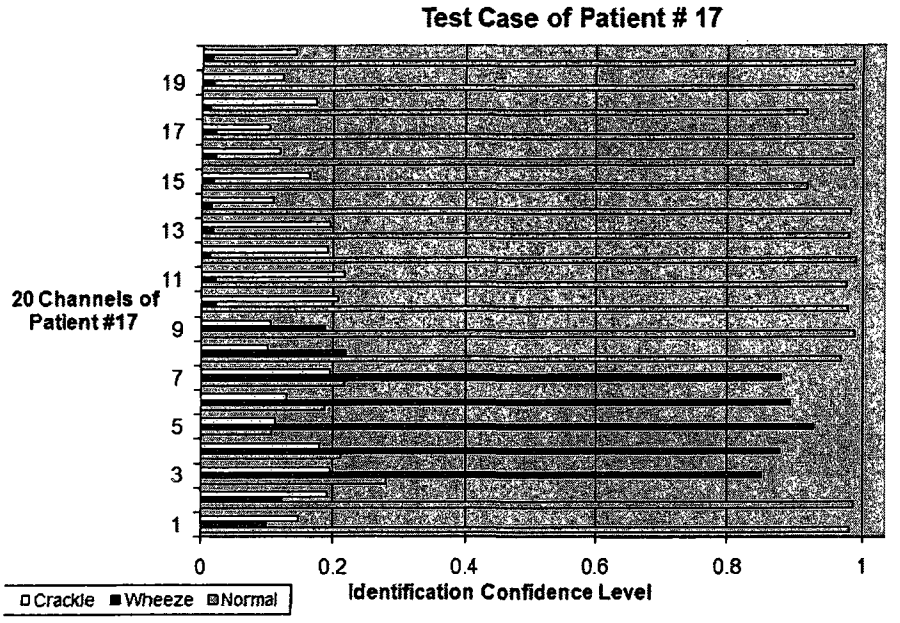

Figure A.17: Test Case Patient # 17 - Identification of Lung Sounds

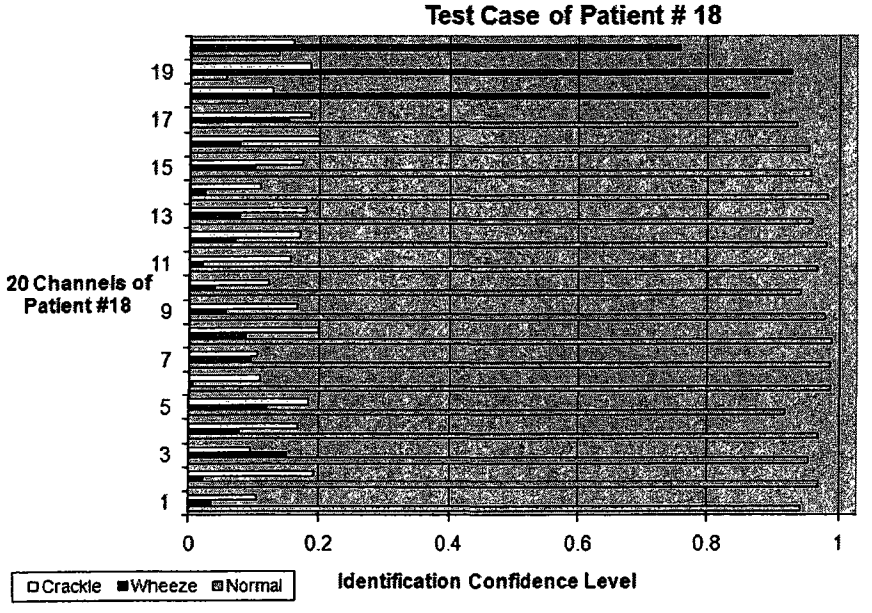

Figure A.18: Test Case Patient # 18 - Identification of Lung Sounds

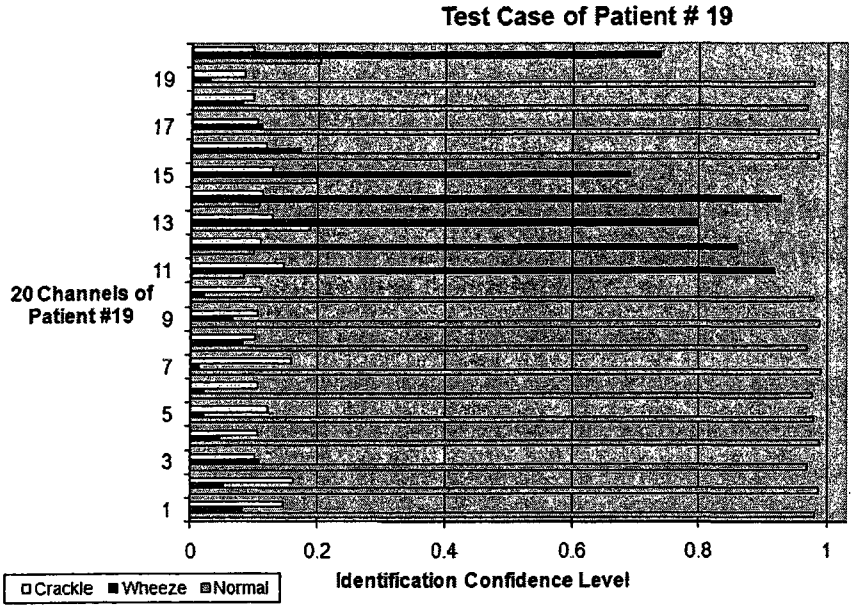

Figure A.19: Test Case Patient # 19 - Identification of Lung Sounds

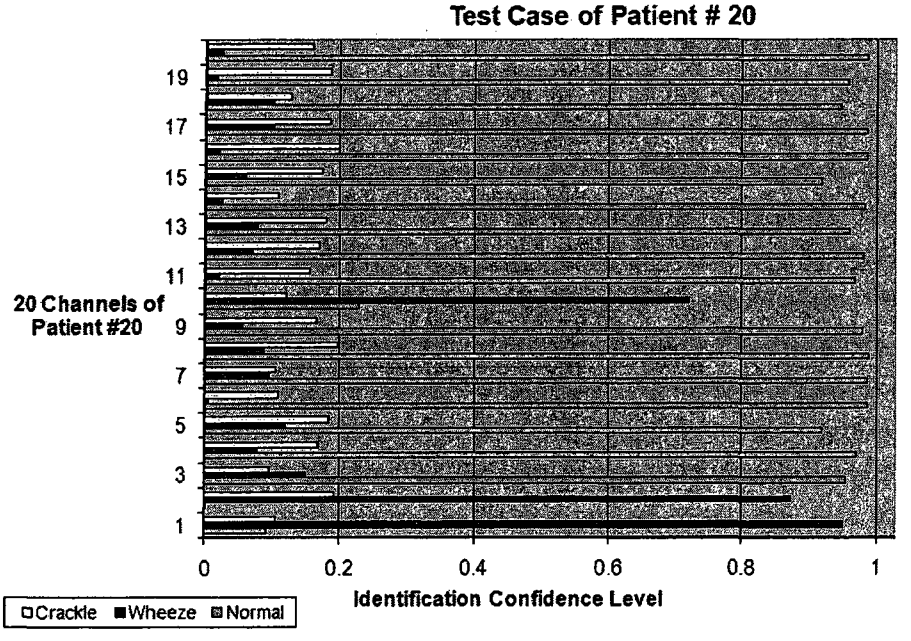

Figure A.20: Test Case Patient # 20 - Identification of Lung Sounds

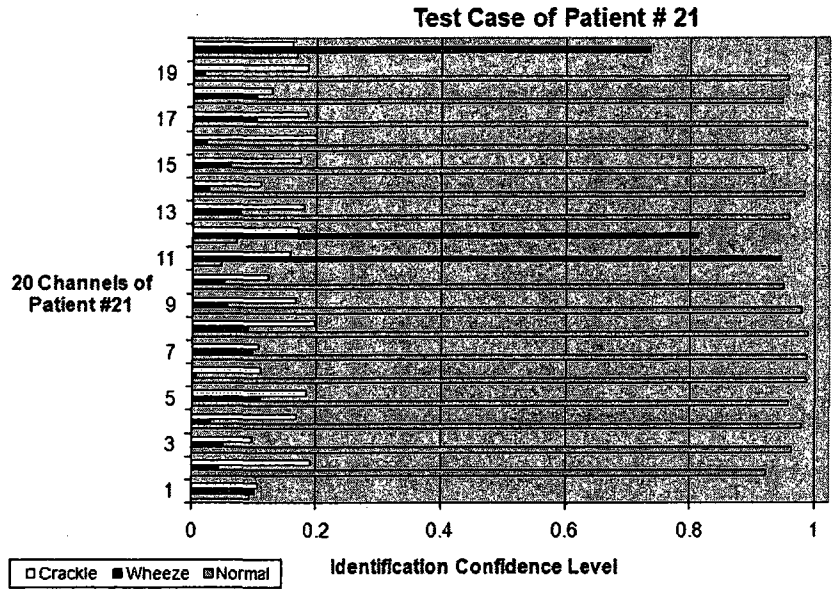

Figure A.21: Test Case Patient # 21 - Identification of Lung Sounds

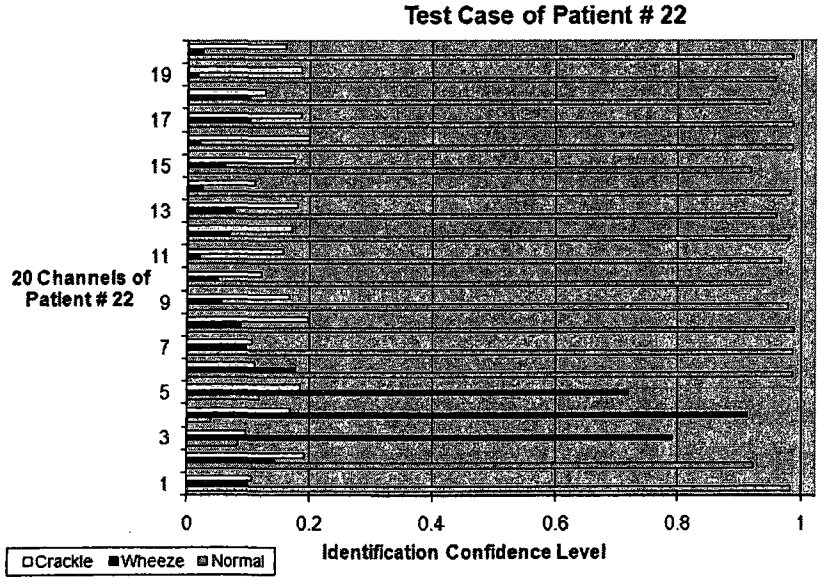

Figure A.22: Test Case Patient # 22 - Identification of Lung Sounds

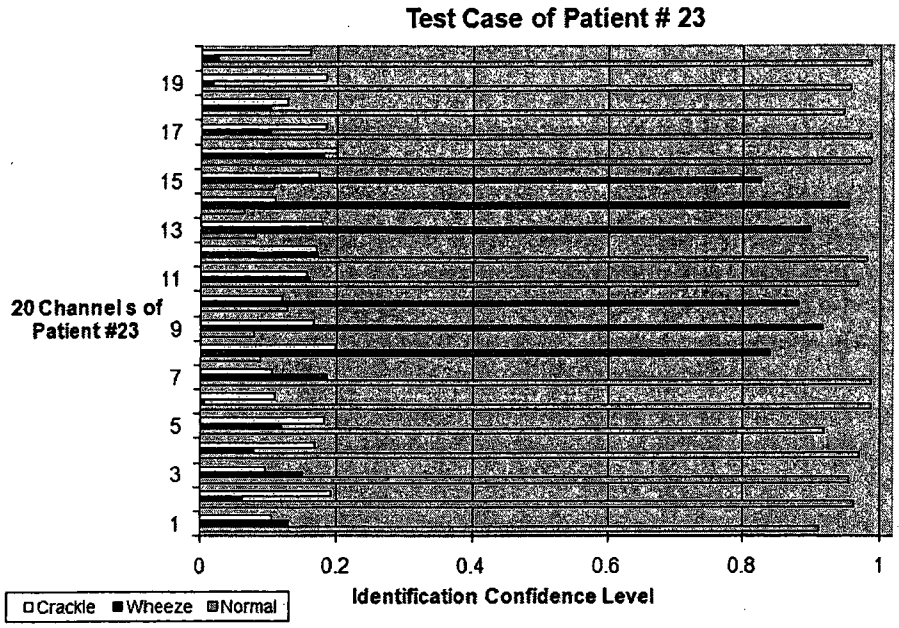

Figure A.23: Test Case Patient # 23 - Identification of Lung Sounds

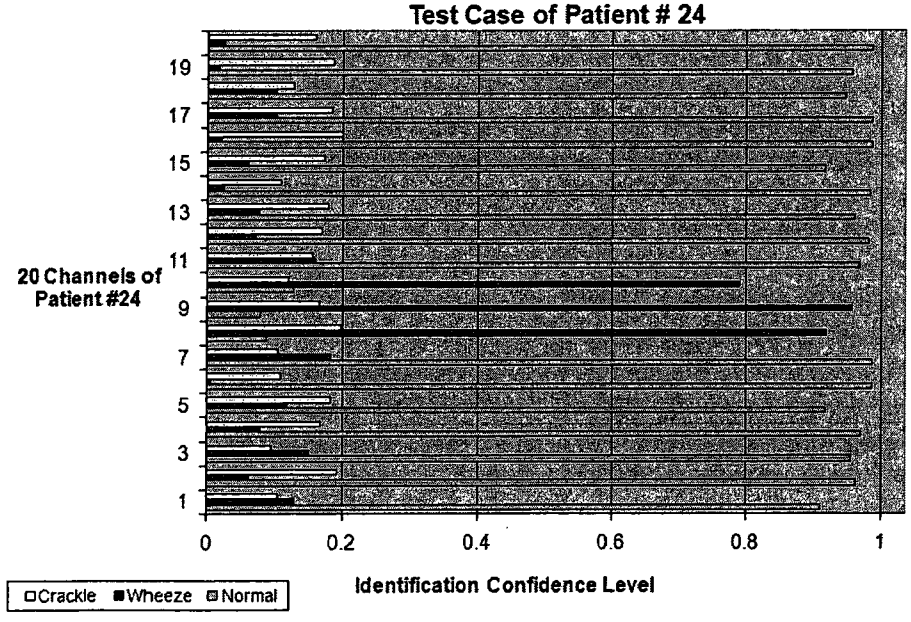

Figure A.24: Test Case Patient # 24 - Identification of Lung Sounds

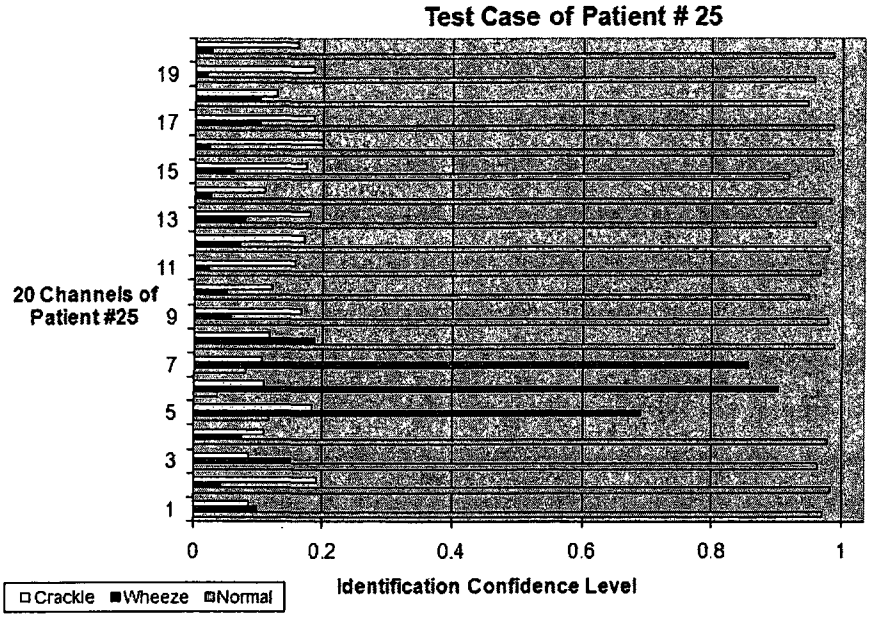

Figure A.25: Test Case Patient # 25 - Identification of Lung Sounds

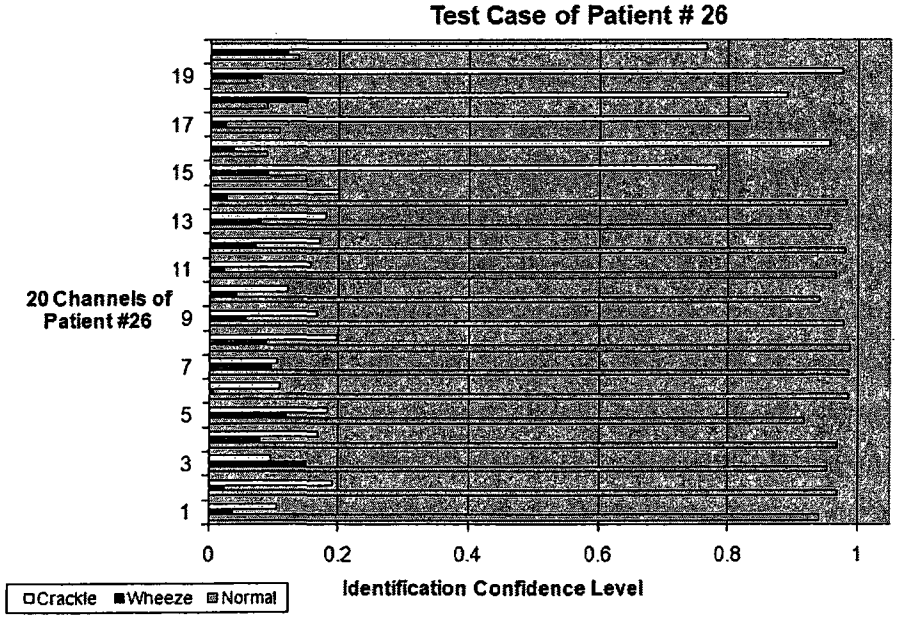

Figure A.26: Test Case Patient # 26 - Identification of Lung Sounds

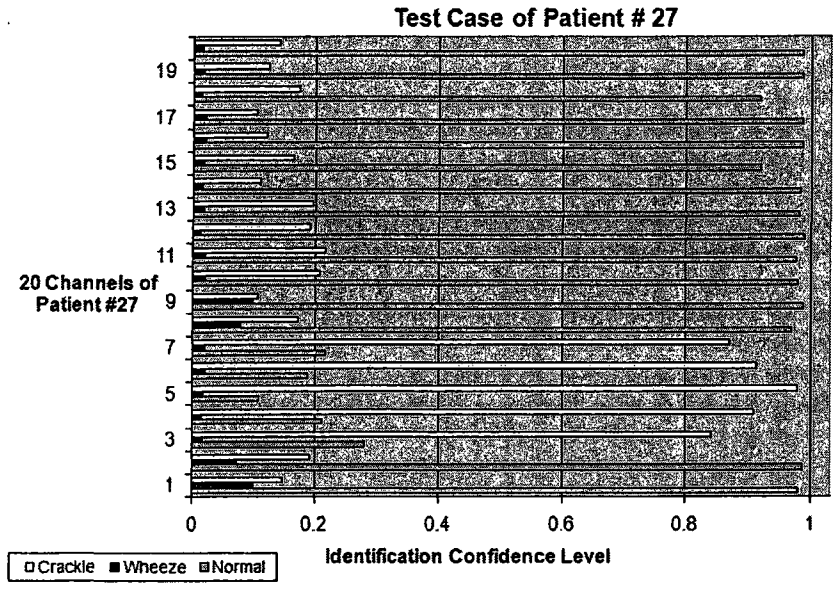

Figure A.27: Test Case Patient # 27 - Identification of Lung Sounds

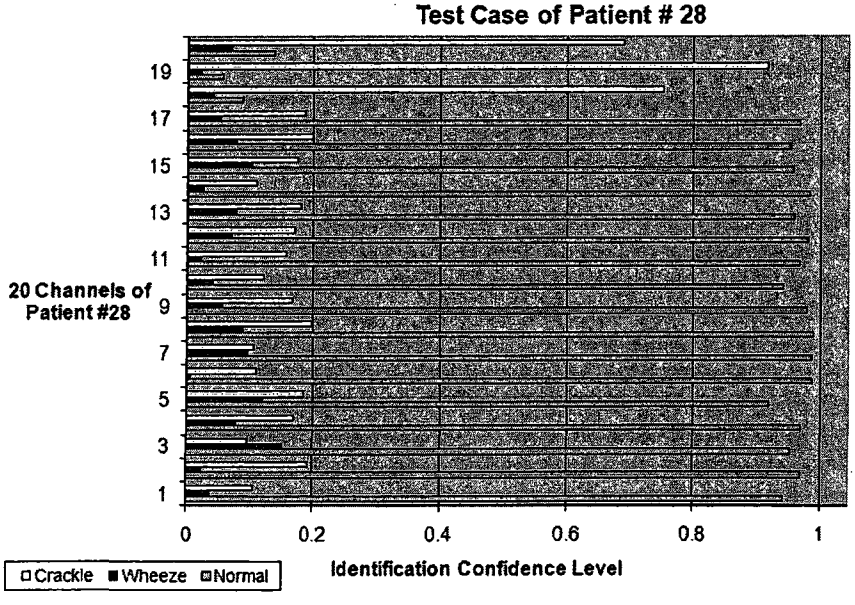

Figure A.28: Test Case Patient # 28 - Identification of Lung Sounds

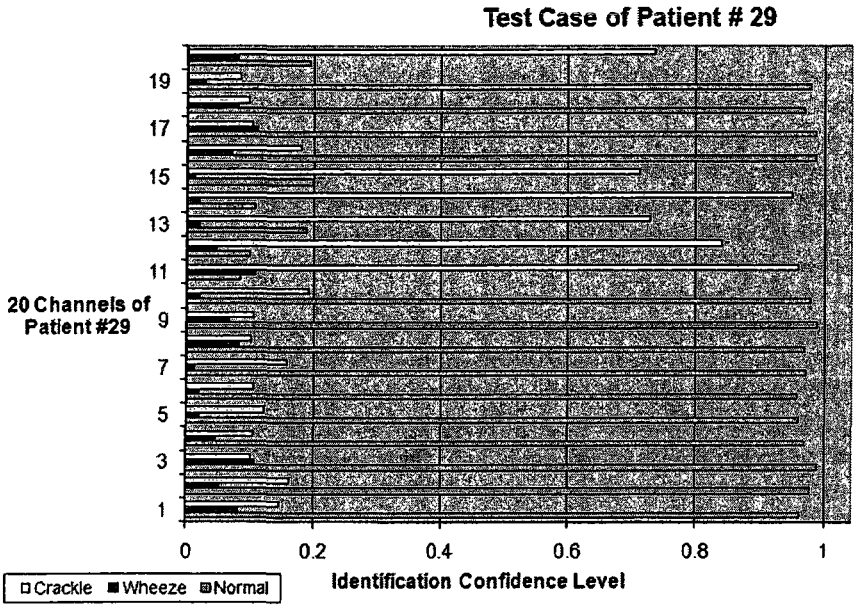

Figure A.29: Test Case Patient # 29 - Identification of Lung Sounds

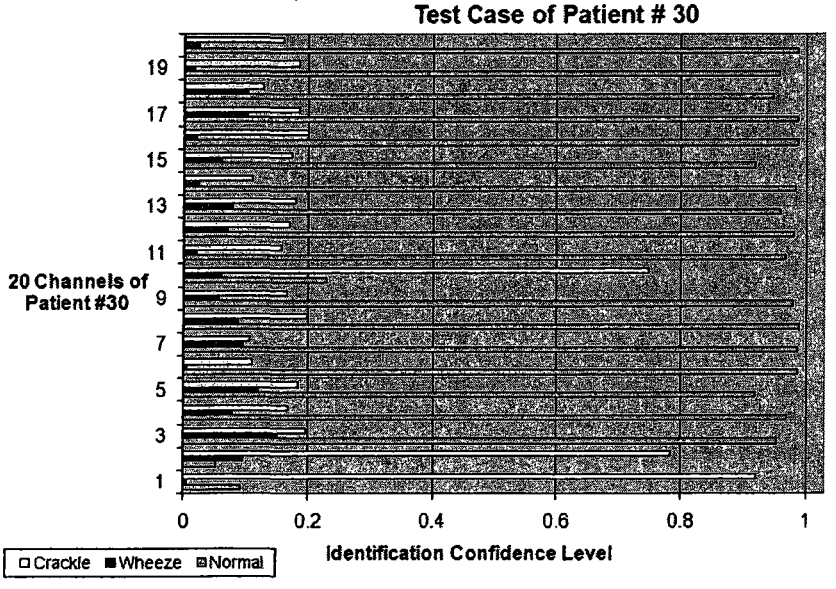

Figure A.30: Test Case Patient # 30 - Identification of Lung Sounds

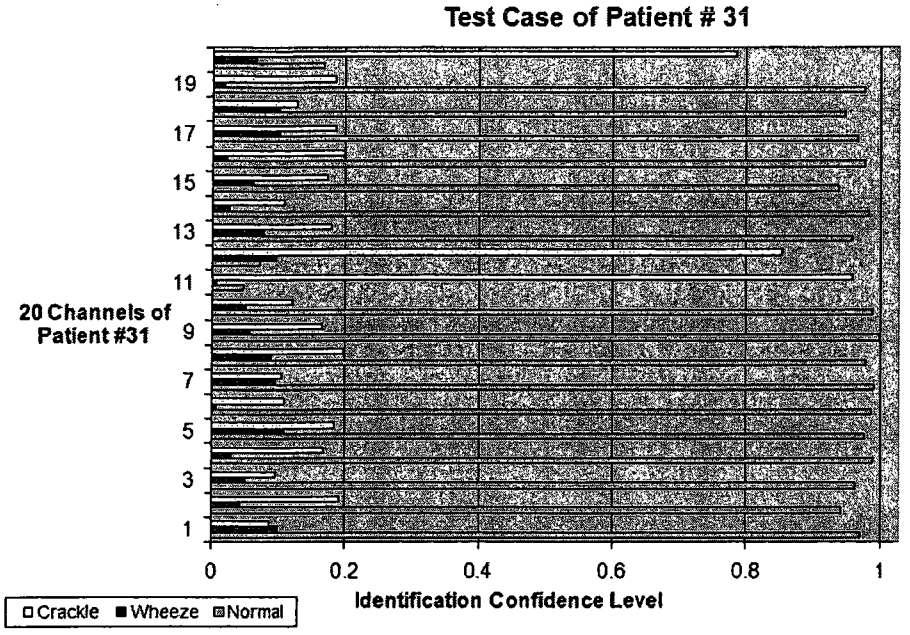

Figure A.31: Test Case Patient # 31 - Identification of Lung Sounds

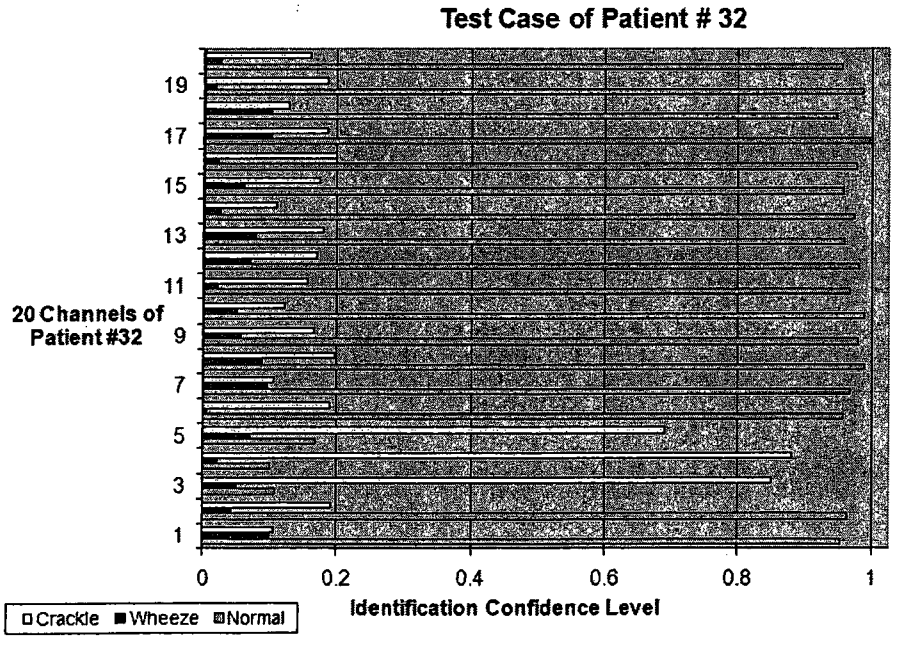

Figure A.32: Test Case Patient # 32 - Identification of Lung Sounds

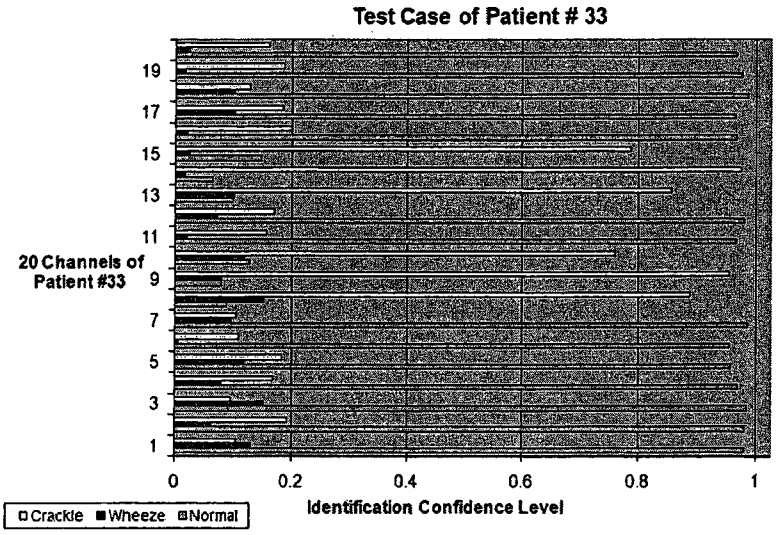

Figure A.33: Test Case Patient # 33 - Identification of Lung Sounds

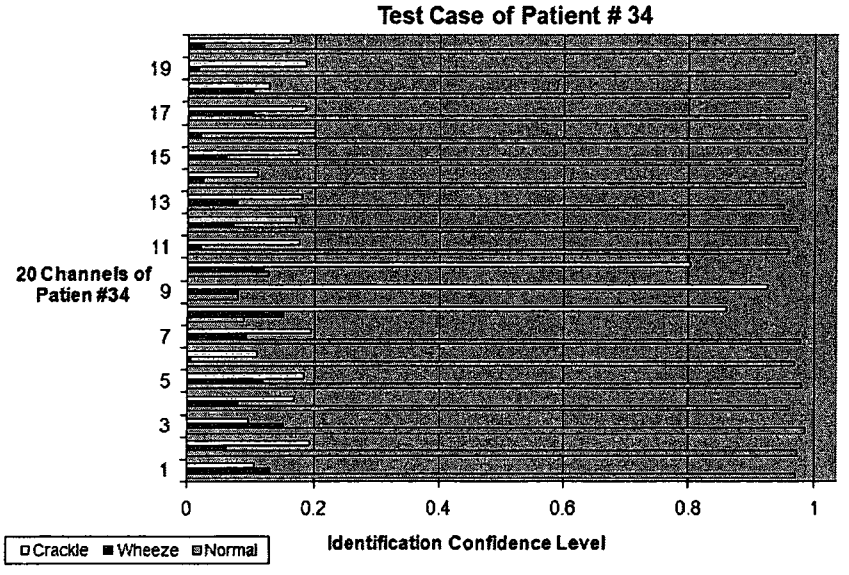

Figure A.34: Test Case Patient # 34 - Identification of Lung Sounds

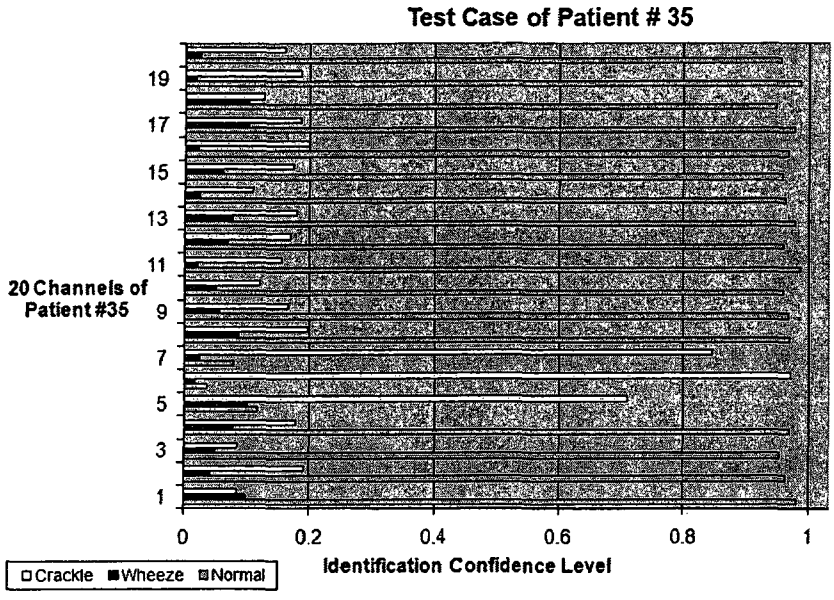

Figure A.35: Test Case Patient # 35 - Identification of Lung Sounds

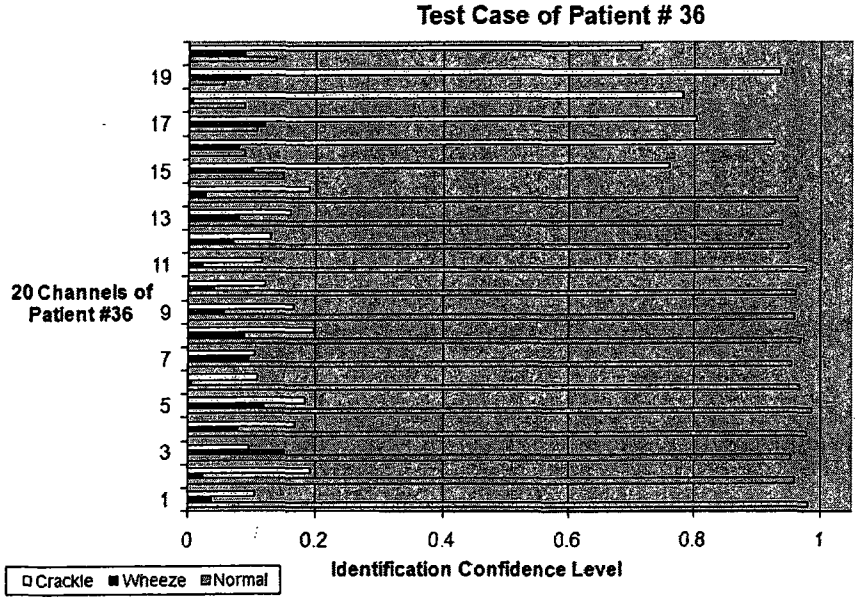

Figure A.36: Test Case Patient # 36 - Identification of Lung Sounds

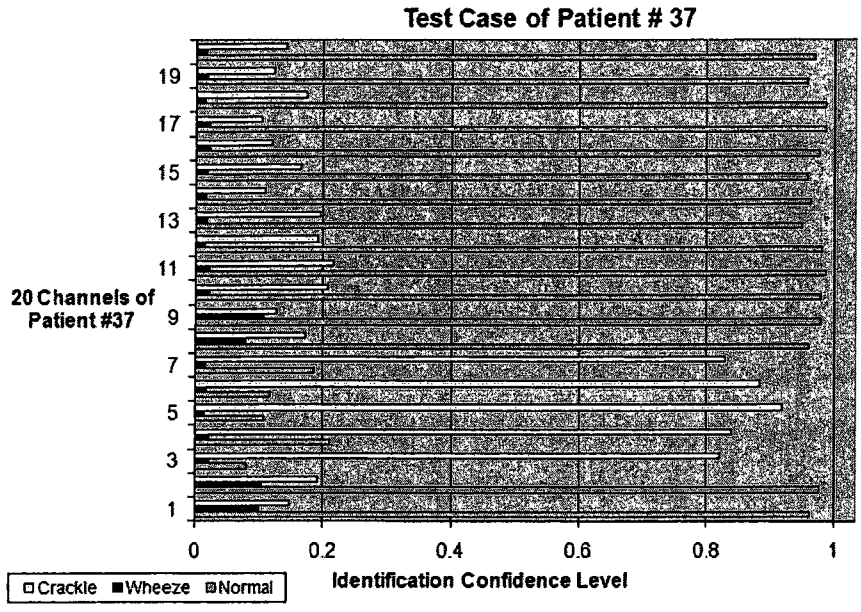

Figure A.37: Test Case Patient # 37 - Identification of Lung Sounds

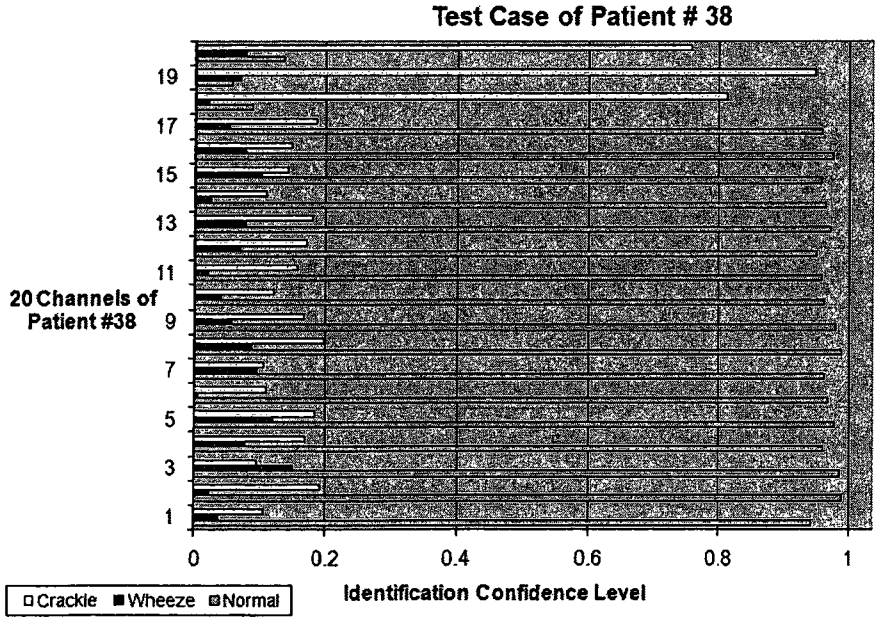

Figure A.38: Test Case Patient # 38 - Identification of Lung Sounds

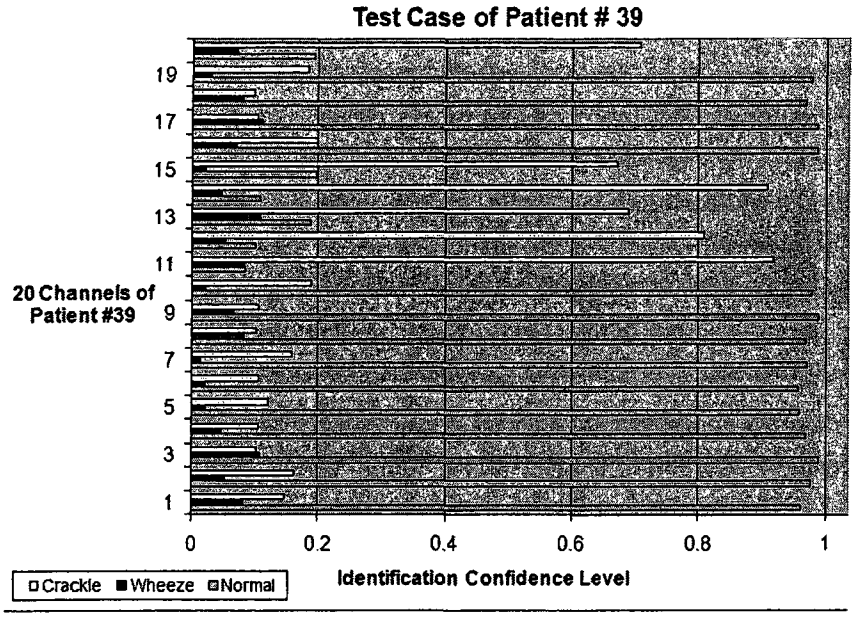

Figure A.39: Test Case Patient # 39 - Identification of Lung Sounds

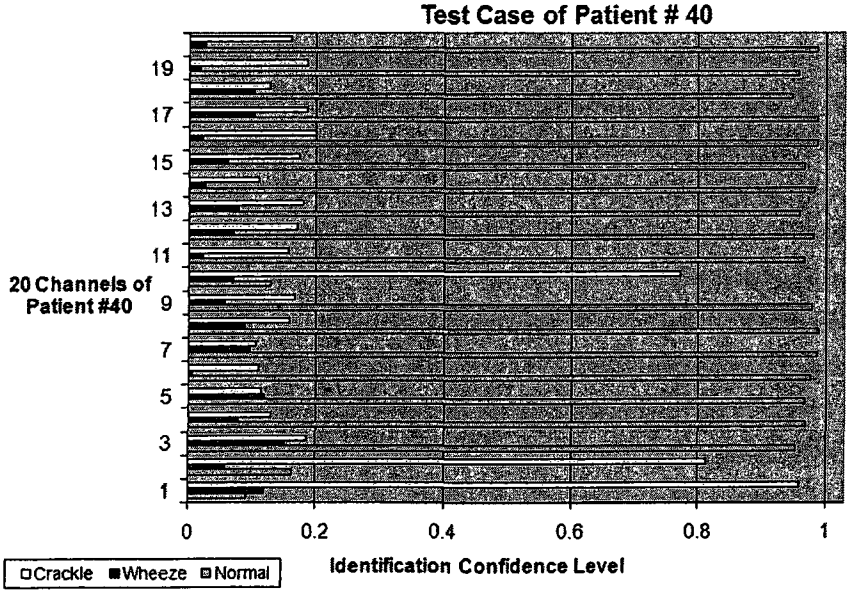

Figure A.40: Test Case Patient # 40 - Identification of Lung Sounds

APPENDIX B

Test Cases of the Localization Module

B.1 Localization Test Results of the Generated Virtual Patients

In order to locate the site of the infection, the adventitious sounds (wheeze or crackle) identified by the identification module of the developed system are presented to the localization module. Cross-correlation between each two of these is carried out. Figures B.1 to B.40 show the outputs of the localization module of the diagnosed adventitious lung sound signals of the 40 test cases presented. With reference to the figures, the bars represent the degree of the cross-correlation between the channels. When the output values of the correlation among the adventitious sound signals are relatively high, these indicate that the adventitious lung sound signals are from the same source of infection. However, when the output values of the correlation among the adventitious sound signals are low, these indicate that the adventitious lung sound signals are from different sources of infection.

The automated auscultation system was tested using the generated forty virtual patients in Table 6.2. Results of site localization of adventitious lung sounds carried out on those virtual patients where extremely significant. The figures show clearly that the system accuracy in all the test cases was perfect and was able to locate all the sites of adventitious lung sounds with very high confidence level. Those test results conclude that the develop system is capable of pinpointing the lung segments and lobes that are the sites of the adventitious sounds.

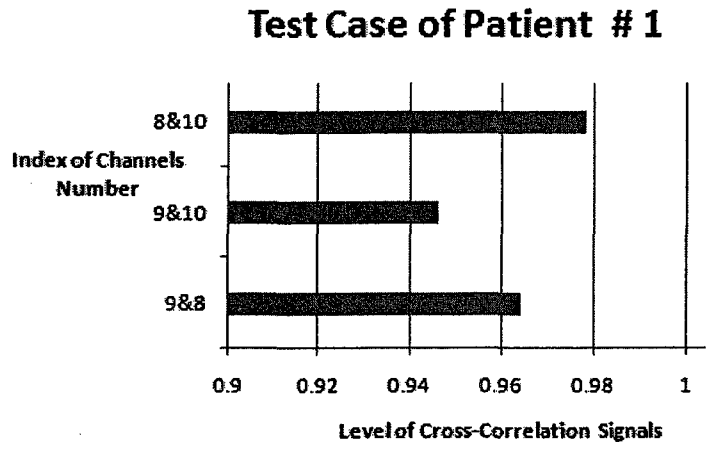

Figure B.1: Test Case Patient #1- Localization of the Source of Infection

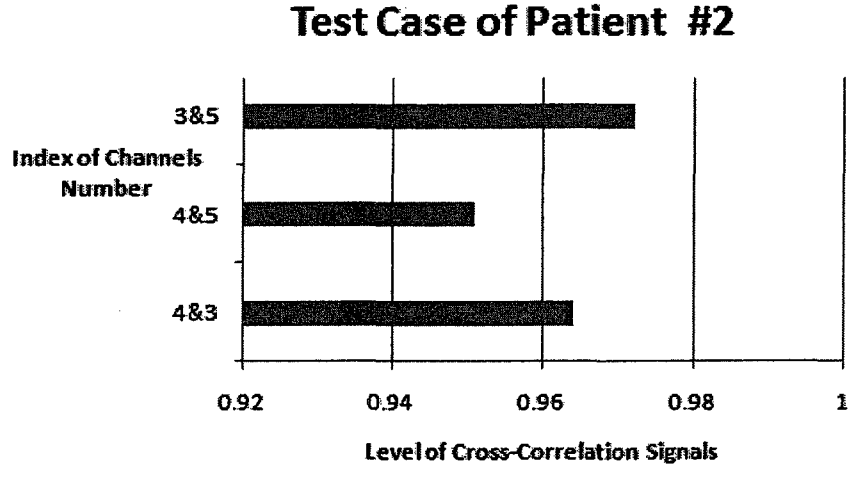

Figure B.2: Test Case Patient #2- Localization of the Source of Infection

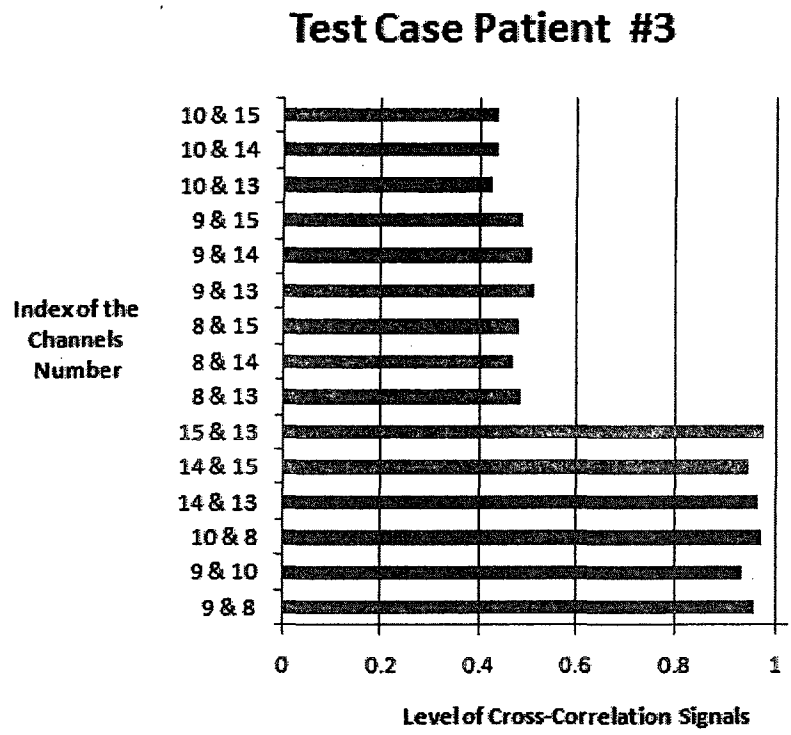

Figure B.3: Test Case Patient #3-Localization of the Source of Infection

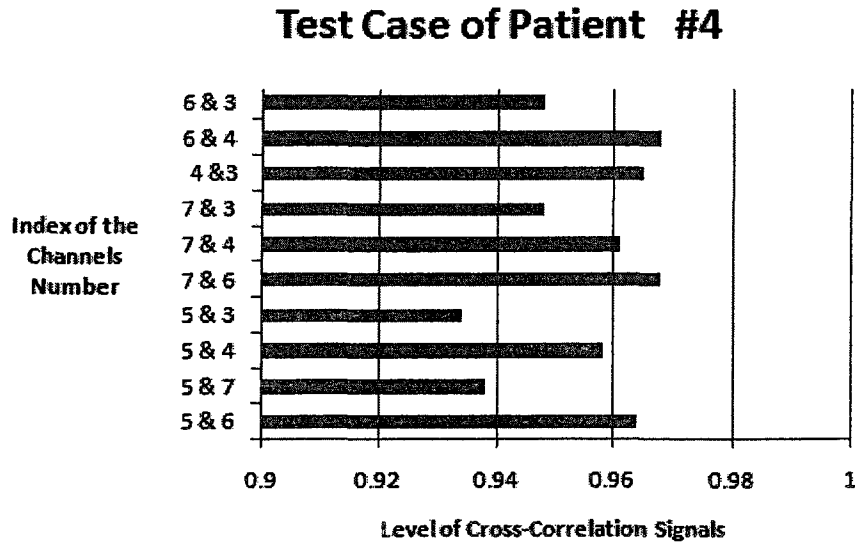

Figure B.4: Test Case Patient #4-Localization of the Source of Infection

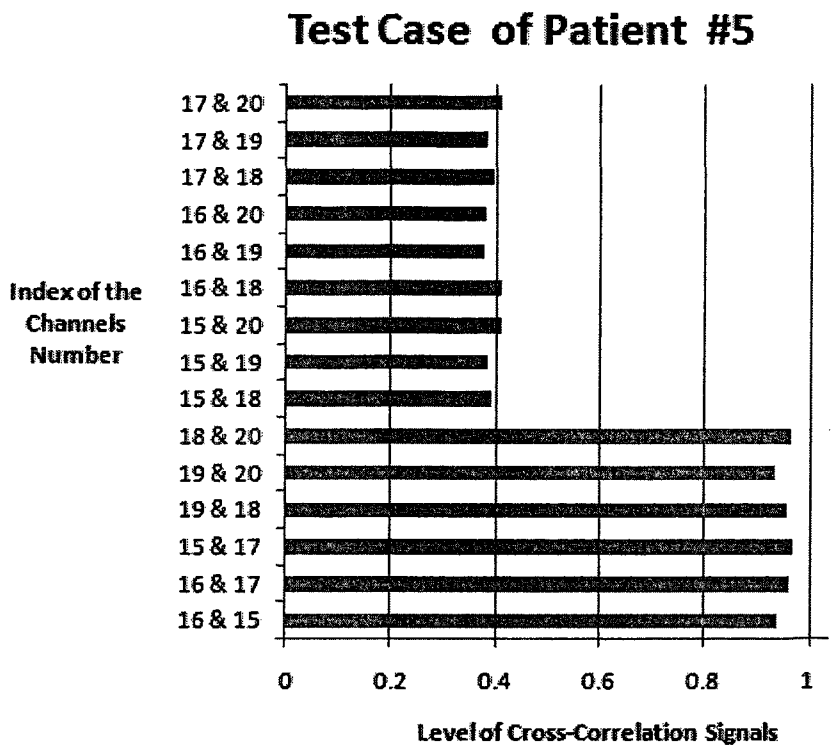

Figure B.5: Test Case Patient #5 - Localization of the Source of Infection

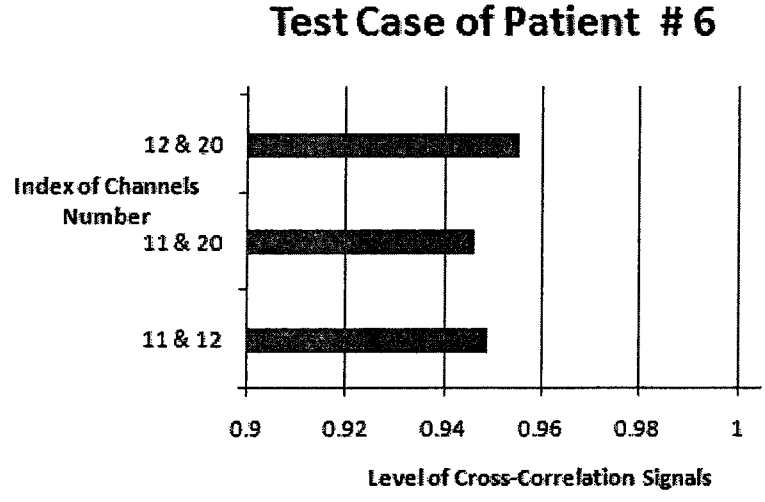

Figure B.6: Test Case Patient #6 - Localization of the Source of Infection

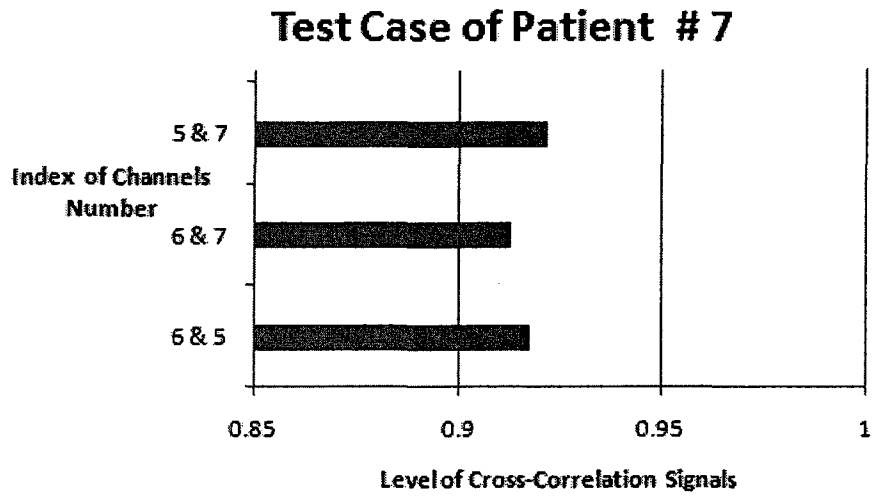

Figure B.7: Test Case Patient #7 - Localization of the Source of Infection

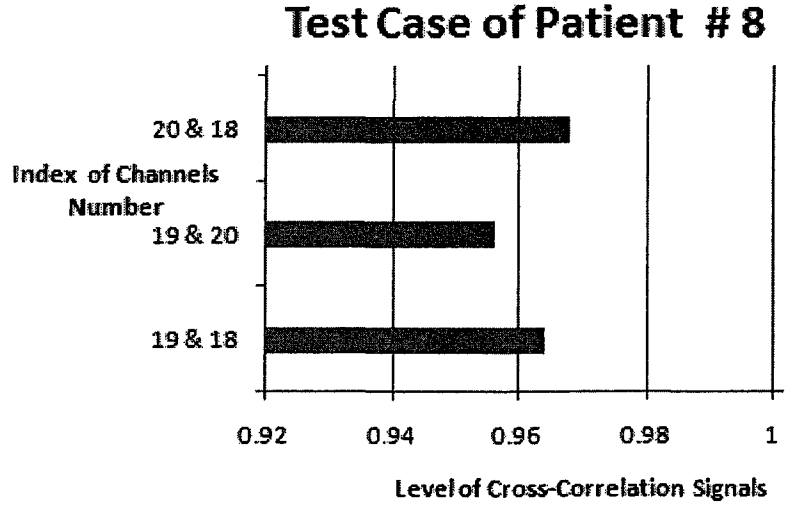

Figure B.8: Test Case Patient #8 - Localization of the Source of Infection

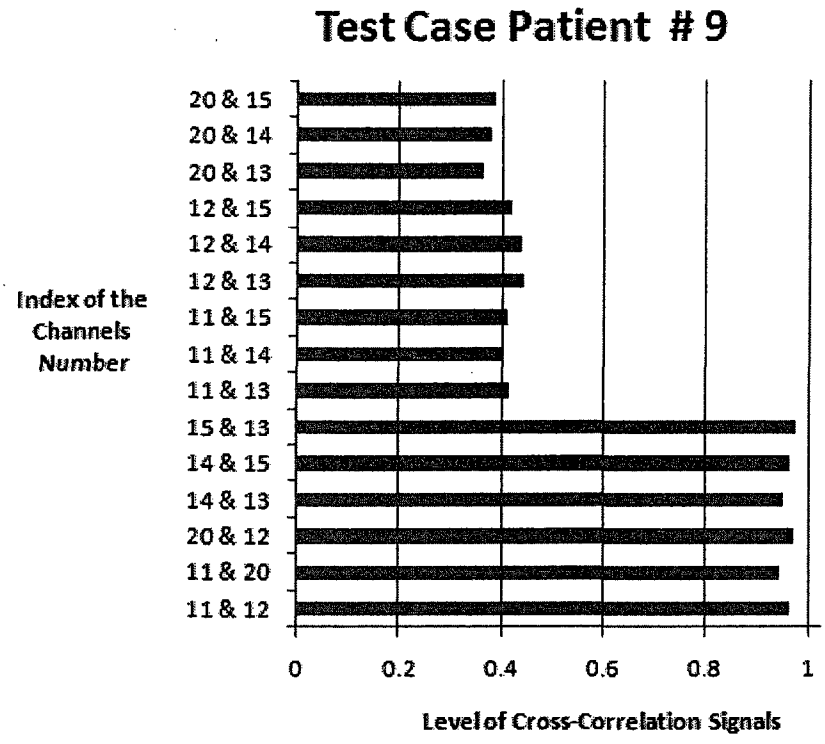

Figure B.9: Test Case Patient #9 - Localization of the Source of Infection

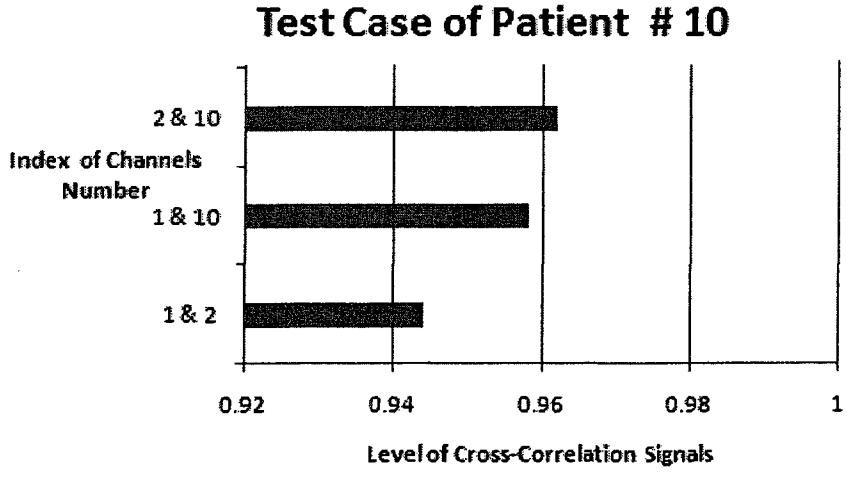

Figure B.10: Test Case Patient #10 - Localization of the Source of Infection

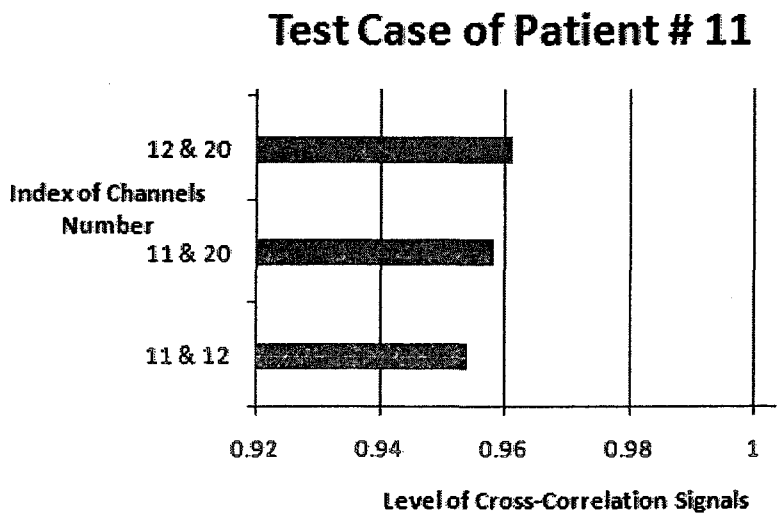

Figure B.11: Test Case Patient #11 - Localization of the Source of Infection

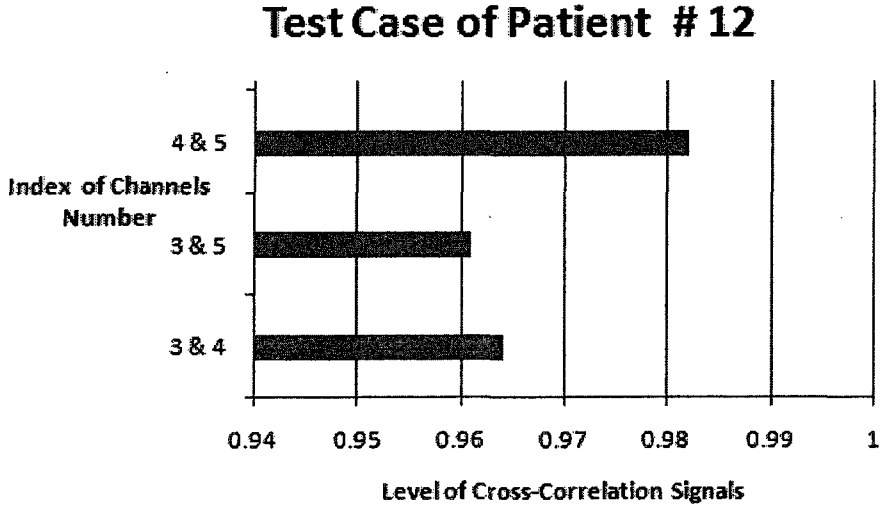

Figure B.12: Test Case Patient #12 - Localization of the Source of Infection

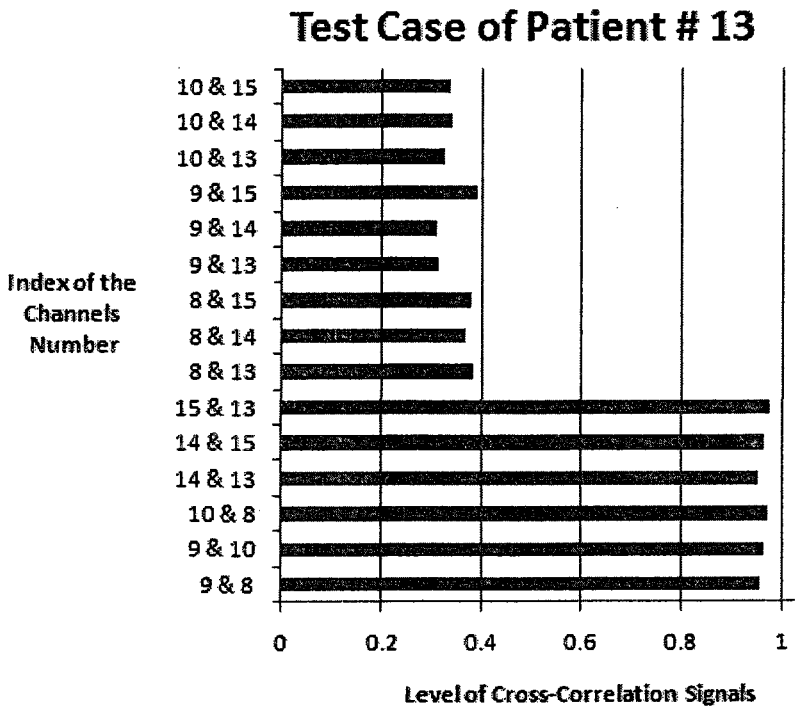

Figure B.13: Test Case Patient #13 - Localization of the Source of Infection

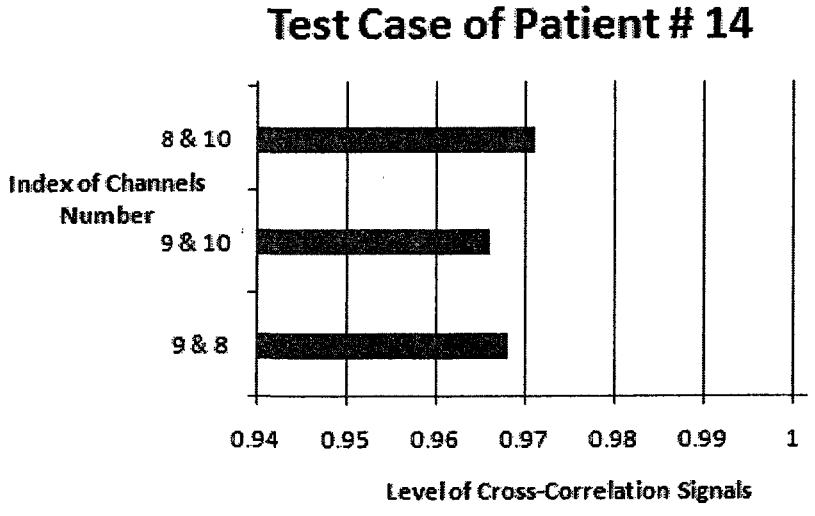

Figure B.14: Test Case Patient #14 - Localization of the Source of Infection

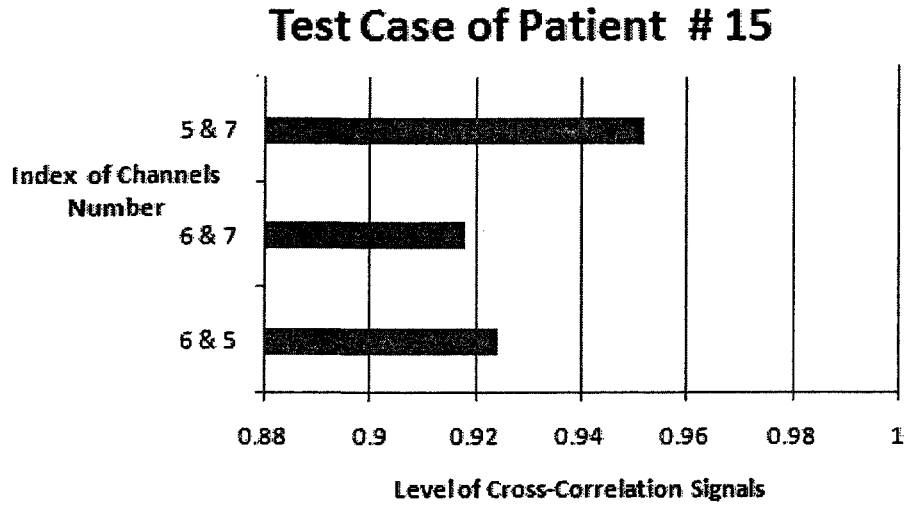

Figure B.15: Test Case Patient #15 - Localization of the Source of Infection

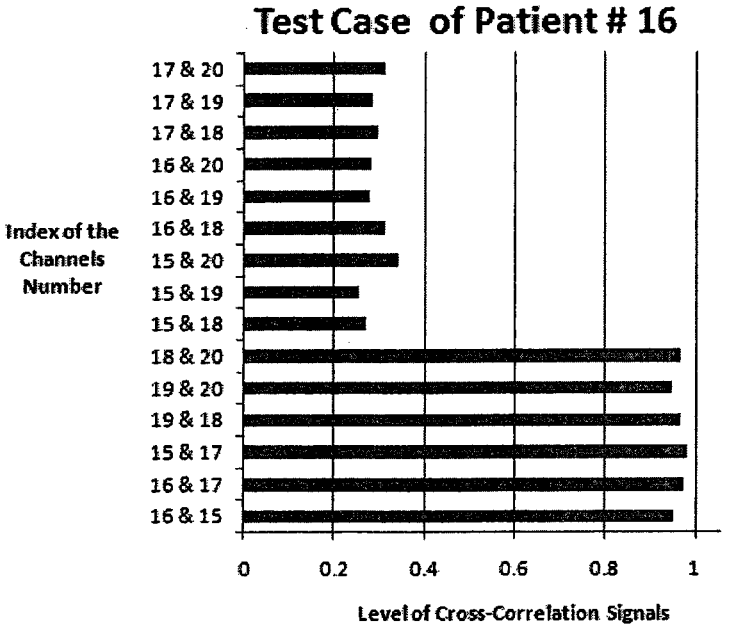

Figure B.16: Test Case Patient #16 - Localization of the Source of Infection

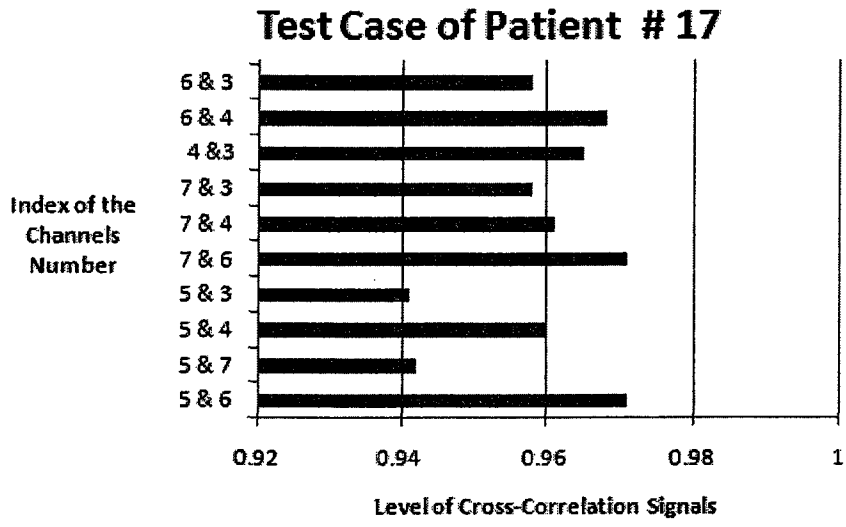

Figure B.17: Test Case Patient #17 - Localization of the Source of Infection

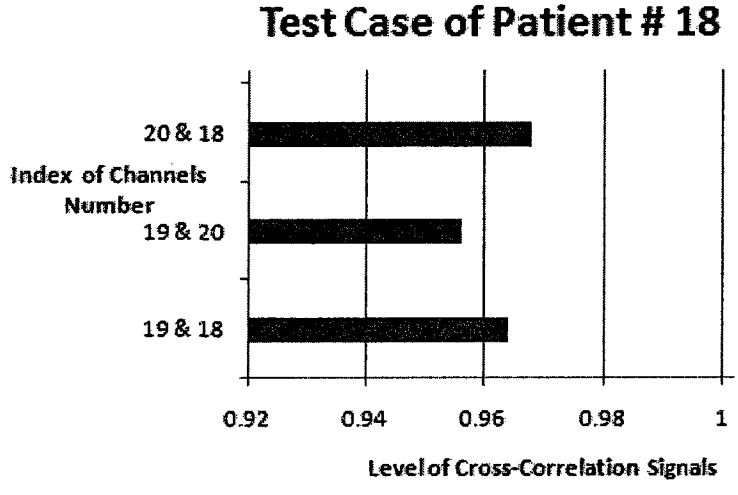

Figure B.18: Test Case Patient #18 - Localization of the Source of Infection

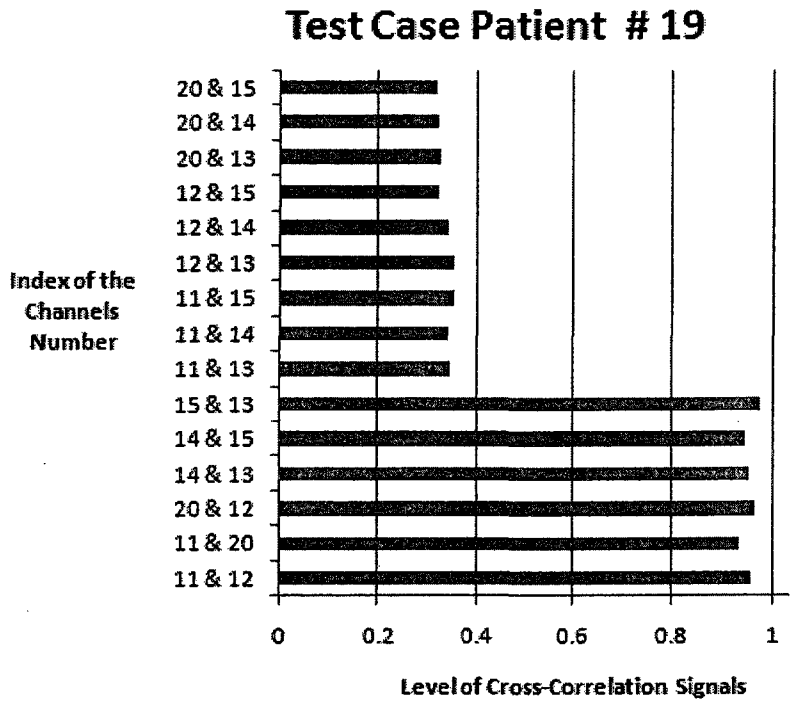

Figure B.19: Test Case Patient #19 - Localization of the Source of Infection

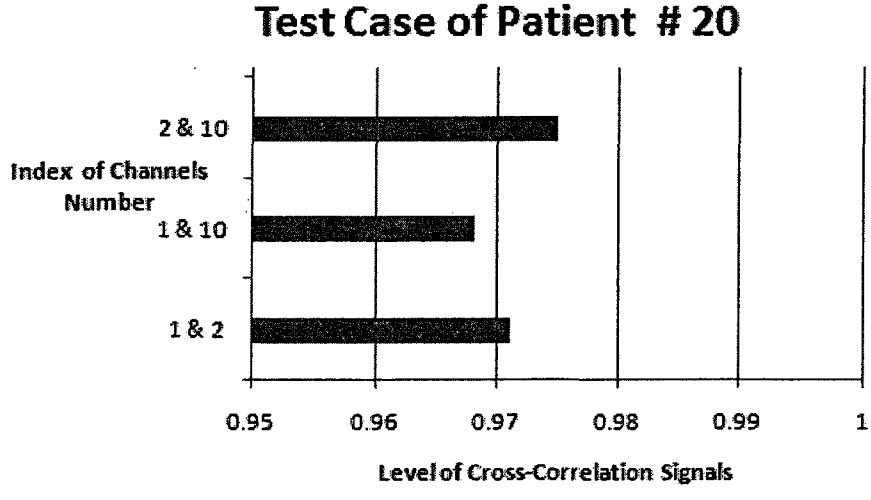

Figure B.20: Test Case Patient #20 - Localization of the Source of Infection

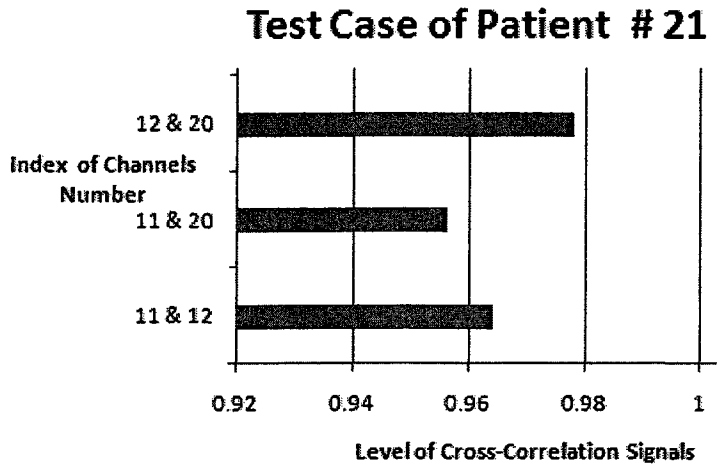

Figure B.21: Test Case Patient #21 - Localization of the Source of Infection

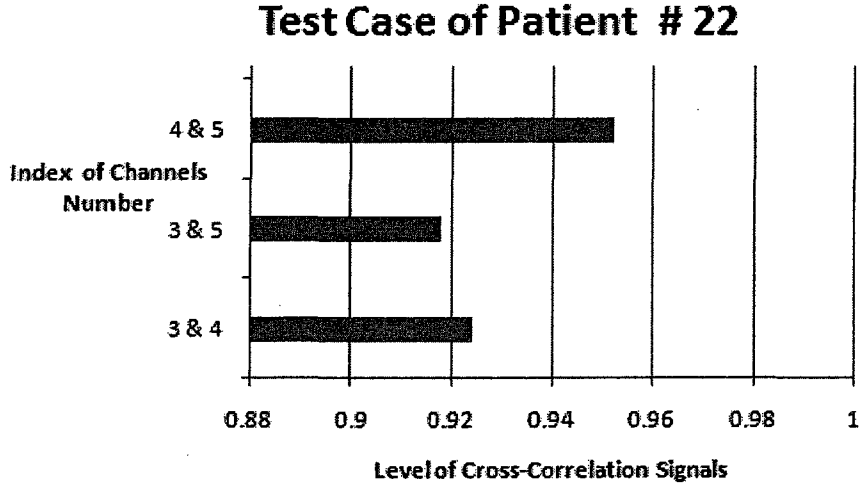

Figure B.22: Test Case Patient #22 - Localization of the Source of Infection

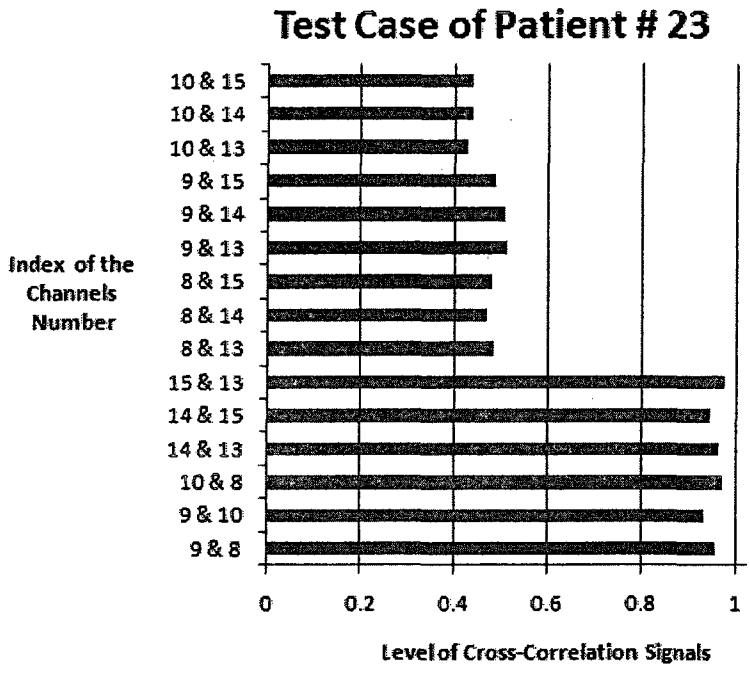

Figure B.23: Test Case Patient #23 - Localization of the Source of Infection

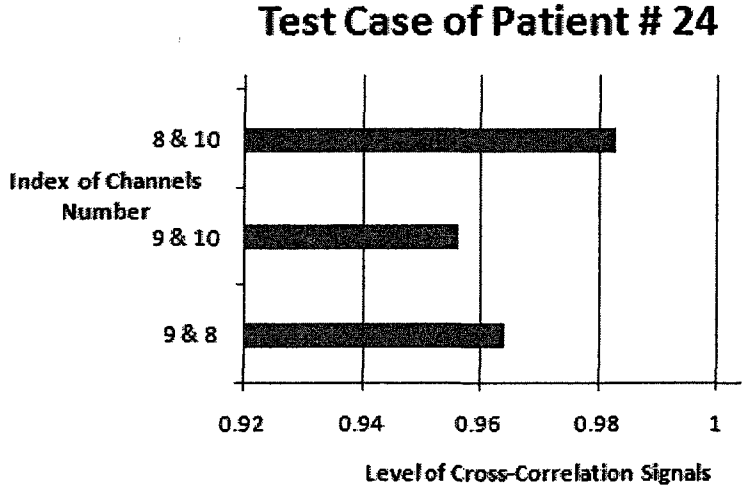

Figure B.24: Test Case Patient #24 - Localization of the Source of Infection

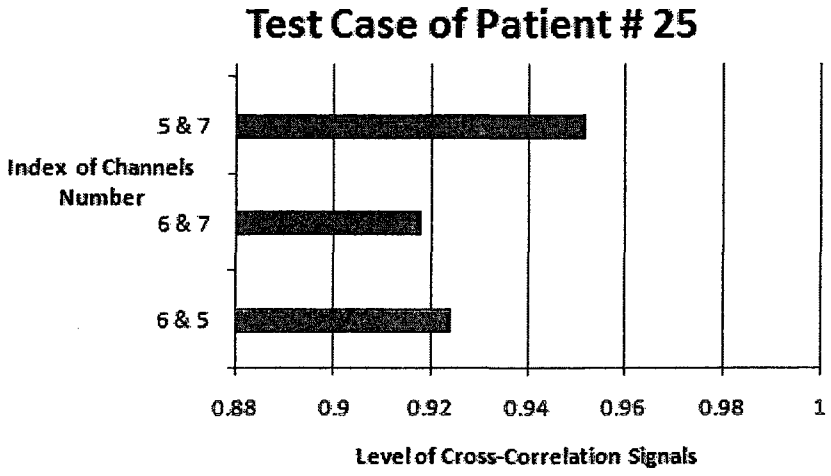

Figure B.25: Test Case Patient #25 - Localization of the Source of Infection

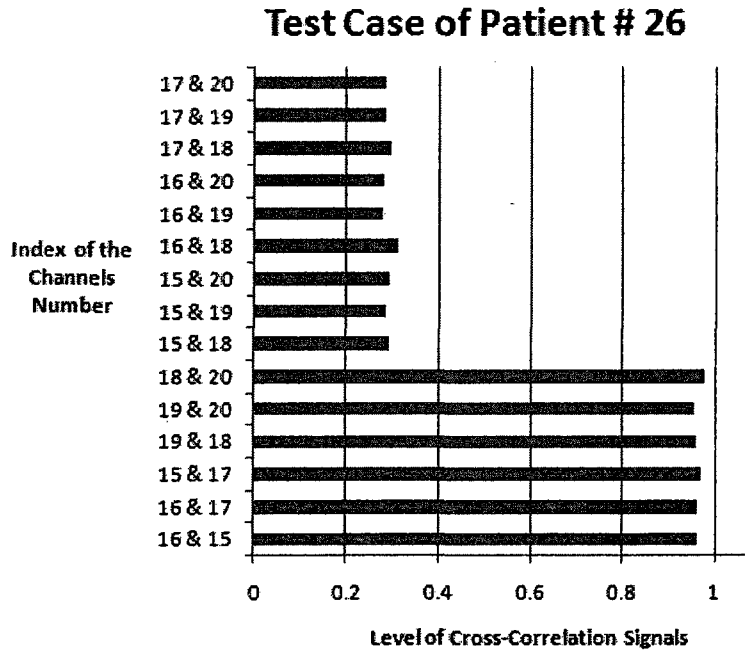

Figure B.26: Test Case Patient #26 - Localization of the Source of Infection

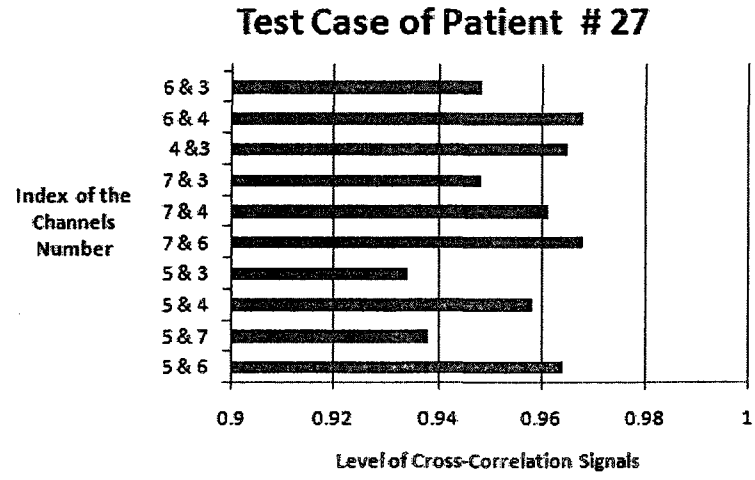

Figure B.27: Test Case Patient #27 - Localization of the Source of Infection

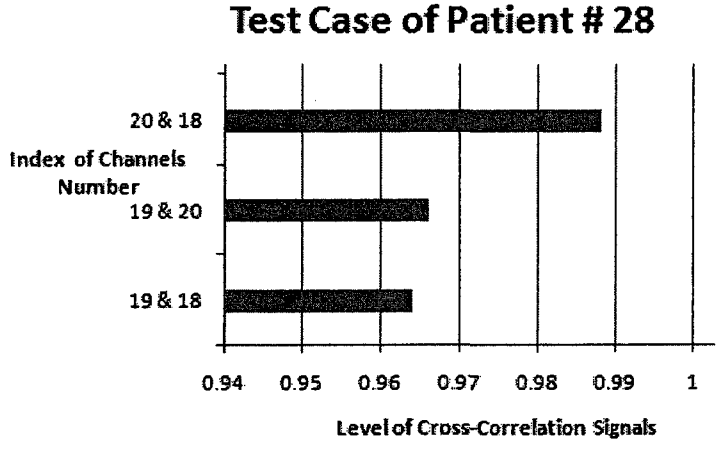

Figure B.28: Test Case Patient #28 - Localization of the Source of Infection

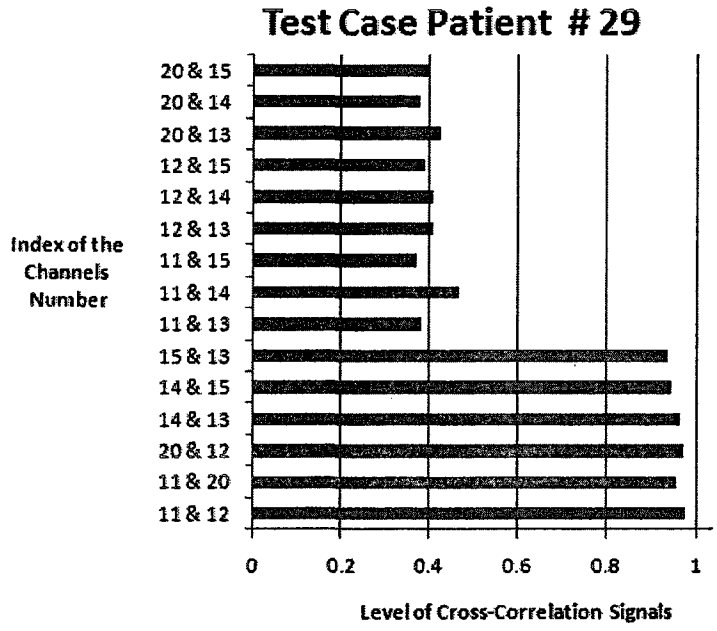

Figure B.29: Test Case Patient #29 - Localization of the Source of Infection

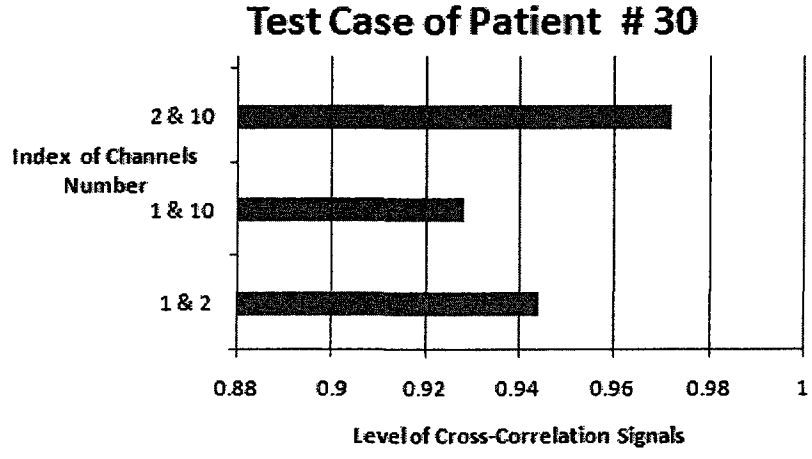

Figure B.30: Test Case Patient #30 - Localization of the Source of Infection

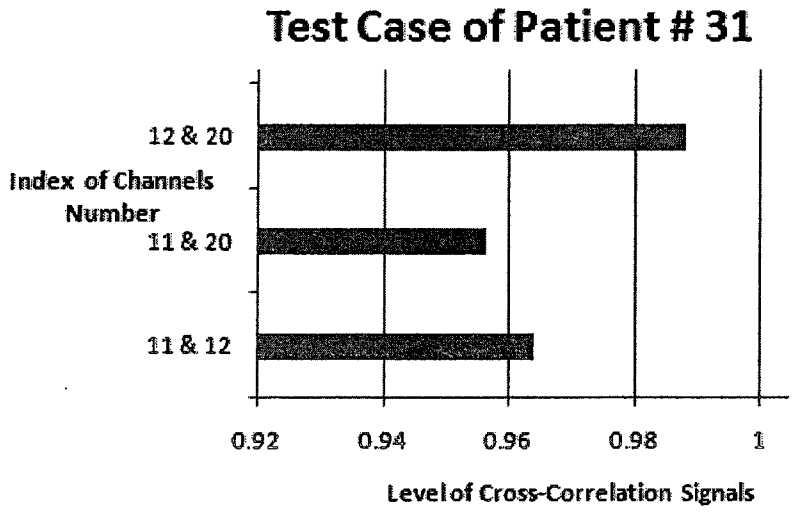

Figure B.31: Test Case Patient #31 - Localization of the Source of Infection

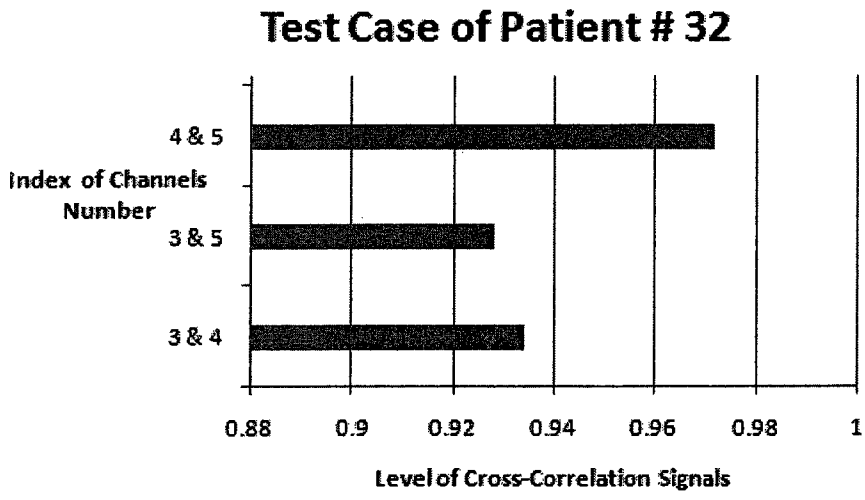

Figure B.32: Test Case Patient #32 - Localization of the Source of Infection

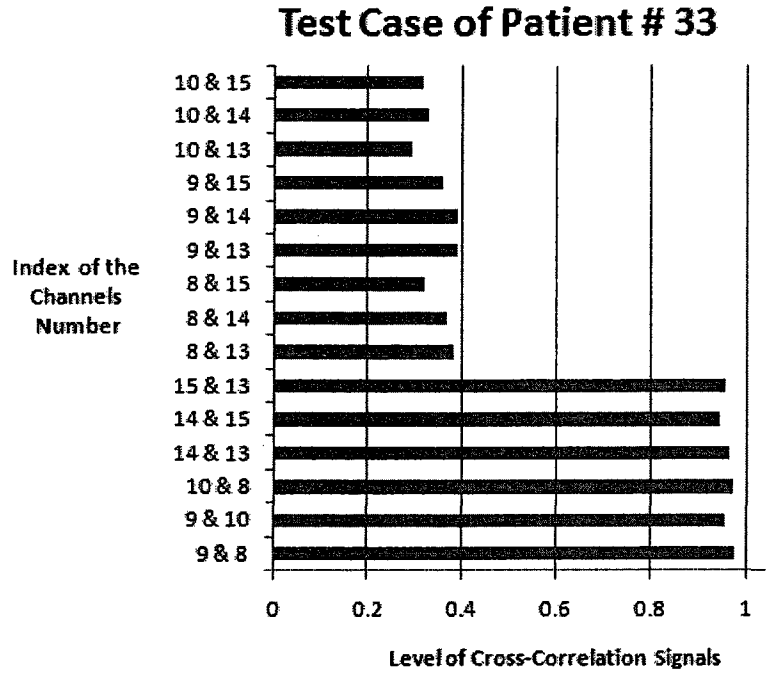

Figure B.33: Test Case Patient #33 - Localization of the Source of Infection

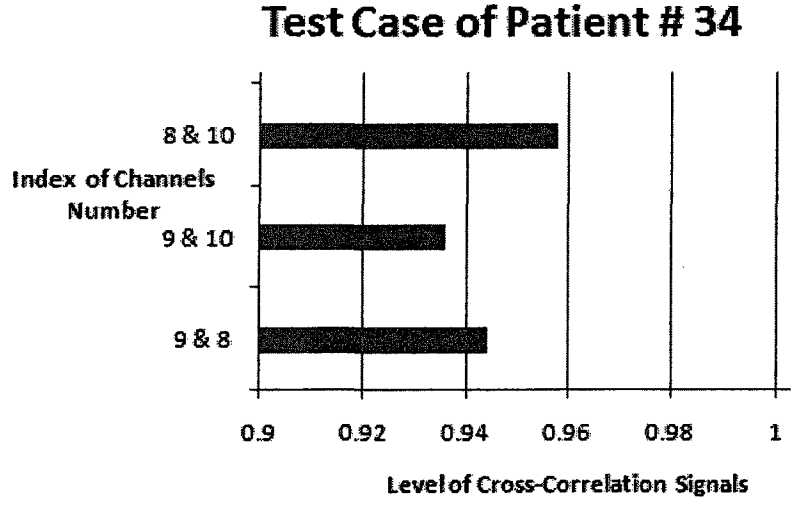

Figure B.34: Test Case Patient #34 - Localization of the Source of Infection

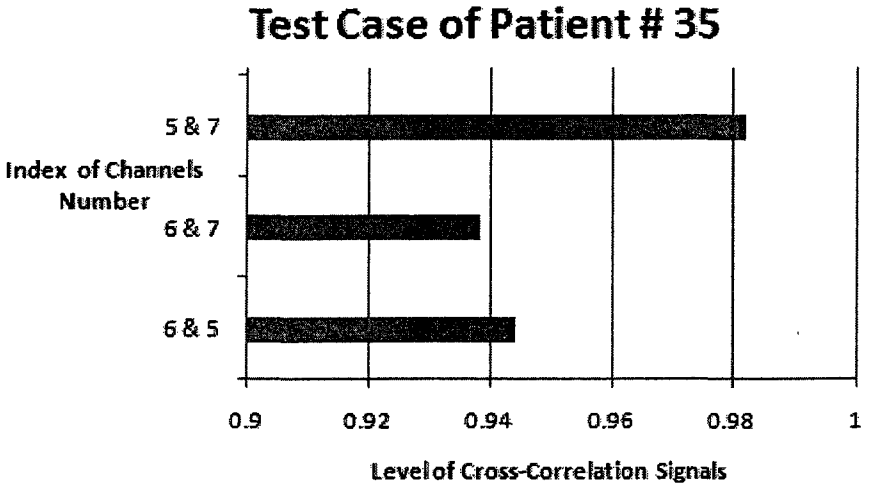

Figure B.35: Test Case Patient #35 - Localization of the Source of Infection

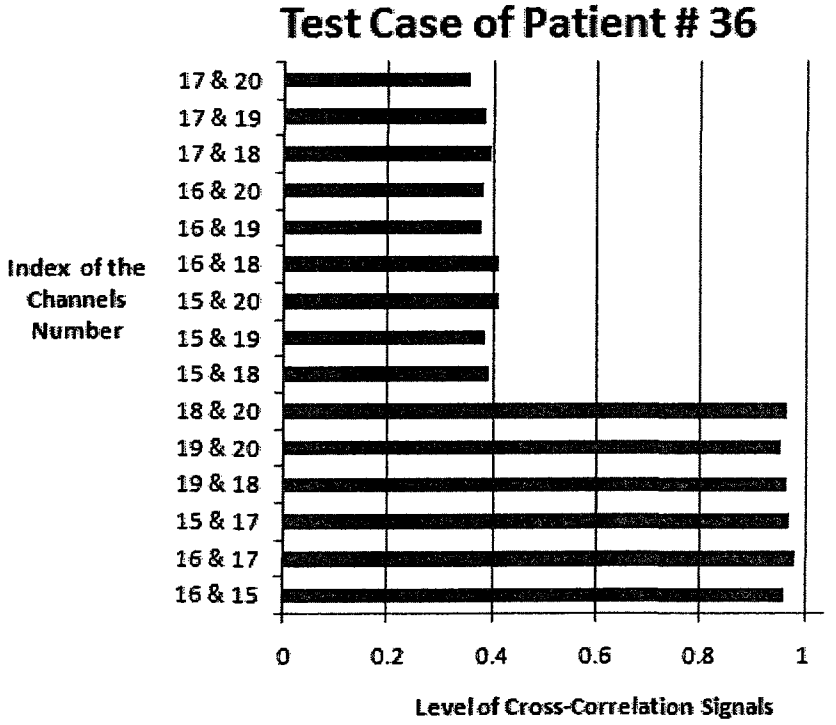

Figure B.36: Test Case Patient #36 - Localization of the Source of Infection

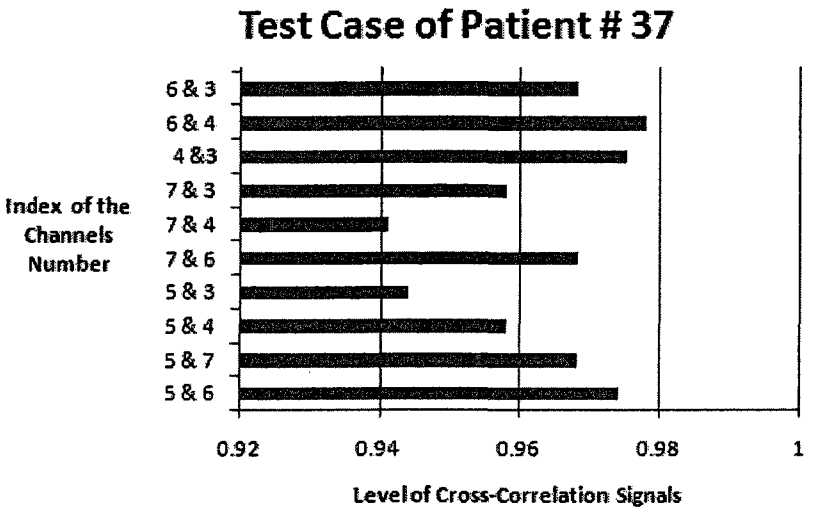

Figure B.37: Test Case Patient #37 - Localization of the Source of Infection

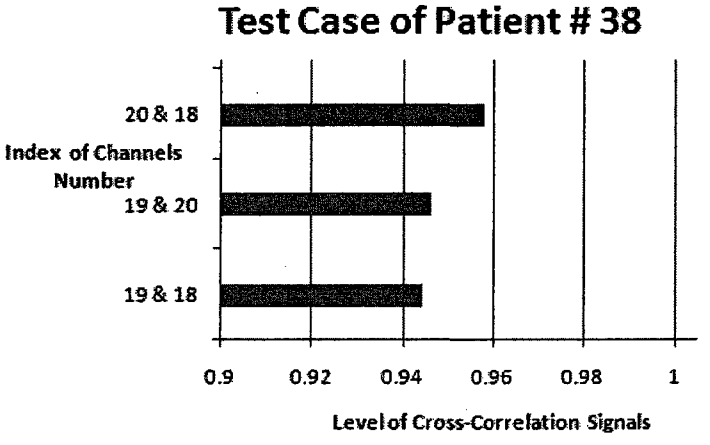

Figure B.38: Test Case Patient #38 - Localization of the Source of Infection

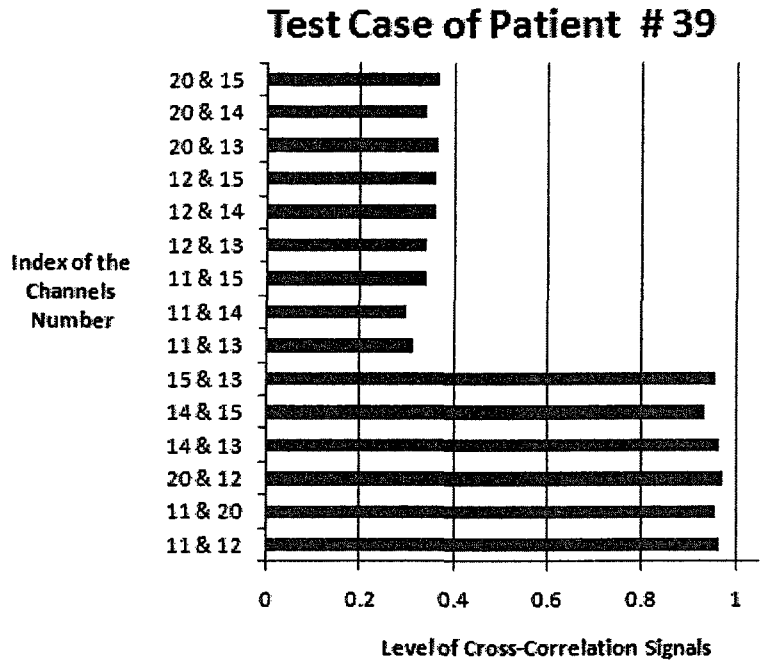

Figure B.39: Test Case Patient #39 - Localization of the Source of Infection

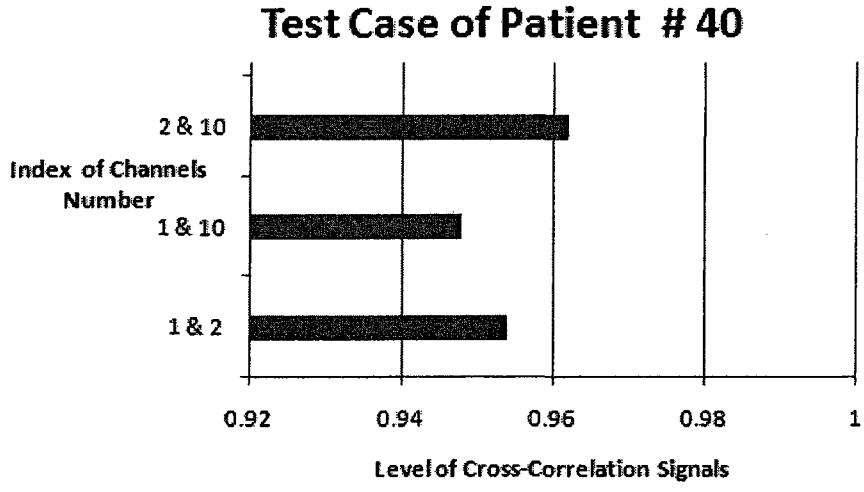

Figure B.40: Test Case Patient #40 - Localization of the Source of Infection